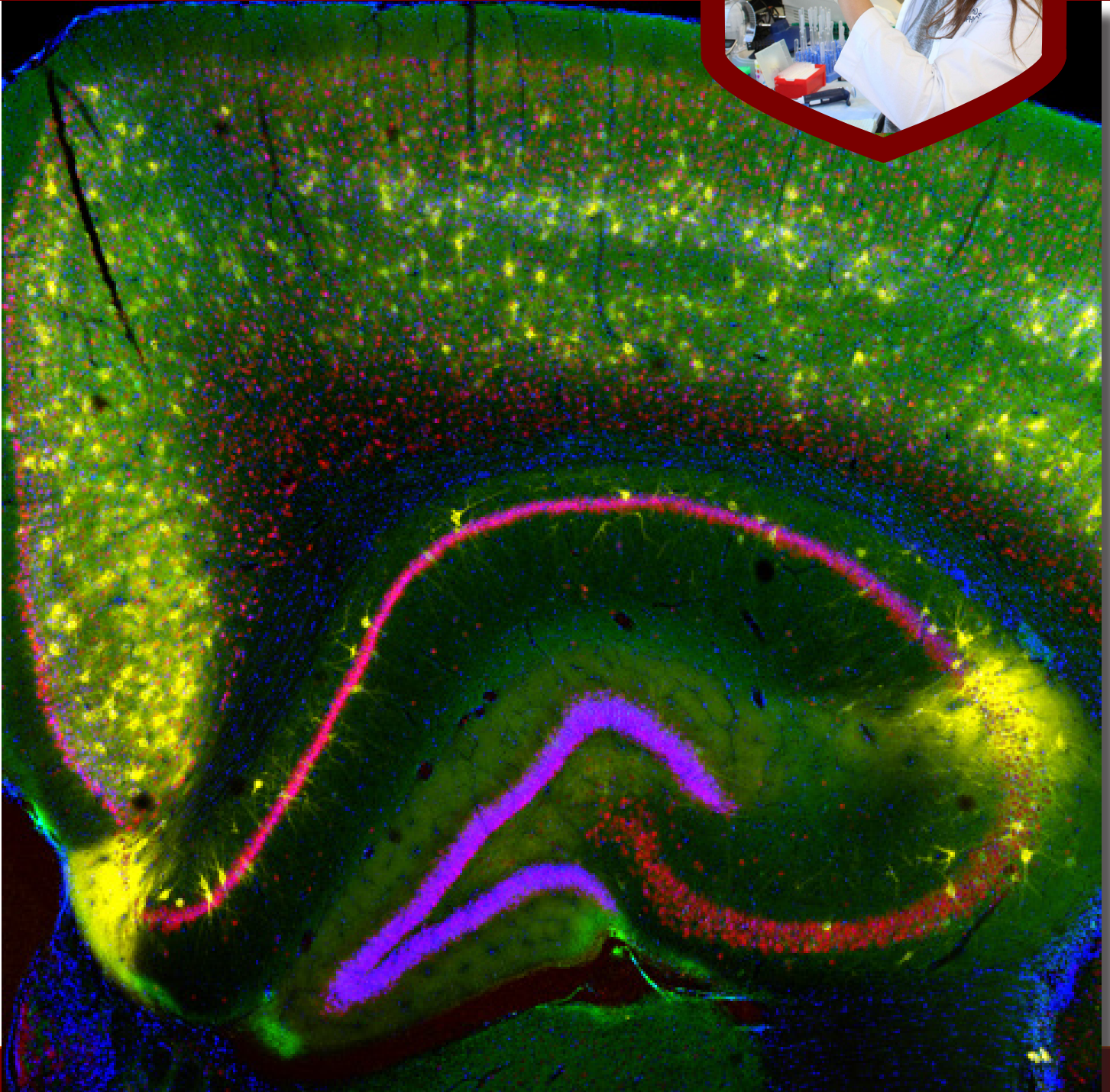
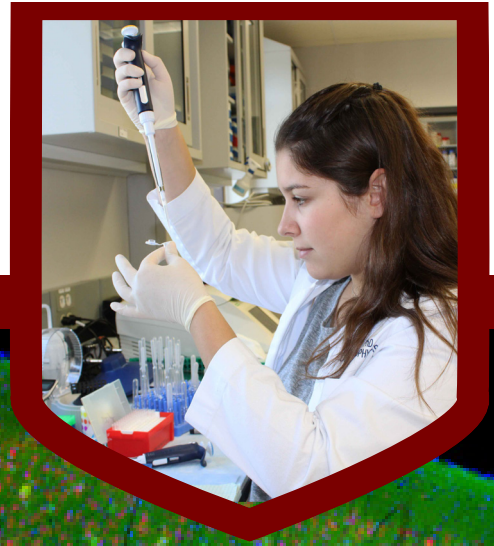


School of Neuroscience EngelNovitt Summer Research Program



The EngelNovitt Undergraduate Research Fellowship in Neuroscience program is a paid summer internship that gives students the opportunity to work within a neuroscience laboratory affiliated with the Virginia Tech School of Neuroscience. Students devote 40 hours per week immersed in a research environment assisting with an ongoing project. The program provides students with a real-world neuroscience research experience and bench skills that can help them as they progress in their research and/or medical careers.

This program was made possible by the generous support from the Washington, D.C.-based law firm EngelNovitt PLLC. EngelNovitt is led by John Engel, a longtime supporter of the Virginia Tech College of Science. The School of Neuroscience is grateful for providing our students with this life-changing opportunity.

Fellowship Recipients

Dallece Curley EngelNovitt Fellowship Recipient
Mentor: Dr. Stefanie Robel
Investigation of Astrocytic Reduction and Proliferation in Response to Mild TBI/Concussion

Alexa Figueroa Baiges EngelNovitt Fellowship Recipient
Mentor: Dr. Chris Thompson
The flavor and fragrance additive maltol appears to act as a thyroid hormone agonist

Matthew Hyland EngelNovitt Fellowship Recipient
Mentor: Dr. Sarah Clinton
The Effects of SSRI Exposure on the Domains of Depression-Like Behavior in Rats

Ian Levine EngelNovitt Fellowship Recipient
Mentor: Dr. Matt Buczynski
Validation of Locomotor Activity as a Model of Nicotine Exposure

Caroline McKenna EngelNovitt Fellowship Recipient
Mentor: Dr. Andrea Bertke
H3K9me3 and H3K27me3 on the Latent Herpes Simplex Virus 1 ICP27 promoter in Sensory and Autonomic Neurons

Madison O'Donnell EngelNovitt Fellowship Recipient
Mentor: Dr. Elizabeth Gilbert
Hypothalamic mechanisms of xenin-induced anorexia in Japanese quail

Amanda Patterson EngelNovitt Fellowship Recipient
Mentor: Dr. Georgia Hodes
Sex and the immune system: Understanding the relationship between stress and cytokines

Abigael Weit EngelNovitt Fellowship Recipient
Mentor: Dr. Michelle Olsen
Examination of GABA Transporter Expression Across Development

Dawn Wright EngelNovitt Fellowship Recipient
Mentor: Dr. Mike Bowers
AAV-Mediated Truncated FOXP2 Splice Variant Injections in Developing Rat Brain Alters Vocalization Complexity and Social Interactions

Sahil Laheri James and Lillian Gay Fellowship Recipient
Mentor: Dr. Blake Johnson
3D Bioprinted Gliovascular Units

Christopher Buenaventura James and Lillian Gay Fellowship Recipient
Mentor: Dr. Mark Cline
Differential anorexigenic mechanisms of substance P in alternative vertebrate models

Katherine Vlahcevic James and Lillian Gay Fellowship Recipient
Mentor: Dr. Martha Ann Bell
36 Month EEG Predicts Reading Achievement at Age Six through Executive Function

Kalirroi Engel School of Neuroscience Fellowship Recipient
Mentor: Dr. Bhanu Tewari
Extracellular Matrix Degradation Causes Reactive Astrogliosis

Emily Barritt School of Neuroscience Fellowship Recipient
Mentor: Dr. Ian Kimbrough
Dysfunctions of the Gliovascular Unit in Alzheimer Disease

Erica Johnson School of Neuroscience Fellowship Recipient
Mentor: Dr. Chris Thompson
Lead induces widespread toxic effects in the developing tadpole brain

Andrew Savoia School of Neuroscience Fellowship Recipient
Mentor: Dr. Susan Campbell
Sulfasalazine as a Treatment for Acquired Epilepsy

Noah Feld School of Neuroscience Fellowship Recipient
Mentor: Dr. Susan Campbell
Alterations in the Expression of Connexins in the Peritumoral Cortex of Pediatric and Adult Glioma Models

Brett Smith School of Neuroscience Fellowship Recipient
Mentor: Dr. Georgia Hodes
Characterizing stress induced sex differences in pre- and post-synaptic plasticity in the Hippocampus and Nucleus Accumbens

Investigation of Astrocytic Reduction and Proliferation in Response to Mild TBI/Concussion

Dallece E. Curley; Alex Winemiller; and Stefanie Robel, Ph.D
Virginia Tech Carilion Research Institute, Roanoke, Virginia

In the United States, a traumatic brain injury (TBI) occurs every 5 seconds, with 75% of these injuries being mild or concussive. Mild TBIs/Concussions can cause patients to suffer from long-term memory loss, concentration difficulties, and general cognitive deficits. Due to an absence of apparent lesions using various imaging modalities, the underlying cellular mechanisms of the progression of this disease have remained a mystery. Astrocytes, the most numerous glial cells in the brain, respond to brain injury with astrogliosis. This process aids in sealing off damaged from uninjured brain areas, but can come at the cost of housekeeping properties of astrocytes that ensure proper neuronal function. However, most research thus far has centered around more severe types of TBI with a clear site of injury, the experimental equivalent of gunshot wounds. Little is known, however, about the astrocytic response to mild TBI/Concussion. The specific aims of this study were to investigate possible astrocytic reduction/loss, as well as the proliferation response in sham (control) compared to mTBI (injured) mouse models.

Here, we used a mouse model of repeated mild TBI/Concussion to assess key features of astrogliosis, which includes astrocyte proliferation. Aldh111-eGFP//FVB/N mice, which label astrocytes with a transgenic green fluorescent protein, were injured using the Modified Marmarou weight drop injury model. Tissue was fixed and collected at several time points after injury, and then immunohistochemistry was performed using antibodies against GFP, Ki67, and BrdU. GFP and similar astrocyte markers were used to assess astrocyte reduction/loss, while Ki67 and BrdU stained acutely proliferating cells and cumulatively proliferating cells respectively. BrdU, a DNA analog that binds during replication, was administered to mice intraperitoneally twice daily until sacrificed, followed by a pretreatment that denatured DNA in order to allow antibody binding and visualization.

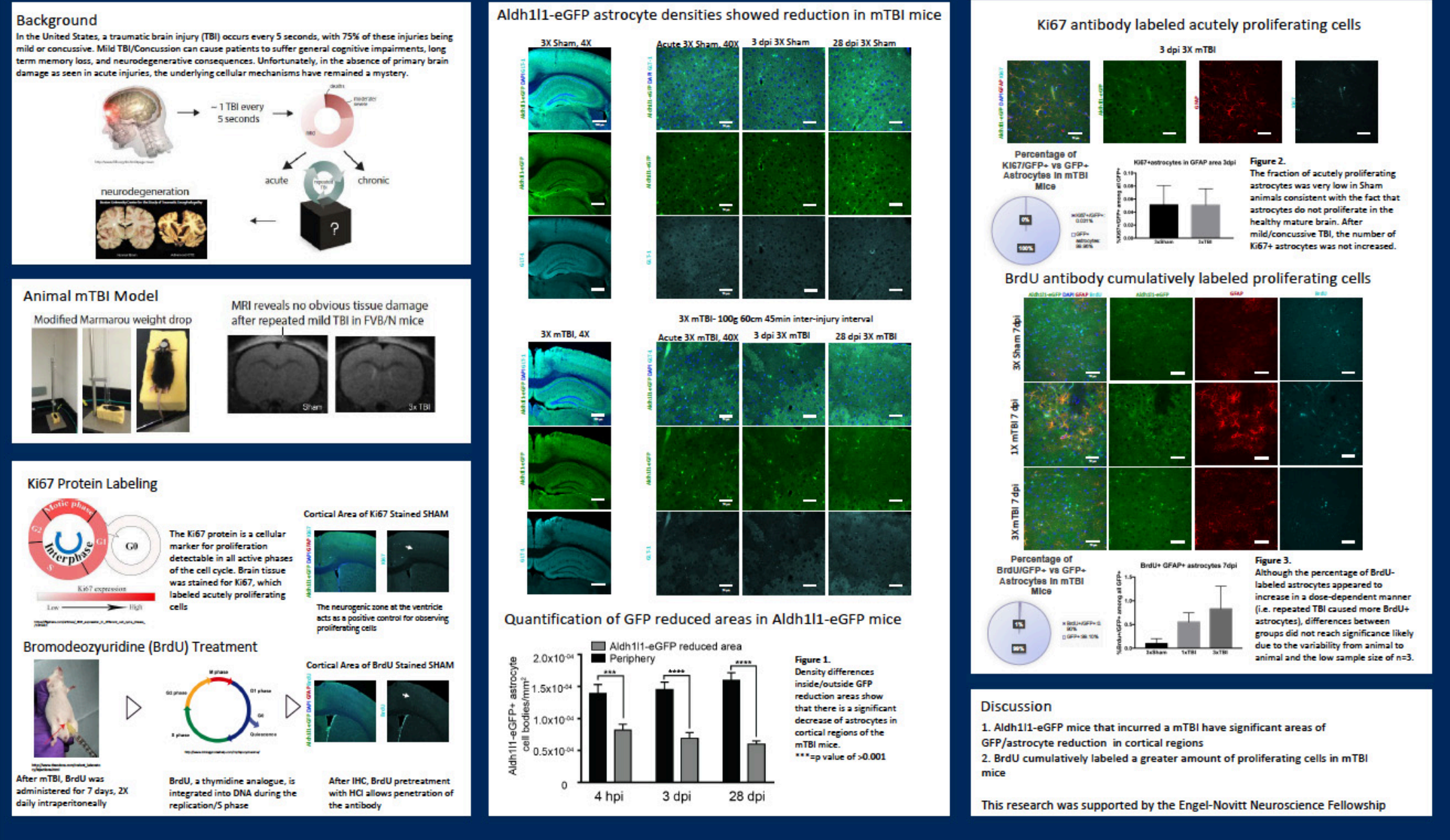
Quantification of astrocyte densities did not show areas



Investigation of Astrocytic Reduction and Proliferation in Response to Mild TBI/Concussion



Dallece E. Curley^{1,2}, Alex Winemiller¹, Stefanie Robel^{1,2}
¹Virginia Tech Carilion Research Institute, Roanoke, Virginia
²Virginia Tech School of Neuroscience, Blacksburg, Virginia



of complete loss of astrocytes in mTBI mice, however we did find uncharacteristic reduction of GFP-reporter and proteins crucial for normal astrocyte functioning in these areas ($p < 0.001$, $n=3$). Astrocyte proliferation acutely stained by Ki67 showed negligible proliferation in mTBI mice (0.031% ki67+/GFP+, $n=3$) compared to shams, so the cumulative BrdU stain was used as a

comparison. BrdU staining clearly indicated higher levels of proliferation in mTBI mice compared to shams, however differences did not reach significance due to variability and low sample size ($n=3$). The astrocytic reduction indicates that astrocytes respond very differently to repeated mild TBIs/Concussions than has previously been observed in other types

of TBI, and that astrocyte dysfunction might contribute to the pathobiology and progression of this disease.

The flavor and fragrance additive maltol appears to act as a thyroid hormone agonist

Alexa Figueroa Baiges, Matthew Emmanuel, Erica Johnson, Shaan Sharma, Christopher K. Thompson
School of Neuroscience, Virginia Tech, Blacksburg VA

Background: Thyroid hormone is essential for normal brain and physical growth in almost all vertebrate animals during development. In *Xenopus laevis* tadpoles, it is one of the most important components to drive them through metamorphosis. It has been shown, however, that many products concerning the agricultural and consumer industries as well as industrial products may disrupt thyroid hormone signaling. In the Tox21 dataset, a collaborative effort between the NIH, the EPA and the FDA, the organic compound maltol was found to be a thyroid hormone agonist at relatively high concentrations. Maltol is used as a flavor enhancer and as an additive to fragrances because of its natural sweet smell. Everyday foods such as cocoa and coffee contain maltol and it is one of the main ingredients in contributing to the odor of bread.

Methods: The current project assessed the effects of Maltol on the development of the visual system in *Xenopus laevis* tadpoles, which are greatly sensitive to changes in thyroid hormone signaling and are therefore useful models for better understanding thyroid hormone disruption. Their development occurs externally, allowing for easier observation and manipulation of brain and physical development. The effects of maltol were assessed using several experiments. Effects on body length were analyzed by measuring tadpoles in increasing doses of maltol and compared to T4 on days 0, 2, 4, and 7. Then effects of maltol in combination with T4 on these same days were assessed. In vivo imaging was also performed, in which tadpoles were imaged every 24 hours and differentiation of neural progenitor cells into neurons was quantified for 3 days. Finally, cell proliferation in the optic tectum, telencephalon and pretegmentum in control, maltol concentrations (100µM, 300µM, 600µM, and 1mM) and T4 groups was quantified and compared. Optic tectum morphology (width: length ratio) was also measured.

Results: Maltol seemed to have more synergistic than agonistic properties in the body length experiment, yet



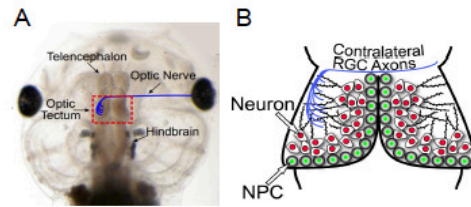
The flavor and fragrance additive maltol appears to act as a thyroid hormone agonist

Alexa Figueroa Baiges, Matthew Emmanuel, Erica Johnson, Shaan Sharma, Christopher K Thompson
School of Neuroscience, Virginia Tech, Blacksburg VA



INTRODUCTION

Thyroid hormone is essential for normal brain and physical growth in almost all vertebrate animals during development. In *Xenopus laevis* tadpoles, it is one of the most important components to drive them through metamorphosis. It has been shown, however, that many products concerning the agricultural and consumer industries as well as industrial products may disrupt thyroid hormone signaling. In the Tox21 dataset, a collaborative effort between the NIH, the EPA and the FDA, the organic compound maltol was found to be a thyroid hormone agonist at relatively high concentrations. Maltol is used as a flavor enhancer and as an additive to fragrances because of its natural sweet smell. Everyday foods such as cocoa and coffee contain maltol and it is one of the main ingredients in contributing to the odor of bread. The current project assessed the effects of Maltol on the development of the visual system in *Xenopus laevis* tadpoles, which are greatly sensitive to changes in thyroid hormone signaling and are therefore useful models for better understanding thyroid hormone disruption. Their development occurs externally, allowing for easier observation and manipulation of brain and physical development. The effects of maltol were assessed by implementing dose-responsive treatments and analyzing the effects on body length and cell proliferation changes in the optic tectum. In vivo imaging was also performed, in which the rates of differentiation of cells into neurons was evaluated. The results of this experiment suggest that maltol can affect thyroid hormone signaling.



A) Dorsal aspect of the head of a *Xenopus laevis* tadpole. B) A schematic diagram of the midbrain area in A illustrating the retino-tectal circuit. Neural progenitor cells (NPC, green) are found in the ventricular proliferative zone. Neurons (red) are generated from NPCs. They extend dendrites (black) into the neuropil where they form synapses with other tectal neurons and/or RGC axons (blue).

METHODS

Animals: *Xenopus laevis* albino tadpoles NF stage 46-47 (7-10 days old).

Hormone and disruptor treatment: Thyroxine (T₄) was dissolved in 50mM NaOH, then diluted in Steinberg's rearing solution to working strength concentration (19 nM). 0.1261g of Maltol was diluted in 50mL H₂O. The stock solution was then diluted into respective concentrations in 200mL of Steinberg's to make working strength of 100µM, 300µM, 600µM and 1mM. Groups of tadpoles were then kept in their corresponding solutions for up to seven days.

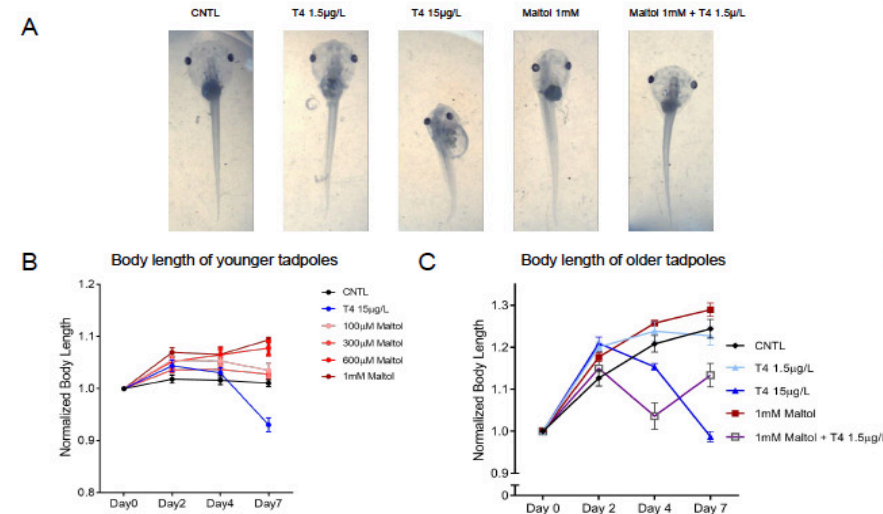
In Vivo Imaging: Tadpoles were kept alive and in their respective groups and imaged every 24 hours for 3 days using a Leica SP8 confocal microscope; images were analyzed using ImageJ. For body length, individual tadpoles were imaged every few days.

Sacrifice and tissue processing: Tadpoles were killed on Day 4 and Day 7, depending on the experiment, with an overdose of MS222 and fixed overnight in 4%PFA. Standard immunohistochemistry methods were used to stain whole-mount brains for CldU (Sigma, 1:500) and Sytox-O (Life Sciences, 1:500).

Imaging and analysis: PFA-fixed brains were imaged on an Leica SP8 confocal microscope, and images were analyzed with ImageJ.

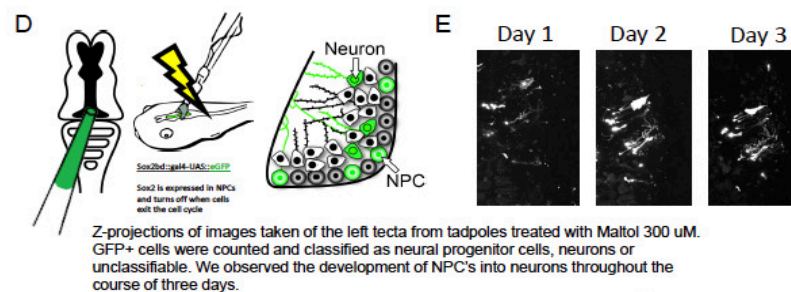
showed very similar results to the T4 group in the in vivo experiment. Brain morphology was also altered, and therefore width/length ratios in the optic tectum were measured in these same groups. Maltol also showed a dose-dependent increase in cell proliferation in the tectum, with the results of the highest concentration being comparable to those of the T4 group. As for brain morphology, the highest concentration of maltol (1mM)

Maltol treatment increased body length relative to CNTL Maltol+T4 decreased body length relative to CNTL

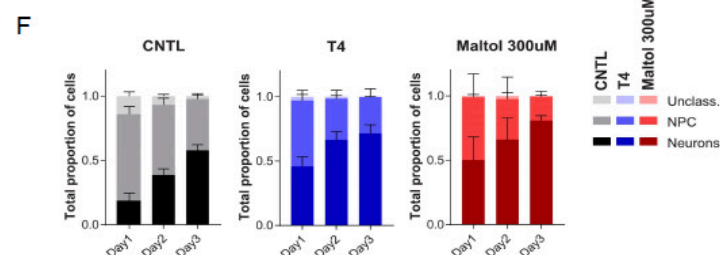


A) Images of example tadpoles from Day 7. Line graphs showing body lengths for tadpoles measured on Day 0, Day 2, Day 4, and Day 7 (B and C). The highest concentration of maltol (1mM, dark red) led to highest increase in body length on Day 7. The highest concentration of maltol plus T4 1.5µg/L caused the most decrease in body length, after the highest concentration of T4 (15µg/L).

Maltol increased differentiation of neural progenitor cells into neurons



Z-projections of images taken of the left tecta from tadpoles treated with Maltol 300µM. GFP+ cells were counted and classified as neural progenitor cells, neurons or unclassifiable. We observed the development of NPC's into neurons throughout the course of three days.

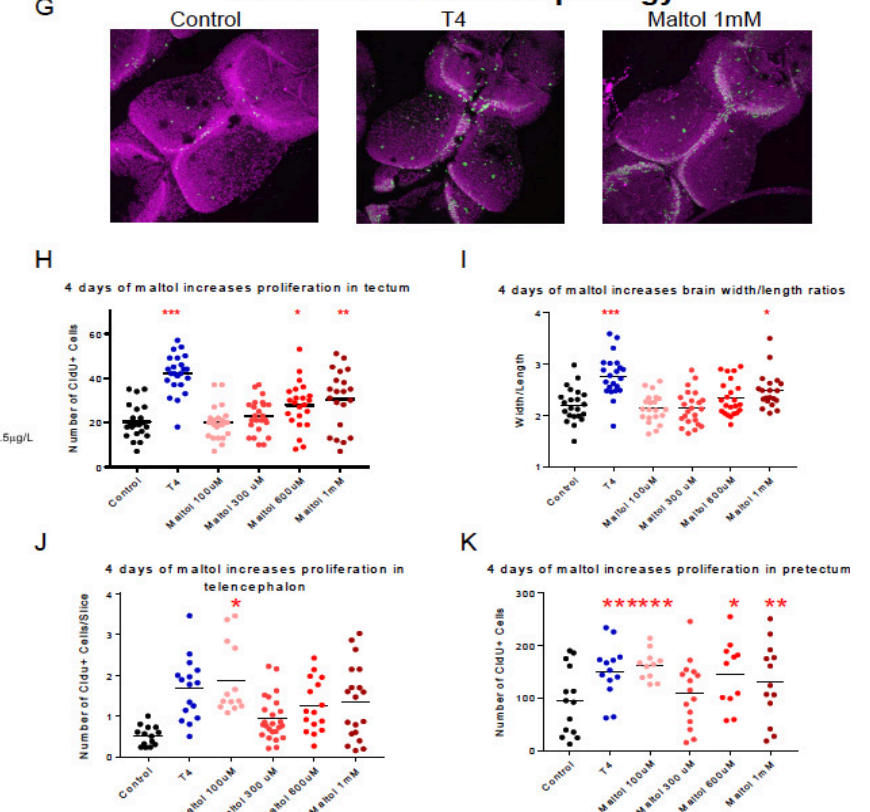


A) Z-projections of confocal stacks of example optic tecta from Day 1, Day 2 and Day 3. B) Maltol demonstrated a greater rate of differentiation of cells turned into neurons when compared to CNTL groups and T4 (15µL) groups.

showed a significant difference from the control, to levels close to those of the T4 group.

Conclusion: Our studies suggest that maltol agonizes thyroid hormone signaling and may impact thyroid hormone sensitive molecular and cellular mechanisms important for brain development. The body length data suggests that maltol may act synergistically with T4 in

Maltol treatment increased overall cell proliferation and altered brain morphology



G) Z-stack projections of indicated treatment groups. H, J and K) Scatter plots depicting effects of various concentrations of maltol on CldU+ cells in the areas of the tectum, telencephalon and pretegmentum. I) Maltol affected brain size in that it increased width/length ratios with increasing concentrations. * = p<0.05, ** = p<0.01, *** = p<0.001

CONCLUSIONS

- Maltol caused an overall increase of body length in a dose-dependent manner. Maltol+T4, however, caused an overall decrease in body length; this suggests that maltol acts synergistically with T4 to induce TH-signaling mechanisms, perhaps via a retinoic acid signaling mechanism.
- Maltol caused an increase in rate of differentiation of neural progenitor cells into neurons. As shown by Figure F, the total number of cells converted into neurons in Maltol 300µM groups was significantly larger than that of the CNTL group.
- Maltol induced TH-like changes in tectum morphology. Maltol also caused a higher number of Cldu+ cells to be expressed in the pretegmentum, telencephalon and tectum, albeit at levels that did not match T4 alone. This suggests that maltol agonizes TH-signaling and may impact TH-sensitive molecular and cellular mechanism important for brain development.

ACKNOWLEDGEMENTS

Many thanks to Dr. Christopher Thompson, Shaan Sharma, Zahabiya Hussain, Matt Emmanuel, Stacy Spitzer, and Erica Johnson for their assistance with this project and in the lab. This work is funded by NIEHS grant R00ES022952

The Effects of SSRI Treatment on Multiple Domains of Depression-Like Behavior in Rats

Matthew Hyland, Matthew Glover, Chelsea McCoy, Erin Kwon, and Sarah Clinton

School of Neuroscience, Virginia Tech, Blacksburg, VA

Background: In the United States, approximately 15 million adults are affected by major depressive disorder every year. This disorder is characterized by a number of symptoms, including depressed mood or loss of interest or pleasure in daily activities for more than two weeks. Selective serotonin reuptake inhibitors (SSRIs) have been the mainstay treatment for these symptoms for the past 25 years. SSRIs block the serotonin reuptake transporter of the presynaptic cell, thereby reducing reabsorption and transiently increasing synaptic serotonin levels. SSRIs are considered safe and generally cause fewer side effects than many other antidepressants. Although SSRIs effectively treat many depressed patients, there is still a limited understanding of the etiology of depression as well as limited understanding of the exact mechanisms whereby SSRIs exert their effects. To better understand how SSRIs affect emotional behaviors relevant to a multifaceted disorder like depression, the present project uses a well validated rodent model organism to examine the effects of SSRI treatment on three behavioral domains commonly affected in the illness: anhedonia, self-neglect, and social withdrawal.

The purpose of the present experiments was to assess new tests that may better measure depression-like behavior in rodents. Adult male Sprague-Dawley rats were treated with the SSRI citalopram dissolved in drinking water (10 mg/kg) or normal water (control condition). After two weeks of citalopram (or control) treatment, rats underwent three behavioral tests to evaluate the effects of SSRIs on three behavioral domains commonly associated with depression in humans – 1) anxiety; 2) anhedonia (loss of interest in pleasurable activities); and 3) self-care. The elevated plus maze (EPM) is a traditional test of rodent anxiety-like behavior. We established the female urine sniffing test in our laboratory to examine sexual motivation and reward-seeking behavior in the drug- and vehicle-treated male rats. Finally, we assessed self-care behavior using the ‘splash test’, a test where sub-

jects are spritzed with sticky sucrose solution and tested to determine the length of time to clean themselves.

In the present study we hypothesized that SSRI treatment would not affect anxiety-like measures in the EPM (in part based on previous reports in the literature). On the other hand, we predicted that male rats treated with citalopram would show improved depression like behaviors (i.e. greater self-care and reward-seeking behavior in the splash test and female urine sniffing tests, respectively).

Methods: For this experiment, we used 16 male Sprague-Dawley rats purchased from Charles River Laboratory (Kingston, NY). For 2.5 weeks, rats received the SSRI citalopram (10mg/kg/day) through their drinking water or normal drinking water as a control. The rats and their water bottles were weighed every Monday, Wednesday, and Friday in order to maintain a proper therapeutic concentration of citalopram. After the 2.5-week treatment period, animals began a behavioral test battery (with one test per day over a week period of time). These tests were intended to evaluate the effects of SSRI treatment on three broad behavioral domains: 1) anxiety; 2) self-neglect; 3) sexual motivation, and reward-seeking behavior. Behavioral testing was conducted under low lighting (15 lux) from the hours of 09:00-12:00. All trials are recorded using Ethovision computer software (Noldus, Leesburg, VA). The EPM consisted of a platform in the shape of a plus that was raised approximately 1 meter off the ground. Two opposite arms of the maze were open platforms and the other two were enclosed by walls (pictured in Fig. 1A below). The rats were placed in the middle of the arms and the time they spent in each type of arm (closed or open) or in the middle of the two was recorded. The splash test is a test in which rats are squirted with a 30% sucrose solution on the middle of their back. They are then allowed to roam around a test box for 15 minutes. The time that rats spend grooming themselves is then scored by a trained observer using computerized software (Observer, Noldus, Leesburg, VA). Finally, the female urine sniffing test (FUST) is a test in which rats are placed in a test box with a few pieces of clean bedding in one of the corners. The rats are allowed to roam for 5 minutes and then the bedding is removed and they are acclimated for 15 minutes. Bedding is then soaked in female urine and placed in the same corner of the box for 5 minutes; the time spent sniffing the different bedding is recorded. Data was analyzed using GraphPad 6 (Prism, La Jolla, CA). Unpaired t-tests and repeated measures ANOVA were used when appropriate; significance was defined as $p < 0.05$.

Results: We first sought to confirm former findings that SSRI treatment does not have a significant effect on anxiety-like behavior in the EPM. We found that there were no differences between SSRI treated rats ($n = 10$) and controls ($n = 6$) in the time spent in the open arms of the maze (Fig. 1B; $p > 0.05$), or how long it took them to begin exploring the open arms (Fig. 1C; $p > 0.05$).

Due to previous studies in which it has been found that SSRIs cause decreased depression-like behavior (most notably in a test called the Forced Swim Test), we sought to determine whether citalopram treatment would also reduce depression-like behavior in two new tests being developed in our laboratory – the splash test of self-care behavior and FUST to evaluate anhedonic behavior. In the FUST, we found no effect of SSRI treatment on time spent sniffing either type of bedding (Fig. 2C; $p > 0.05$), nor in the number of times they frequented the bedding (Fig. 2D; $p > 0.05$). However, we

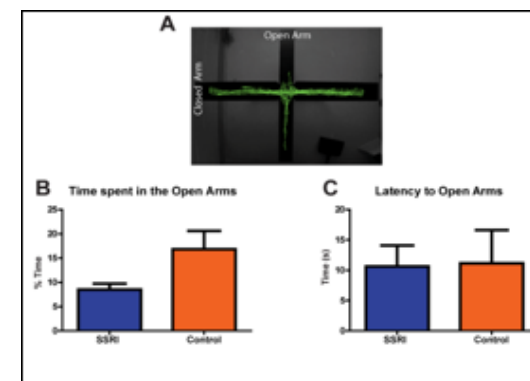


Figure 1: SSRI treatment did not affect anxiety-like behavior in the elevated plus maze (EPM). A representative image of the EPM, with exploration track marked by a green line (A). SSRI treated rats and vehicle-treated controls spent similar amounts of time in the open arms of the EPM (B), and showed similarly low latency to explore the open arms (C).

did find a difference in the time animals spent investigating the female urine-soaked bedding versus control/clean bedding, with males spending significantly more time sniffing the female-urine soaked bedding (main effect of the type of bedding, Fig. 2C; $p = 0.0004$). In the splash test, we found no significant difference between treatment groups in overall locomotor activity (distance they traveled in the test apparatus during the assessment; Fig. 3A; $p > 0.05$). There were also no group differences in latency to begin grooming (Fig. 3B; $p > 0.05$) or time spent grooming, although we did see a trend of SSRI-treated rats grooming more than controls (Fig. 3C; $p = 0.06$).

Conclusion: When we began our study, we hypothesized that SSRI treatment would not affect anxiety-like measures in the EPM, but that rats treated with citalopram would show improved depression-like behavior (such as greater self-care in the splash test and more reward-seeking behavior in the FUST). As expected, we found no group differences in overall locomotion or time spent in the open arms of the elevated plus maze. In the FUST – a test of anhedonia and sexual motivation – there were no effects of SSRI treatment on time sniffing female urine,

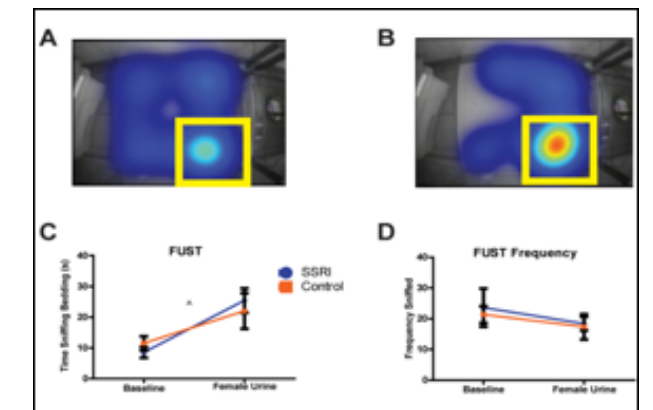


Figure 2: SSRI treatment did not affect male rats' exploration of female urine. The heatmaps show the amount of time the rats spent sniffing clean bedding (A) versus female urine (B) over the 5 minutes of recorded time. All male rats spent greater time sniffing the female urine compared to clean bedding (C), however, there were no significant differences between the two drug treatment groups. There were no group differences in the number of times the rats visited the corner of the box where the bedding was placed ($p > 0.05$) (D).

which was unexpected. We did, however, see a main effect of the type of bedding, with male rats spending more time sniffing female urine soaked bedding compared to clean bedding; this suggests that the main mechanisms of the test are working as expected. Although we did not see significant effects of SSRI treatment, there may be technical aspects of the current paradigm that influenced our results. For instance, some other studies using this test allow experimental rats to acclimate to the test box for 40 minutes instead of just 15 minutes (as we did in our experiment). Other studies using FUST suggest that the female rats providing urine should be in estrous (a time when they are most fertile/sexually receptive), since this could enhance male rats' sexual motivation and interest. Thus, future experiments will refine our FUST protocol to determine whether these procedural details affect the overall outcome of the study. In the Splash Test, we did

not find group differences between the SSRI treated and control rats (i.e., no differences in time spent grooming). This was also unexpected, although our data showed a non-significant trend of control rats grooming less than SSRI-treated rats. It may be useful to refine our procedure for this test. For instance, we may put the sucrose solution on the rats' upper neck as opposed to the middle of the back; this area moves more as a rat explores and might prompt more grooming. Furthermore, our sample sizes were somewhat small (n=10 per group), so we may have been underpowered to detect significant effects of SSRI treatment. Overall, this experiment helped us to make important first steps for establishing new depression-relevant behavior tests in our laboratory (i.e. the FUST and splash tests) and we will continue to refine our procedures to utilize these tests in future experiments.

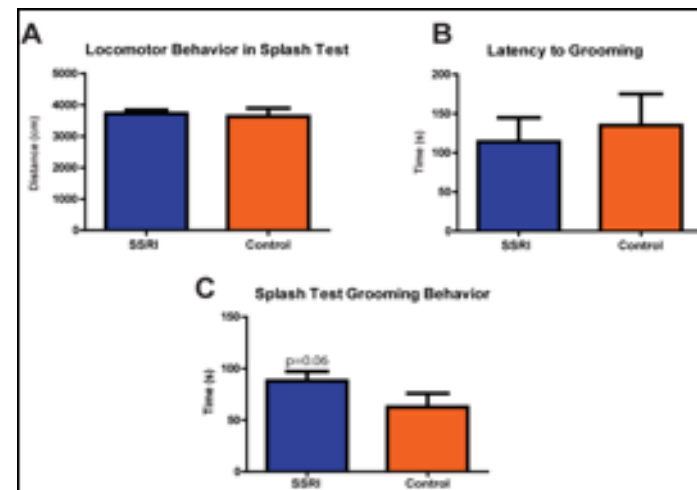



Figure 3: SSRI treatment did not significantly affect self-care behavior in the splash test. There was no group difference in overall activity (A) or in the latency to start grooming (B). There was no significant difference between treatment groups in the amount of time spent grooming, however there was a trend toward SSRI-treated rats grooming more ($p = 0.06$) (C).

Our results so far suggest that in rodents, SSRI treatment may be most effective in changing behavioral despair (as in the Forced Swim Test, which has been demonstrated in our lab and many others in previously published studies) and hedonic behavior (Sucrose Preference Test).



The Effects of SSRI Exposure on the Domains of Depression-Like Behavior in Rats

Matthew Hyland, Matthew Glover, Chelsea McCoy, Erin Kwon, and Sarah Clinton
Virginia Tech, School of Neuroscience

Introduction

In the United States, approximately 15 million adults are affected by major depressive disorder every year. This disorder is characterized by a depressed mood or loss of interest or pleasure in daily activities for more than two weeks. Selective serotonin reuptake inhibitors (SSRIs) have been the mainstay treatment for these symptoms for the past 25 years. SSRIs block the serotonin transporter of the presynaptic cell, reducing reabsorption and transiently increasing serotonin levels in the synapse. They are considered safe and generally cause fewer side effects than many other antidepressants.

Unfortunately, neither the etiology of depression, nor the full effects of SSRIs, are completely understood. To better understand the effects of SSRIs in the clinical setting, it is imperative to further elucidate the effects of SSRIs in this multifaceted disorder. To do so, a well validated model organism should be used to demonstrate the different domains of depression, including anhedonia, self-neglect, and social withdrawal.

The purpose of this experiment is to assess new tests which may better measure depression-like behavior in rodents. For this experiment, male Sprague-Dawley rats were treated with the SSRI citalopram or normal water (control). On postnatal day (P)75, they underwent three behavioral tests to evaluate the effects of SSRI treatment on these behavioral domains. The elevated plus maze (EPM) is a measure of anxiety-like behavior, the female urine sniffing is a measure of sexual motivation and reward-seeking behavior, and the splash test is measure self-care behavior.

We hypothesize that SSRI treatment will not affect anxiety-like measures in the EPM, but that rats treated with citalopram will show greater self-care and reward-seeking behavior. The results of this study will help determine whether these tests, in their current form, are suitable measures of these behavioral domains.

SSRIs had no Effect on Anxiety-Like Behavior

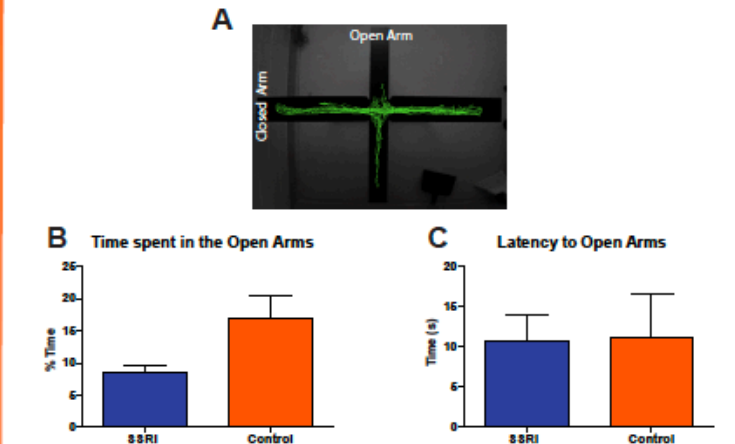


Figure 1: SSRI treatment does not affect anxiety-like behavior as measured by the elevated plus maze. (A) This is an image of the EPM tracking we used to obtain our data. (B) SSRI treated rats showed no significant difference in the percent of time they spent on open arms of the EPM. (C) nor in the time it took them to start exploring the open arms.

SSRIs did not Affect Self-Care Behavior

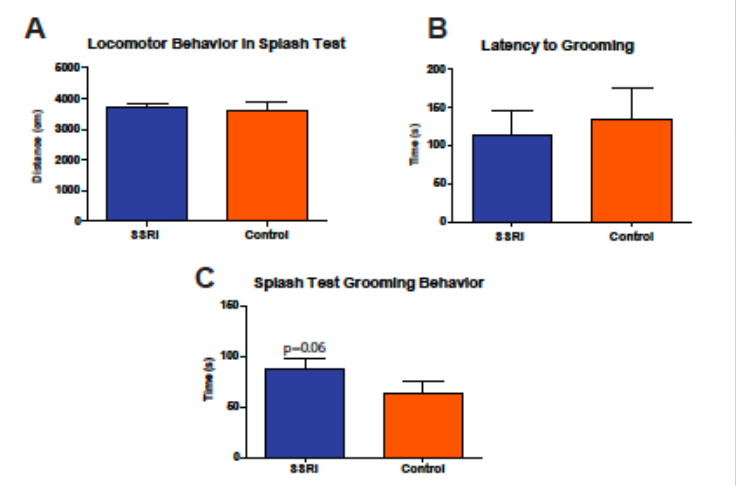


Figure 3: SSRI treatment did not significantly affect self-care behavior. (A) There was no significant difference between groups in the distance rats moved (B) or time before they started grooming. (C) There was no significant difference between treatment groups in the amount of time spent grooming, however there did seem to be a slight trend toward SSRI treated rats grooming more ($p = 0.06$).

Methods

For this experiment, we used 16 male Sprague-Dawley rats purchased from Charles River Laboratory (Kingston, NY). For 2.5 weeks, 10 of the rats received the SSRI citalopram through their drinking water and 6 received normal drinking water as a control. The rats and their water bottles were weighed every Monday, Wednesday, and Friday in order to maintain a proper therapeutic concentration of citalopram. After the 2.5 weeks, on postnatal day (P)75, the animals underwent three behavioral tests to evaluate the effects of SSRI treatment on these behavioral domains: anxiety, self-neglect, sexual motivation, and reward-seeking behavior.

The elevated plus maze (EPM) consists of a platform in the shape of a plus and is raised approximately 3 feet of the ground. Two opposite arms of the maze are simply open platforms and the other two are enclosed by walls. The rats are placed in the middle of the arms and the time they spend in each type of arm (closed or open) or in the middle of the two is recorded.

The splash test is a test in which rats are squirted with a 30% sucrose solution on the middle of their back. They are then allowed to roam around phenotypic boxes for 15 minutes. The time the rats spend grooming themselves is then measured.

The female urine sniffing test (FUST) is a test in which rats are placed in phenotypic boxes with a few pieces of clean bedding in one of the corners. The rats are allowed to roam for 5 minutes and then the bedding is removed and they are acclimated for 15 minutes. Then bedding soaked in female urine is placed in the same corner of the box for 5 minutes and the time spent sniffing the different bedding is recorded and compared between groups.

SSRIs caused no change in Sexual Motivation/Reward-Seeking Behavior

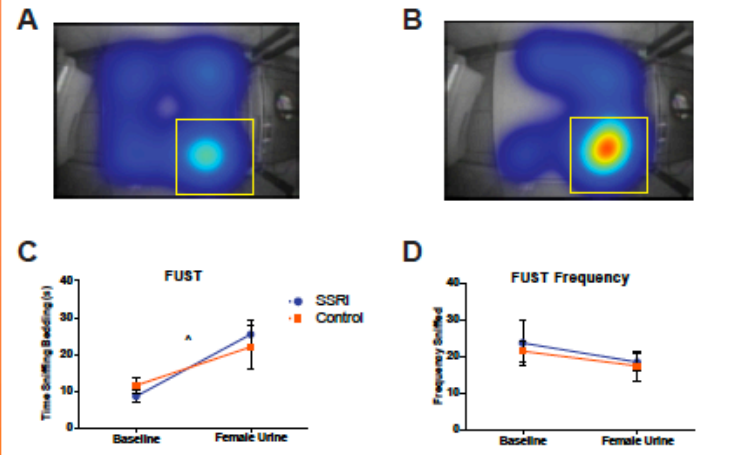


Figure 2: SSRI treatment did not seem to lead to a greater interest in female urine. (A-B) The heatmaps show the amount of time the rats spent in different places over the 5 minutes of recorded time. A is the clean bedding trial and B shows the urine trial. (C) The time spent sniffing the female urine was significantly greater than the time spent sniffing clean bedding ($p = 0.0004$), however, there were no significant differences between the two treatment groups. (D) There was no significant difference between treatment groups, nor between the different types of bedding, in the number of times the rats visited the corner of the box where the bedding was placed.

Conclusions/Future Directions

- We hypothesized that SSRI treatment would not affect anxiety-like measures in the EPM, but that rats treated with citalopram would show greater self-care and reward-seeking behavior.
- As expected, there were no significant differences in the locomotion or time spent in the open arms of the elevated plus maze.
- In the Splash test, there was not a significant difference between the SSRI treated rats and control rats in the time they spent grooming.
- To improve the splash test, we may put the sucrose solution on the rats' upper neck as opposed to the middle of the back. This area moves more as a rat explores and might prompt more grooming.
- In the FUST there was no significant difference between the treatments in amount of time sniffing urine.
- To improve FUST, literature suggest to allow the rats to acclimate to the box for 40 minutes instead of just 15 and that the female rats that the urine came from should be in estrous.
- We were underpowered for all of these tests, so having a greater sample size may lead to more significant differences in the data.
- This experiment has shown us that we can still rely on the EPM, and where we can improve the FUST and splash tests to acquire more accurate measurements of depression-like behavior in rats.
- Further tests will attempt to confirm the well-established effects of SSRI treatment on behavioral despair (Forced Swim Test) and hedonic behavior (Sucrose Preference Test).

Support and Funding

This work was supported by the EngleNovitt Undergraduate Research Fellowship and NIH R01MH105447-01 (SMC).

Validation of Locomotor Activity as a Model of Chronic Nicotine Exposure

Ian S. Levine, Sidharth S. Madhavan E. Reilly Scott¹, Ann M. Gregus,
Matthew W. Buczynski
School of Neuroscience and Department of Biochemistry
Virginia Polytechnic Institute and State University, Blacksburg,
VA 24060

Nicotine addiction is a complex disorder that results from drug-induced changes in brain signaling alter addiction-related behaviors including reward, dependence, and relapse. To uncover these drug-related molecular changes, we utilize mouse models of forced nicotine exposure to recapitulate components of addiction. Nicotine reward is difficult to model because it acts as both a stimulant and an anxiolytic. We aim to establish a mouse model of nicotine exposure because of the extensive amount of genetic and pharmacological tools available for this species. Specifically, we utilize the locomotor activity model to model reward behavior. Past studies have reported that assorted doses yield results of higher activity, lower activity, or increased activity over time. To measure the acute effects of nicotine, we measured locomotor activity (distance, m) before and after drug exposure. Each mouse is placed in a plexiglass cage (35 x 22 cm) under red light for 60 minutes before (habituation) and after (drug exposure) nicotine injection. Video of session is digitally captured and analyzed using AnyMaze software to determine distance traveled (m), immobility time (sec), and immobility episodes (n) for each mouse. Nicotine locomotor activity was analyzed at four doses (0.05, 0.2, 0.4, 1.0 mg/kg, s.c.) on the 1st and 5th session of drug exposure. Each nicotine group was compared with in-session vehicle control using the Student's T-test ($p < 0.05^*$, $p < 0.01^{**}$, $p < 0.001^{***}$). We concluded that nicotine (0.4 and 1 mg/kg) produce changes in locomotor activity in session one, and chronic exposure to all doses sensitized mice to the effects of nicotine so that it did not alter locomotor activity on day five. This project established a model for acute effects of nicotine.

Validation of Locomotor Activity as a Model of Nicotine Exposure



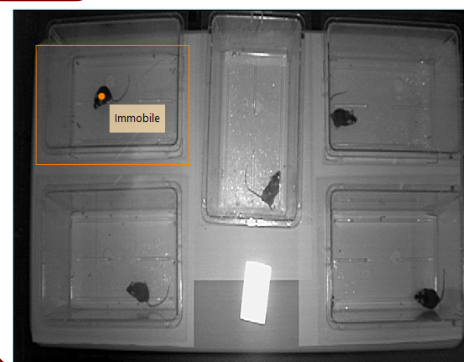
Ian S. Levine¹, E. Reilly Scott¹, Sidharth S. Madhavan¹,
Ann M. Gregus², Matthew W. Buczynski¹
¹School of Neuroscience and ²Department of Biochemistry
Virginia Polytechnic Institute and State University, Blacksburg, VA 24060



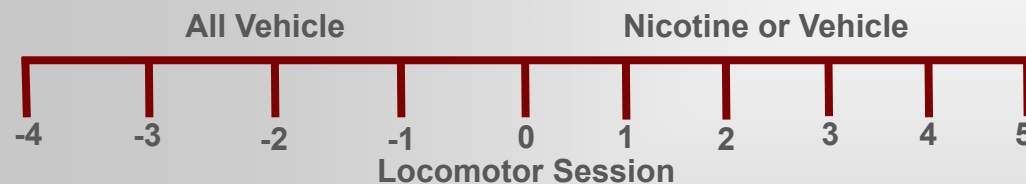
Background

Nicotine addiction is a complex disorder that results from drug-induced changes in brain signaling alter addiction-related behaviors including reward, dependence, and relapse. To uncover these drug-related molecular changes, we utilize mouse models of forced nicotine exposure to recapitulate components of addiction. Nicotine reward is difficult to model because it acts as both a stimulant and an anxiolytic. We aim to establish a mouse model of nicotine exposure because of the extensive amount of genetic and pharmacological tools available for this species. Specifically, we utilize the locomotor activity model to model reward behavior. Past studies have reported that assorted doses yield results of higher activity, lower activity, or increased activity over time.

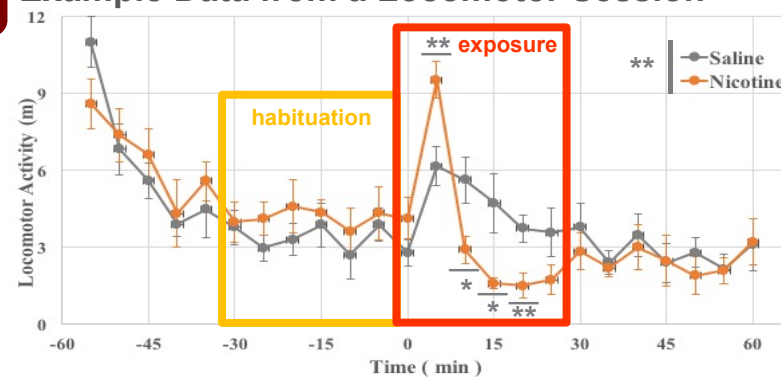
1 Model of Locomotor Activity Using AnyMaze Software



To measure the acute effects of nicotine, we measured locomotor activity (distance, m) before and after drug exposure. Each mouse is placed in a plexiglass cage (35 x 22 cm) under red light for 60 minutes before (habituation) and after (drug exposure) nicotine injection. Video of session is digitally captured and analyzed using AnyMaze software to determine distance traveled (m), immobility time (sec), and immobility episodes (n) for each mouse.

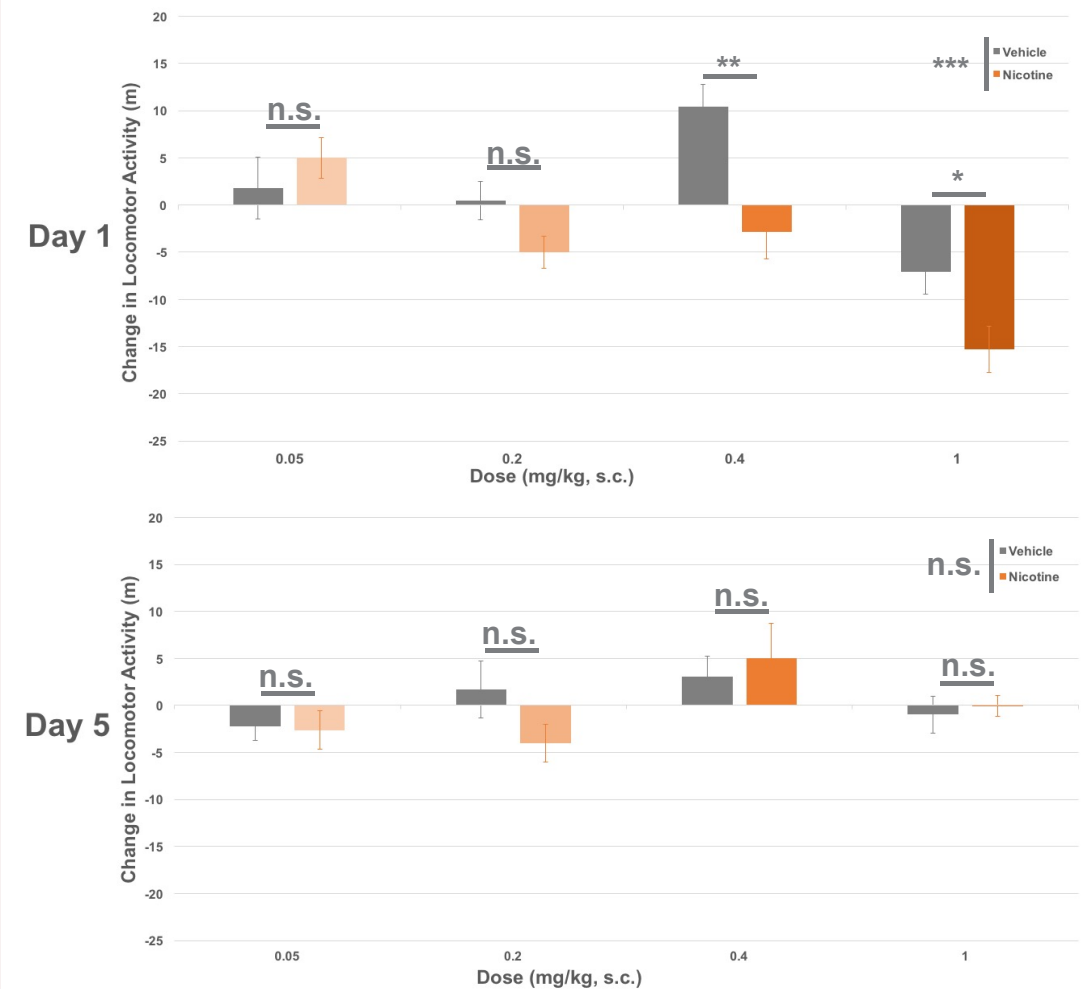


2 Example Data from a Locomotor Session



Mice were injected with either vehicle (saline) or nicotine (0.4 mg/kg, s.c.).

3 Acute Nicotine Reduces Locomotor Activity (Day 1) and Chronic Nicotine Exposure Causes Sensitization (Day 5)



Nicotine locomotor activity was analyzed at four doses (0.05-1 mg/kg, s.c.) on the 1st and 5th session of drug exposure. On Day 1, 2-way ANOVA identified an effect of Drug ($p < 0.001$), Dose ($p < 0.001$), and Drug x Dose Interaction ($p < 0.05$). Follow-up analysis of Drug was performed at each Dose by ANOVA. On Day 5, 2-way ANOVA showed no significant effect of Drug, Dose, or Drug x Dose Interaction. Significance indicated at $p < 0.05^*$, $p < 0.01^{**}$, and $p < 0.001^{***}$

Conclusions and Future Directions

- Multiple nicotine doses (0.4 and 1 mg/kg) produce changes in locomotor activity (Day 1)
- Multiple nicotine doses (0.4 and 1 mg/kg) sensitizes locomotor changes (Day 5)
- Future study to identify if doses of 0.4 and 1 mg/kg cause withdrawal (EPM, Open Field)

Support provided by NIH (MWB), Fralin SURF (SSM), and EngelNovitt Fellowship Program (ISL).

H3K9me3 and H3K27me3 on the Latent Herpes Simplex Virus 1 ICP27 promoter in Sensory and Autonomic Neurons

Caroline M. McKenna, Anna R. Cliffe, Andrea S. Bertke

Virginia Tech School of Neuroscience, University of Virginia School of Medicine,

Virginia-Maryland College of Veterinary Medicine

Blacksburg, VA; Charlottesville, VA

Background: Herpes Simplex Virus-1 (HSV-1) is a major human pathogen, causing disease in more than 75% of the US population. During primary infection, HSV-1 establishes latency in sensory and autonomic neurons, from which it can reactivate to cause recurrent skin or ocular lesions throughout life. Although a variety of stimuli are known to reactivate the virus, the specific mechanism of reactivation within the neurons is unknown. We recently showed that cellular stress can remodel viral chromatin during HSV-1 reactivation (Cliffe), but stress hormones induce reactivation selectively in autonomic neurons, rather than sensory neurons (Bertke). Therefore, *we hypothesized that different types of neurons maintain the latent HSV-1 genome in different chromatin conformations, allowing reactivation to occur more readily in autonomic neurons in response to stress.*

Virus: HSV-1 (strain 17+)

Mouse infections: 6 week old female Swiss Webster mice (Envigo) were infected ocularly with 10⁶ pfu HSV-1 in each eye and maintained for 28 days to allow the virus to establish latency. Sensory trigeminal (TG), sympathetic superior cervical (SCG) and parasympathetic ciliary ganglia (CG) were collected after euthanasia.

Chromatin immunoprecipitations (ChIP): ChIP assays were performed with antibodies against H3 (Abcam ab1791), H3K9me3 (Abcam ab8898), H3K27me3 (Millipore 07-449) and IgG control (Active Motif), followed by qPCR with primers/probe specific for the ICP27 promoter to quantify trimethyl deposition on histone H3 at the ICP27 promoter. Results: The results section is the most important part of the abstract and nothing should compromise its range and quality. The results section should be the longest part of the abstract and should contain as much detail about the findings as the journal word count permits. Major findings include but are not limited to key quantitative H3K9me3 is associated with constitutively silenced chromatin while H3K27me3 is associated and/or qualitative results or identified trends.

Conclusions: H3K9me3 is associated with constitutively silenced chromatin while H3K27me3 is associated with facultatively silenced chromatin, which is thought to be more reversible. The ICP27 promoter lacks H3K9me3 in ciliary ganglia, suggesting that the HSV-1 genome is not as strongly silenced in these neu-

rons. Although H3K9me3 can be remodeled during reactivation, its presence in sensory and sympathetic neurons can be a barrier to reactivation, while its absence in parasympathetic neurons could allow HSV-1 to reactivate more easily in response to reactivation stimuli.

H3K9me3 and H3K27me3 on the Latent Herpes Simplex Virus 1 ICP27 promoter in Sensory and Autonomic Neurons

Caroline M. McKenna¹, Anna R. Cliffe², Andrea S. Bertke³

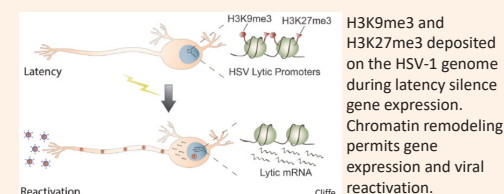
¹Virginia Tech School of Neuroscience, ²University of Virginia School of Medicine,

³Virginia-Maryland College of Veterinary Medicine



Background

Herpes Simplex Virus-1 (HSV-1) is a major human pathogen, causing disease in more than 75% of the US population. During primary infection, HSV-1 establishes latency in sensory and autonomic neurons, from which it can reactivate to cause recurrent skin or ocular lesions throughout life. Although a variety of stimuli are known to reactivate the virus, the specific mechanism of reactivation within the neurons is unknown. We recently showed that cellular stress can remodel viral chromatin during HSV-1 reactivation (Cliffe), but stress hormones induce reactivation selectively in autonomic neurons, rather than sensory neurons (Bertke). Therefore, **we hypothesized that different types of neurons maintain the latent HSV-1 genome in different chromatin conformations, allowing reactivation to occur more readily in autonomic neurons in response to stress.**



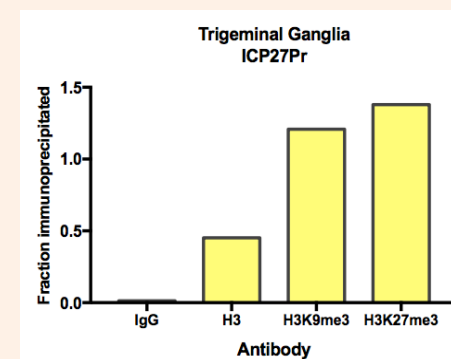
Materials and Methods

Virus: HSV-1 (strain 17+)

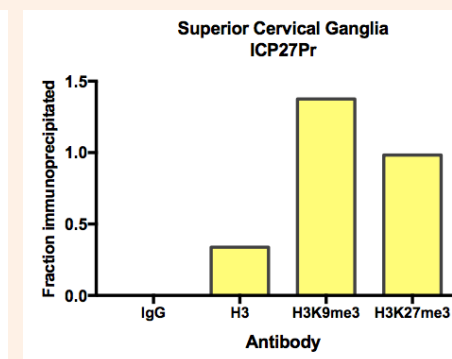
Mouse infections: 6 week old female Swiss Webster mice (Envigo) were infected ocularly with 10⁶ pfu HSV-1 in each eye and maintained for 28 days to allow the virus to establish latency. Sensory trigeminal (TG), sympathetic superior cervical (SCG) and parasympathetic ciliary ganglia (CG) were collected after euthanasia.

Chromatin immunoprecipitations (ChIP): ChIP assays were performed with antibodies against H3 (Abcam ab1791), H3K9me3 (Abcam ab8898), H3K27me3 (Millipore 07-449) and IgG control (Active Motif), followed by qPCR with primers/probe specific for the ICP27 promoter to quantify trimethyl deposition on histone H3 at the ICP27 promoter.

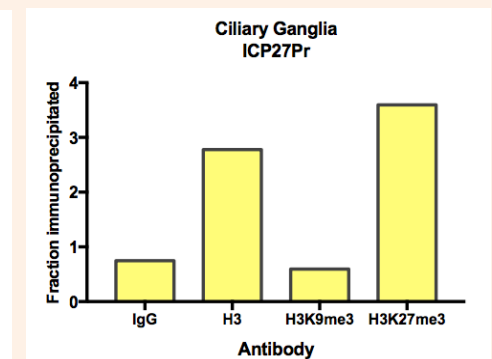
Results



In sensory trigeminal ganglia, silenced chromatin marks H3K9me3 and H3K27me3 were detected on the ICP27 promoter of the HSV-1 viral genome during latency.



In sympathetic superior cervical ganglia, H3K9me3 and H3K27me3 were also detected on the ICP27 promoter during latency.



In parasympathetic ciliary ganglia, the presence of H3K9me3 was very low, compared to the presence H3K27me3, at the ICP27 promoter.

Discussion

- H3K9me3 is associated with constitutively silenced chromatin
- H3K27me3 is associated with facultatively silenced chromatin, which is thought to be more reversible
- The ICP27 promoter lacks H3K9me3 in ciliary ganglia, suggesting that the HSV-1 genome is not as strongly silenced in these neurons
- Although H3K9me3 can be remodeled during reactivation, its presence in sensory and sympathetic neurons can be a barrier to reactivation, while its absence in parasympathetic neurons could allow HSV-1 to reactivate more easily in response to reactivation stimuli

Future Directions

- Additional repetitions to enable statistical analyses of the data
- Additional qPCR studies to quantify H3K9me3 and H3K27me3 on other HSV-1 promoters, such as ICP0, ICP4, and VP16, which are important in the reactivation process
- Additional ChIP assays to identify chromatin marks associated with active open chromatin (H3K4me2/3)
- Comparisons of chromatin composition of HSV-1 and HSV-2 in sensory and autonomic neurons, since HSV-2 reactivates more frequently than HSV-1

Acknowledgments

This project was supported by the Engel Novitt undergraduate research fellowship and the VT-UVA Collaborative Neuroscience Seed Grant. Special thanks to Angela Ives and Rebecca Powell-Doherty for their assistance in the lab.

Hypothalamic mechanisms of xenin-induced anorexia in Japanese quail

Madison O'Donnell, Mark A. Cline and Elizabeth R. Gilbert
Neuroendocrinology Laboratory, Virginia Polytechnic Institute and State University, Blacksburg, VA

Background: Xenin is a 25-residue amino acid peptide that was detected in the gastrointestinal tract of humans, Rhesus monkeys and dogs. Xenin has been isolated from the hypothalamus near satiety centers. It is best known as a factor that controls appetite. More specifically it has been demonstrated to act as an anorexigenic factor, meaning that it decreases food intake. When xenin was centrally injected into rats, food intake was decreased. The lab in which the research was conducted previously studied the effect of xenin in broiler chickens. It was found that when xenin was injected into the Ventromedial hypothalamus, food intake was decreased and the Quantity amount of c-Fos immunoreactive cells was increased, indicating activity within the nuclei. It was this finding that led the lab to study the effects of xenin within a different avian species. Japanese quail were studied due to their more wild-type behavior. The Cob 500 broiler chickens that were previously studied have been selected to develop rapid muscle growth, not representing an accurate depiction of appetite. Therefore, quail were studied in order to test xenin in a more natural host. Since it was known that xenin decreases food intake, we sought to elucidate the molecular mechanisms by which xenin mediates its anorectic effect on appetite.

Methods and Results: In Experiment 1, 7 day-old quail were centrally (intracerebroventricularly; into the left lateral ventricle) injected with 0 (vehicle; artificial cerebrospinal fluid), 0.25, 0.5 or 1.0 nmol xenin and food and water intake were measured for 180 minutes. On a cumulative basis, quail that received 0.5 nmol xenin reduced food intake for 120 minutes. Water intake was not affected in any experiments. Experiment 2 measured the behavior of the quail to ensure that the neuropeptide did not have any competitive behaviors adverse side effects.

Results yielded that exploratory pecks increased, as well as jumps. This data suggest that in fact the neuropeptide did not cause distress to the birds. In Experiment 3, the whole hypothalamus was isolated from xenin injected chicks at 1 hour post-injection. Next, total RNA isolation was performed and real time PCR performed to measure mRNA abundance of several appetite-associated factors. Quail injected with xenin expressed an increase in the opioid receptor delta, and neuropeptide Y (NPY) mRNA expression level. Experiment 4 examined appetite-associated nuclei within the hypothalamus, these being the Ventromedial hypothalamus (VMH), Lateral hypothalamus (LH), Paraventricular nucleus (PVN), and Arcuate nucleus(ARC). Upon performing c-Fos immunohistochemistry, results displayed activa-

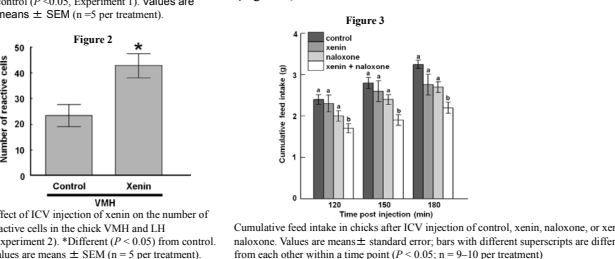
This research was supported by the EngelNovitt Fellowship.

Abstract

Xenin, a 25 amino acid peptide first isolated from the gastric mucosa, reduces food intake in birds and mammals. The objective of this experiment was to determine the effects of xenin on food and water intake, behavior, and hypothalamic c-Fos immunoreactivity and appetite-associated mRNA in Japanese quail (*Coturnix japonica*). At 7 days post hatch, quail fasted for 3 hours were intracerebroventricularly (ICV) injected with 0, 0.25, 0.5, or 1 nmol of xenin and food and water intake were recorded every 30 minutes for 180 minutes. In experiment 2, chicks injected with 0.5 nmol of xenin were monitored for 30 minutes in an arena where various appetite-associated behaviors were measured. In experiment 3, chicks were injected with 0.5 nmol of xenin and the hypothalamus was collected to measure appetite-associated factor mRNA. In experiments 4 and 5, chicks were injected with 0.25 nmol xenin and hypothalamic nuclei were collected at 1 h to determine c-Fos immunoreactivity and the abundance of certain mRNAs, respectively. Food intake was reduced at 30 minutes up to 120 min in quail injected with 0.5 nmol xenin. Water intake was not affected by treatment. Feeding pecks, exploratory pecks and deep rest were increased by xenin between 10 and 30 min post-injection. There were more c-Fos immunoreactive cells in the arcuate nucleus (ARC), ventromedial hypothalamus (VMH), and paraventricular nucleus (PVN) of xenin- than vehicle-treated chicks at 1 h post-injection. In the whole hypothalamus, neuropeptide Y (NPY) and delta opioid receptor mRNA were increased at 1 h post-injection in response to xenin treatment. In the PVN, corticotropin-releasing factor receptor subtype 2 (CRFR2) and urotensin 2 (UTS2) mRNAs increased in response to xenin, while in the ARC, expression of agouti-related peptide (AgRP) was increased in xenin-treated quail relative to vehicle-injected birds. Results suggest that CRF receptor signaling in the PVN is involved in mediating xenin's effects. The increase in NPY and AgRP gene expression might reflect a compensatory response to restore homeostatic food intake. Because of xenin's appetite suppressant effects, it could be explored as a pathway to target for developing therapies for eating disorders.

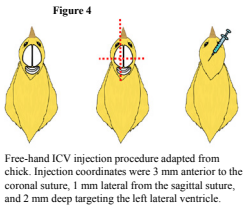
Background on Xenin

- A 25-residue peptide that was detected in the gastrointestinal tract of humans, Rhesus monkeys and dogs (Hanscher et al., 1995).
- Isolated from the hypothalamus near satiety centers (Hanscher et al., 1995).
- Decreased food intake when centrally injected into rats (Alexiou et al., 1998).
- Decreased food intake (Figure 1) and the number of feed pecks between 15 and 30 minutes post-injection (Nandar et al., 2008)
- Increased c-Fos in the VMH (Figure 2)
- Low-dose-induced anorexia is countered by endogenous opioids (Figure 3)



Experimental Design

- Experiment 1**
 - 7 day old
 - ICV injected with 0, 0.25, 0.5, and 1 nmol xenin
 - Food and water intake measured in 30 minute intervals for 180 minutes
- Experiment 2**
 - 6 day old
 - ICV injected 0 or 0.5 nmol xenin
 - Comprehensive behavior analysis for 30 minutes
- Experiment 3**
 - 7 day old
 - ICV injected with 0 or 0.5 nmol xenin
 - Collected whole hypothalamus at 1 hour
 - Total RNA isolation and real time PCR
- Experiment 4**
 - 7 day old
 - ICV injected with 0 or 0.25 nmol xenin
 - Hypothalamic c-Fos immunohistochemistry at 1 hour
- Experiment 5**
 - 8 days old; ICV injected with 0 or 0.25 nmol xenin
 - Hypothalamic nucleus punch biopsy at 1 hour; arcuate nucleus, ventromedial hypothalamus, lateral hypothalamus, dorsomedial nucleus, paraventricular nucleus
 - Total RNA isolation and real time PCR

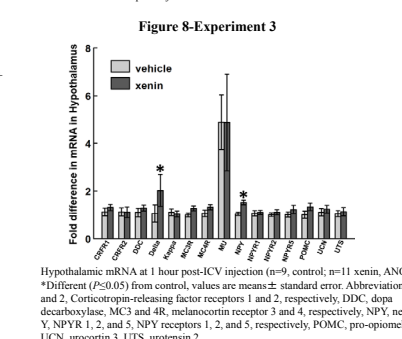
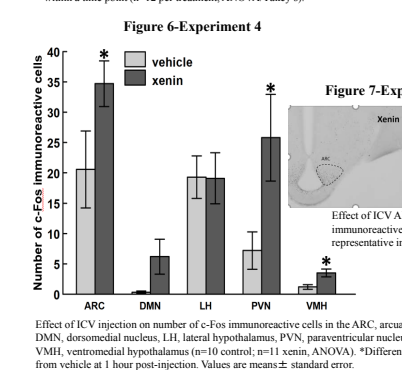
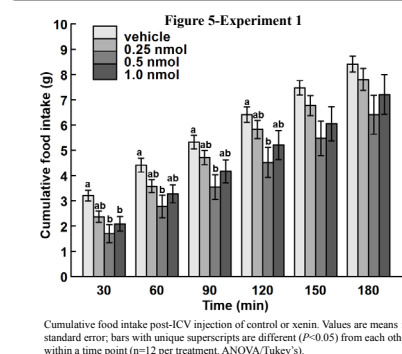


Hypothalamic mechanisms of xenin-induced anorexia in Japanese quail

Madison L. O'Donnell, Mark A. Cline, and Elizabeth R. Gilbert
Neuroendocrinology Laboratory, Virginia Tech, Blacksburg, Virginia 24061

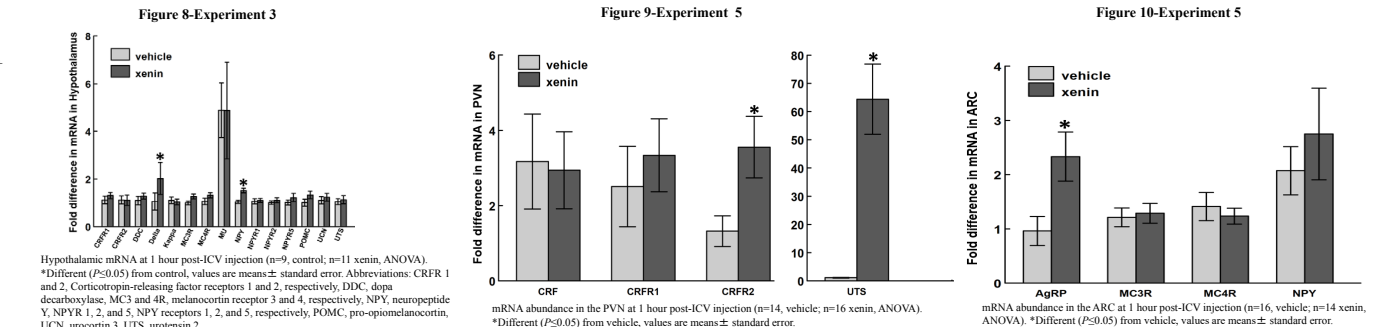


Results



Behavior		5	10	15	20	25	30
Locomotion	Control	3.91±0.92	9.44±1.79	14.75±2.84	19.15±3.16	23.68±3.98	28.88±4.83
	Xenin	3.25±0.99	8.13±2.23	13.72±3.18	20.55±4.47	25.68±5.81	29.31±6.91
Feed pecks	Control	11.36±11.26	48.45±33.88	106.54±51.17	151.54±55.64	227.18±70.07	1053.70±80.91
	Xenin	5.09±4.89	17.18±16.98	46.90±18.62	69.27±55.64	570.90±58.10*	292.36±88.46
Steps	Control	147.90±34.24	369.45±59.52	578.09±88.69	771.81±97.61	939.54±128.51	1,173.18±168.9
	Xenin	119.81±30.85	308.81±66.40	528.09±105.89	785.45±154.43	970.27±194.88	1,096.64±44.4
Jumps	Control	0.09±0.09	0.36±0.27	0.81±0.32	1.0±0.35	1.18±0.35	1.45±0.45
	Xenin	0	0.09±0.09	0.27±0.14	0.54±0.36	0.63±0.45	0.63±0.45*
Defecations	Control	0	0	0	0	0	0
	Xenin	0	0	0	0	0	0
Exploratory pecks	Control	48.54±12.64	147.81±28.64	331.54±35.91	304.18±45.92	361.27±63.09	414.81±77.56
	Xenin	26.63±9.71	64.45±18.47*	126.0±29.27*	171.18±39.19*	215.09±40.73*	244.54±48.96*

Behavior	Treatment	5	10	15	20	25	30
Perch	Control	3.02±2.73	10.71±7.15	17.70±8.32	17.84±8.37	28.45±10.79	36.22±15.11
	Xenin	0	0.07±0.07	4.01±3.93*	8.03±7.57	17.06±12.50	34.22±19.66
Preen	Control	0.81±0.57	1.10±0.70	1.40±0.84	1.65±0.95	2.30±0.99	2.94±0.97
	Xenin	0	1.52±1.27	9.37±6.21	11.48±6.28	17.55±7.73	19.87±8.29
Rest	Control	2.97±2.97	4.27±4.27	4.72±4.72	26.50±21.82	40.16±35.27	40.16±35.27
	Xenin	30.60±26.41	62.89±52.84*	63.06±52.83*	65.99±54.60	76.56±58.56*	111.32±73.34*
Stand	Control	287.16±3.69	576.89±7.61	863.99±10.51	1137.66±33.19	1390.15±50.42	1663.09±62.43
	Xenin	262.96±26.67	523.12±53.02	782.38±78.83	1046.82±105.28	1296.26±118.21	1511.01±137.72
Sit	Control	0.20±0.20	0.60±0.42	4.71±3.52	8.40±6.86	30.06±17.26	35.40±17.40
	Xenin	0.39±0.39	5.16±3.31	33.25±27.34	58.81±52.53	80.60±62.36	106.56±68.78



Discussion

- Xenin had anorexigenic effects in quail, similar to those reported in other species
- Compared to the chick, the quail responded earlier to the same doses suggesting that they have a lower threshold in the sensitivity to the response to xenin
- Xenin had no effect on water intake in quail or chicken
- Deep rest and perch time were increased in response to xenin. It remains to be determined whether this indicates that the anorexigenic effect of xenin is due to malaise
- The VMH, ARC, and PVN were activated in response to xenin. As these are key appetite regulatory nuclei, these data suggest that these are the sites of action for xenin's effects on appetite
- Gene expression data suggest that CRF receptor signaling in the PVN is involved in mediating xenin's effects
- Differences between whole hypothalamus and nuclei suggest that the whole hypothalamus might mask differences at the nucleus level
- Increases in NPY and AgRP gene expression might reflect a compensatory response to restore homeostatic food intake
- The objective of our next experiment is to determine the effect of blocking CRF receptor signaling on xenin-induced anorexia
- Because of xenin's appetite suppressant effects, it could be explored as a pathway to target eating disorders



Conclusions: Central injection of xenin has been known to decrease food intake in rodent and avian species. However, until the current study, the molecular mechanisms by which xenin mediates its effects were poorly understood. Upon completing this study, a proposed pathway was identified due to the increased expression of CRFR2 and UTS 2. The potent anorectic factor UTS 2 binds to CRFR2, indicating that this interaction within the PVN may be the central mechanism exerting xenin's anorexigenic effect within the quail model.

Sex and the immune system: Understanding the relationship between stress and cytokines

Amanda Patterson, Brett Smith, Jennifer Rainville, Georgia E. Hodes
Department of Neuroscience, Virginia Tech, Blacksburg, VA

Men and women display different symptomatology during depression (Martin, Neighbors, & Griffith, 2013), but in pre-clinical trials attempting to find biomarkers or new treatments, females continue to be marginalized (Prendergast, Onishi, & Zucker, 2014). Depression-like behavior of mice is quantifiable and can be used to distinguish differences in the stress response between sexes (Hodes et al., 2015; Laplant et al., 2010). This summer my project, under Dr. Georgia Hodes' leadership, was focused on correlating stress susceptibility behavior in mice with their individual cytokine profiles. Here we focus on the underlying peripheral biological influences to these behavioral differences, specifically cytokine types and quantities. Cytokines are signaling proteins secreted by cells of the immune system that allow communication with a number of different types of cells throughout the brain and body. The presence of cytokines can indicate an abundance of cellular activity, and with 80 classified cytokines, each cytokine may reveal specificities of cellular interactions (Cannon, 2000). This project was important because it provides preliminary data on sex differences regarding immune response to stress that may develop into depression-like behavior. Our hypothesis for this experiment was the males and females regulated different immune pathways in response to stress. Furthermore, we propose that the mice's immune response will correlate with their individual stress susceptibility behavior.

C57BL/6J mice (n = 40, n = 10 mice/group/sex; The Jackson Laboratory) at 8 weeks of age were assigned a condition of either control or stress after acclimation to the facility. To induce the neurological state of depression-like symptomatology, the stressed mice underwent three stressors; foot shock, tail suspension, and restraint tube. Each stressor was an hour per day in the experiment's timeline. After the last stressor, a submandibular bleed was taken to collect a blood sample from each stressed mouse. The blood sample contained cytokines secreted due to the stressors that could be correlated with the subsequent behavior of the individual. The next day we began behavioral testing. There were three behavioral tests administered one per day in the following order. For the splash test, the mice were sprayed with a 10%

sucrose solution 3 times onto the fur of their backs. They were then placed in a novel cage with no bedding and grooming behavior was digitally recorded for a 5-minute period for subsequent analysis. Following the initiation of back grooming, we recorded all cumulative grooming over a 5-minute period with a stopwatch. Both latency

and total time of grooming were noted. The next behavioral test was novelty suppressed feeding. The stressed mice were put on food restriction over night as motivation to eat during the behavioral test. A single mouse would be placed in a novel arena with a single piece of kibble was placed in the center of the arena. The mouse



Sex and the immune system: Understanding the relationship between stress and cytokines

Amanda Patterson, Brett Smith, Jennifer Rainville, Georgia E. Hodes
Department of Neuroscience, Virginia Tech



Introduction

Men and women display different symptomatology during depression (Martin, Neighbors, & Griffith, 2013), but in pre-clinical trials attempting to find biomarkers or new treatments, females continue to be marginalized (Prendergast, Onishi, & Zucker, 2014). Depression-like behavior of mice is quantifiable and can be used to distinguish differences in the stress response between sexes (Hodes et al., 2015; Laplant et al., 2010). Previous studies determined that female mice experiencing 6-day variable stress are more stress susceptible than males. Here we focus on the underlying peripheral biological influences to these behavioral differences, specifically cytokine types and quantities. Cytokines are signaling proteins secreted by cells of the immune system that allow communication with a number of different types of cells throughout the brain and body. The presence of cytokines can indicate an abundance of cellular activity, and with 80 classified cytokines, each cytokine may reveal specificities of cellular interactions (Cannon, 2000).

Hypothesis: Different immune pathways are regulated by stress in males and females. Additionally, we propose that immune response will correlate with stress susceptible behavior. Therefore we examined the behavior of male and female mice exposed to 6 days of variable stress. Behavior was analyzed across a test battery including splash test, forced swim test, and novelty suppressed feeding test.

Methods

Mice: C57BL/6J mice (n = 40, n = 10 mice/group/sex; The Jackson Laboratory) at 8 weeks of age were assigned a condition of either control or stress after acclimation to the facility. Mice were group housed 5 to a cage until behavioral testing, maintained on a 12 hour light/dark cycle. Mice were given *ad-libitum* access to water and food during stress exposure. Stressed male and females were subjected to subchronic variable stress (SCVS) over 6 days. Stressors used were foot shock (0.45 mA/2 second duration/100 shocks at random for 1 hour), tail suspension (1 hour total), and restraint tube (1 hour total). During the 6-day term, the stressed mice would experience each stressor twice in a repeated order of foot shock, tail suspension, restraint tubes. In preparation of the behavioral tests, all control and stress mice were single housed to trace individual performance. All mice had a tail marker to track and obtain specific data to the individual mouse.

Splash Test: Testing was performed under red light to reduce anxiety. The mice were sprayed with a 10% sucrose solution 3 times onto the fur of their backs. They were then placed in a novel cage with no bedding and grooming behavior was digitally recorded for a 5-minute period for subsequent analysis. Following the initiation of back grooming, we recorded all cumulative grooming over a 5-minute period with a stopwatch. Both latency and total time of grooming were noted.

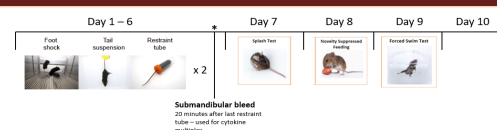
Novelty Suppressed Feeding Test (NSF): All mice were put on food restriction over night as motivation to eat during the behavioral test. The test was performed under red light conditions to reduce anxiety. An arena (50 cm x 50 cm x 50 cm) with the same bedding material (1/8 inch cob bedding) as the single home cages was prepared for the novelty suppressed feeding test. A single piece of kibble was placed in the center of the arena. The mouse undergoing testing was then placed in the corner of the arena in a consistent manner. Behavior was measured in real time by an observer. A stopwatch was used to record the latency until the mouse initiated its first bite of food. A trial was ended at 10 minutes and the latency to eat was recorded as 600 seconds when animals did not eat within the allocated time. Following testing in the novel space animals are tested for latency to eat in the home cage. A new piece of kibble is placed in the center of the home cage. The trial ends when the animal has taken a bite of food or 10 minutes expires. Both latency times are recorded and analyzed.

Forced Swim Test (FST): The test was conducted under white light. The stressed mice were placed in individual 4000 mL beakers filled to the 3000 mL mark with room temperature water (25°C ± 1) with coded identification cards attached to track their identities. The mice were placed in the beakers of water, with body submerged. Each mouse's test lasted for 6 minutes during which they were digitally recorded for subsequent analysis by an investigator blind to their conditions. A stopwatch was used to record latency till the mouse first bout of immobility. The stopwatch was also used to record the cumulative time the mouse spent immobile.

Submandibular Bleed: Blood was drawn within 20 minutes of the last stressor (restraint stress) from the submandibular vein. A 20-gauge needle was used to collect blood into a heparin lined tube. 200µL of blood was drawn per individual. The blood sample is then placed on ice and spun in a centrifuge at 2400 x g. The mouse was then returned to their home cage and monitored for recovery.

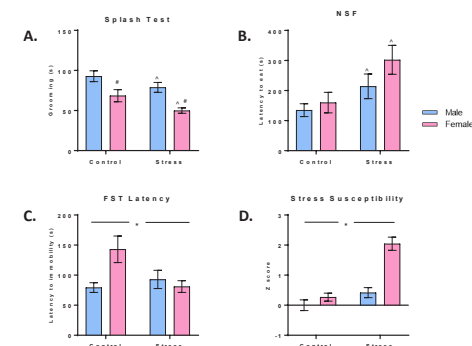
Multiplex ELISA: The multiplex enzyme-linked immunosorbent assay (ELISA) is an advanced assay technique that allows for the detection of multiple cytokines simultaneously (Elshal & McCoy, 2006). The multiplex ELISA uses spherical magnetic beads coated with a multitude of specific immobilized antibodies. When the processed blood samples are exposed to the multiplex ELISA, targeted cytokines bind to their designated antibodies. After the multiplex analysis is complete, a machine is used to measure the intensity of fluorescence. Based on the fluorescence intensity, a quantity can be discerned as the amount of cytokines present in a specific blood sample.

Stress and Behavior Timeline



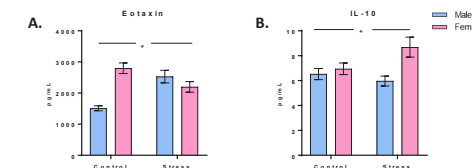
Behavior

A. There was a main effect of stress ($F_{(1,36)} = 6.912$, p -value < 0.05) and sex ($F_{(1,36)} = 18.59$, $p < 0.001$) in the splash test. Males spent a 8% less time grooming due to stress, while females displayed a 15% decrease. B. In the NSF test there was a significant main effect of stress ($F_{(1,36)} = 8.751$, $p < 0.05$). Males had 22% increase in latency to eat while females displayed a 30% increase in latency to eat. C. In the FST there was significant interaction between stress and sex ($F_{(1,33)} = 5.957$, $p < 0.05$). Post hoc testing with a Bonferroni correction indicated that stressed males displayed a 7% increase in latency to immobility compared with unstressed males, whereas stressed females displayed a 27% decrease in latency to immobility. D. Z-scores of data combined across all tests found that stressed females had higher stress susceptibility scores than all other groups as indicated by a significant interaction ($F_{(1,36)} = 14.55$, $p < 0.001$) with a post-hoc Bonferroni correction.



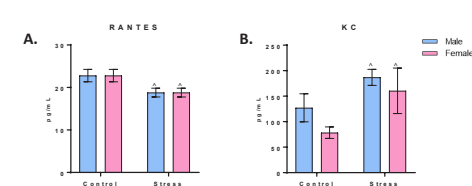
Cytokines: Significant interactions between sex and stress

A. Eotaxin ($F_{(1,36)} = 25.13$, $p < 0.0001$). Post-hoc analysis indicated that stress increased eotaxin in males but decreased it in females. B. IL-10 ($F_{(1,34)} = 4.134$, $p < 0.05$). Stress increased IL-10 in females but decreased it in males.



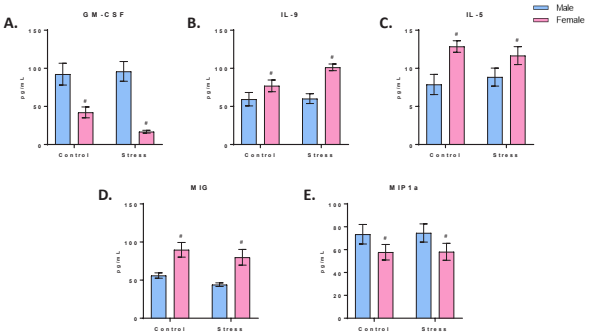
Chemokines: Main effect of stress

A. RANTES/CCL5 ($F_{(1,36)} = 10.02$, $p < 0.01$). B. KC/CXCL1 ($F_{(1,35)} = 6.152$, $p < 0.05$).



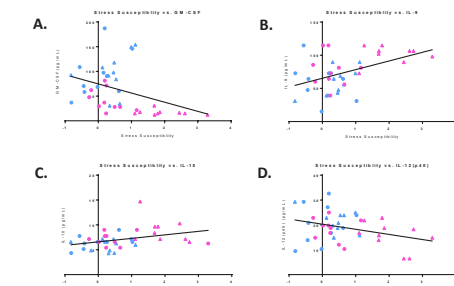
Cytokines and Chemokines: Main effect of sex

A. GM-CSF ($F_{(1,35)} = 37.17$, $p < 0.0001$). B. IL-9 ($F_{(1,35)} = 16.8$, $p < 0.001$). C. IL-5 ($F_{(1,32)} = 11.39$, $p < 0.01$). D. Chemokine MIG/CXCL9 ($F_{(1,35)} = 21.3$, $p < 0.0001$). E. Chemokine MIP1a/CCL3 ($F_{(1,36)} = 4.396$, $p < 0.05$).



Correlations of Stress Susceptibility Score and Cytokines

A. GM-CSF negatively correlated with stress susceptibility scores across sex ($r = -0.37$, $p < 0.05$). B. IL-9 positively correlated with stress susceptibility scores across sex ($r = 0.46$, $p < 0.01$). C. IL-10 positively correlated with stress susceptibility scores across sex ($r = 0.35$, $p < 0.05$). D. IL-12(p40) negatively correlated with stress susceptibility scores across sex ($r = -0.33$, $p < 0.05$).



Conclusion and Future Research

- Females show a stronger behavioral response to 6-day SCVS than males.
- Different patterns of cytokines are regulated by SCVS in males and females.
- Cytokine patterns in females suggest an allergy-like response to stress (Goswami & Kaplan, 2011; Shi et al., 2006).
- A comparison of cytokine patterns following 28 days of stress, when both males and females are stress susceptible, is necessary to determine whether the different patterns of cytokine response reported here are due to stress resilience in the males or a sex difference.

References

- Cannon, J. G. (2000). Inflammatory Cytokines in Nonpathological States. *News in Physiological Sciences*, 15(December), 298–303.
- Elshal, M. F., & McCoy, J. P. (2006). Multiplex bead array assays: Performance evaluation and comparison of sensitivity to ELISA. *Methods*, 38(4), 317–323. <https://doi.org/10.1016/j.jmeth.2005.11.010>
- Goswami, R., & Kaplan, M. H. (2011). A Brief History of IL-9. *The Journal of Immunology*, 186(6), 3283–3288. <https://doi.org/10.1093/immuni/1003049>
- Hodes, G. E., Pfau, M. L., Purnushothaman, L., Ahn, H. F., Golden, S. A., Christoffel, D. J., ... Russo, S. J. (2015). Sex Differences in Nucleus Accumbens Transcriptome Profiles Associated with Susceptibility versus Resilience to Subchronic Variable Stress. *The Official Journal of the Society for Neuroscience*, 35(50), 16362–76. <https://doi.org/10.1523/JNEUROSCI.1392-15.2015>
- Laplant, G., Chakraverty, S., Valiso, V., Maheshwari, S., Xiao, J., W. Kishimoto, G., ... Russo, S. J. (2010). Hypersensitivity in Female Mice. *ESMO*, 874–880.
- Martin, L. A., Neighbors, H. W., & Griffith, D. M. (2013). The experience of symptoms of depression in men vs women: analysis of the National Comorbidity Survey Replication. *JAMA Psychiatry*, 70(10), 1100–6. <https://doi.org/10.1001/jamapsychiatry.2013.1985>
- Prendergast, B. J., Onishi, K. G., & Zucker, I. (2014). Female mice liberated for inclusion in depression and biomedical research. *Neuroscience and Biobehavioral Reviews*, 40, 1–5. <https://doi.org/10.1016/j.neubiorev.2014.01.001>
- Shi, Y., Liu, C. H., Roberts, A. L., Dai, J., Xu, G., Ren, G., ... Dewalds, S. (2006). Granulocyte-macrophage colony-stimulating factor (GM-CSF) and T-cell responses: what we do and don't know. *Cell Research*, 16(2), 126–133. <https://doi.org/10.1038/cr.2010017>

Funding and Support: Special thanks to the Engel Novitt Fellowship, Brain & Behavior Research Foundation for funding and support.

undergoing testing was then placed in the corner of the arena in a consistent manner. Behavior was measured in real time by an observer. A stopwatch was used to record the latency until the mouse initiated its first bite of food. A trial was ended at 10 minutes and the latency to eat was recorded as 600 seconds when animals did not eat within the allocated time. Following testing in the novel space animals were tested for latency to eat in the home cage. A new piece of kibble was placed in the center of the home cage. The trial ended when the animal took a bite of food or 10 minutes expired. Both latency times were recorded and analyzed. The final behavioral test was the force swim latency test. The stressed mice were placed in individual 4000 mL beakers filled to the 3000 mL mark with room temperature water ($25^{\circ}\text{C} \pm 1$) with coded identification cards attached to track their identities. The mice were placed in the beakers of water, with body submerged. Each mouse's test lasted for 6 minutes during which they were digitally recorded for subsequent analysis by an investigator blind to their conditions. A stopwatch was used to record latency till the mouse first bout of immobility. The stopwatch was also used to record the cumulative time the mouse spent immobile. Each behavioral response per individual was used to compile an overall stress susceptible score, indicating how stress susceptible the individual mouse was based on their times from the three behavioral tests. These individual stress susceptibility scores were correlated with cytokine levels. susceptibility scores were correlated with cytokine levels.

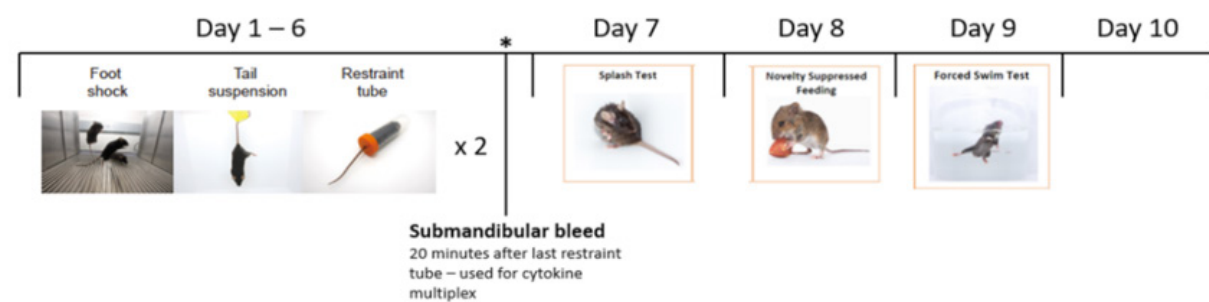


Figure 1: Timeline of stressors, submandibular blood, and behavioral tests. Stressed male and females were subjected to subchronic variable stress (SCVS) over 6 days. Stressors used were foot shock (0.45 mA/2 second duration/100 shocks at random for 1 hour), tail suspension (1 hour total), and restraint tube (1 hour total). During the 6-day term, the stressed mice would experience each stressor twice in a repeated order of foot shock, tail suspension, restraint tubes.

The behavioral results are as followed. In the splash test, there was a significant main effect of stress and sex, meaning overall the stressed females groomed the least compared to all other groups. The less time spent grooming, the more indicative that the group is experiencing depression-like symptomology by lacking in hygienic care. In the novelty suppressed feeding test there was a significant main effect of stress. Overall the stressed female took the longest to venture out to the center and take the first bite of their food. This indicates that the stressed females are experiencing a level of anxiety and fear. In the force swim test, there was a significant interaction between sex and stress. Overall, the stressed females were quick to adapt a passive coping mechanism rather than actively try to escape. Ultimately stress susceptibility scores were largest in the stress female group, indicating after 6 day subchronic stress they are stress susceptible while their stress counterparts, stressed males, show stress resilience based on their low stress susceptibility scores.

After screening for 36 cytokines in the blood samples retrieved from the submandibular bleed, the four cyto-

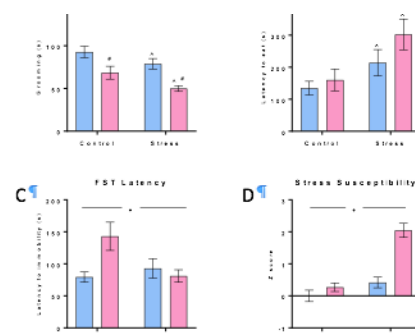


Figure 2: A. There was a main effect of stress ($F(1, 36) = 6.912$, p -value < 0.05) and sex ($F(1, 36) = 18.59$, $p < 0.001$) in the splash test. Males spent a 8% less time grooming due to stress, while females displayed a 15% decrease. B. In the NSF test there was a significant main effect of stress ($F(1, 36) = 8.751$, $p < 0.05$). Males had 22% increase in latency to eat while females displayed a 30% increase in latency to eat. C. In the FST there was significant interaction between stress and sex ($F(1, 33) = 5.957$, $p < 0.05$). Post hoc testing with a Bonferroni correction indicated that stressed males displayed a 7% increase in latency to immobility compared with unstressed males, whereas stressed females displayed a 27% decrease in latency to immobility. D. Z-scores of data combined across all tests found that stressed females had higher stress susceptibility scores than all other groups as indicated by a significant interaction ($F(1, 36) = 14.55$, $p < 0.001$) with a post-hoc Bonferroni correction.

kines that showed significance between their concentrations and stress susceptibility scores were as followed. Both GM-CSF (granulocyte macrophage colony stimulating factor) and IL-12p (40) are pro-inflammatory cytokines, while IL-9 and IL-10 are anti-inflammatory cytokines. Our correlations suggest that stress susceptibility scores increase as pro-inflammatory cytokines decrease, while anti-inflammatory activity increases. These effects seemed to be predominately driven by the stressed females indicated by the pink triangles. Focusing on the stress female group, there seems to be an anti-inflammatory response occurring to stress similar to the immune response to a parasitic worm or an allergy. Further research is needed to determine whether this is due to stress susceptibility or a sex differences in response to stress.

Conclusion: this experiment shows that there are both behavioral differences and immune response differences based on cytokine concentrations. It also supports that stressed females may be perceiving stress as an allergy and is responding as such. To understand if the stress like response is a result of a sex difference or a state of stress susceptibility versus a state of stress resilience, the next step of this project is to extend the term of the subchronic variable stress paradigm to a long-term test. Past research has shown with 28 days of this same SCVS model, the stressed males are no longer stress resilient. If we eliminate stress resiliency as a factory is this test, then we can determine if the overall stress response type is due to a sex difference or a stress susceptibility difference.

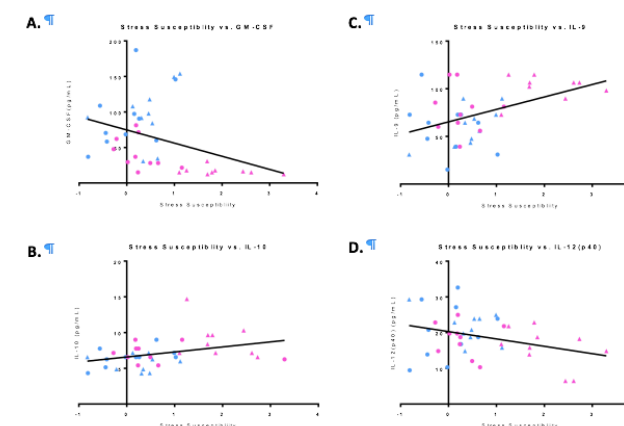


Figure 3 A. GM-CSF negatively correlated with stress susceptibility scores across sex ($r = -0.37$, $p < 0.05$). B. IL-9 positively correlated with stress susceptibility scores across sex ($r = 0.46$, $p < 0.01$). C. IL-10 positively correlated with stress susceptibility scores across sex ($r = 0.35$, $p < 0.05$). D. IL-12(p40) negatively correlated with stress susceptibility scores across sex ($r = -0.33$, $p < 0.05$).

References

- Cannon, J. G. (2000). Inflammatory Cytokines in Nonpathological States. *News in Physiological Sciences*, 15(December), 298–303.
- Hodes, G. E., Pfau, M. L., Purushothaman, I., Ahn, H. F., Golden, S. A., Christoffel, D. J., ... Russo, S. J. (2015). Sex Differences in Nucleus Accumbens Transcriptome Profiles Associated with Susceptibility versus Resilience to Subchronic Variable Stress. *The Journal of Neuroscience: The Official Journal of the Society for Neuroscience*, 35(50), 16362–76. <https://doi.org/10.1523/JNEUROSCI.1392-15.2015>
- Laplant, Q., Chakravarty, S., Vialou, V., Mukherjee, S., Koo, J. W., Kalahasti, G., ... Russo, S. J. (2010). Hypersensitivity in Female Mice, 65(10), 874–880.
- Martin, L. A., Neighbors, H. W., & Griffith, D. M. (2013). The experience of symptoms of depression in men vs women: analysis of the National Comorbidity Survey Replication. *JAMA Psychiatry*, 70(10), 1100–6. <https://doi.org/10.1001/jamapsychiatry.2013.1985>
- Prendergast, B. J., Onishi, K. G., & Zucker, I. (2014). Female mice liberated for inclusion in neuroscience and biomedical research. *Neuroscience and Biobehavioral Reviews*, 40, 1–5. <https://doi.org/10.1016/j.neubiorev.2014.01.001>

Examination of GABA Transporter Expression Across Development

Abbie Weit, Helen Vanderpool, Leanne Holt, Michelle Olsen
 School of Neuroscience, Virginia Polytechnic and State University,
 Blacksburg, VA
 EngelNovitt Undergraduate Research Fellowship Program

Background: Astrocytes are one of the most abundant cell types in the brain. These glial cells enwrap over 90% of glutamatergic synapses and decades of research indicate glutamate uptake via astrocytic glutamate transporters is critical for the termination of glutamatergic synaptic transmission. In contrast, little is known regarding a role for astrocytes at GABAergic synapses. Preliminary data we have generated in the laboratory by RNA sequencing revealed GABA transporters (GAT) are found in abundance in mature cortical astrocytes, and indeed appear enriched in astrocytes relative to other CNS cell populations. These transporters play an important role in the removal of GABA from extracellular space to prevent excess neuronal inhibition. The function and spatial distribution of GAT1 and GAT3 has been previously examined; however, their developmental expression has not been determined.

Methods: In the current study we utilized quantitative PCR and Western blot to examine to examine gene and protein expression levels of GAT1 and GAT3 in the cortex. We evaluated gene and protein expression at multiple time points during early postnatal development.

Examination of GABA Transporter Expression Across Development

Abbie Weit^{1,2}, Helen Vanderpool¹, Leanne Holt¹, Michelle Olsen¹
¹School of Neuroscience, Virginia Polytechnic and State University, Blacksburg, VA
²EngelNovitt Undergraduate Research Fellowship Program



Abstract

Astrocytes are one of the most abundant cell type in the brain. These glial cells enwrap over 90% of glutamatergic synapses and decades of research indicate glutamate uptake via astrocytic glutamate transporters is critical for the termination of glutamatergic synaptic transmission. In contrast, little is known regarding a role for astrocytes at GABAergic synapses. Preliminary data we have generated in the laboratory by RNA sequencing revealed GABA transporters (GAT) are found in abundance in mature cortical astrocytes, and indeed appear enriched in astrocytes relative to other CNS cell populations. These transporters play an important role in the removal of GABA from extracellular space to prevent excess neuronal inhibition. The function and spatial distribution of GAT1 and GAT3 has been previously examined; however, their developmental expression has not been determined. This project examined RNA and protein expression of GAT1 and GAT3 across cortical development in both males and females. Our preliminary studies reveal interesting developmental and sex-specific trends in cortical GAT expression which may contribute to early cortical development and maturation. These studies lay the groundwork for future experiments in the Olsen lab which will examine GAT expression in isolated astrocyte and neuron populations.

Background

Astrocytes

- Astrocytes are the most abundant cell type in the brain
- Responsible for many supportive functions including the production, removal, and breakdown of multiple neurotransmitters

GABA and GABA Transporters

- GABA is the major inhibitory neurotransmitter in the adult, mature CNS
- GABA acts in an excitatory nature in early development
- GABA transporters are used to remove excess GABA from the synaptic cleft
- Three main GATs:
 - GAT1 and GAT3 are expressed in the brain
 - GAT2 is expressed in the periphery

Methods

Tissue Collection

- Cortical tissue was extracted from male and female mice at several developmental time points. These time points included postnatal days 0, 7, 14, 21, 30, 45, and 60.

qPCR

- Real time PCR was completed to examine mRNA expression. Comparisons were made between developmental time points as well as between sexes. GAT1 and GAT3 mRNA expression was normalized to GAPDH mRNA expression.

Western Blotting

- Western Blotting techniques were done to look at protein expression in cortical samples across development. Comparisons were made across sexes. GAT1 and GAT3 protein expression was normalized to GAPDH protein expression.

Results: Our results indicate that mRNA for the GAT1 transporters reaches a peak at postnatal day 7 in male and female mice and remains stable throughout development. Whereas GAT3 expression peak-

Project Goals

- Isolate brain tissue across postnatal development
- Examination of RNA and protein expression of GAT1 and GAT3 GABA transporters across development

Protein expression across development

GAT1

Female

Male

Figure 1. GAT1 protein expression across female cortical development. Western blot analysis demonstrates an increase in GAT1 protein expression following postnatal day 0. *statistically different from p0. #statistically different from p7.

GAT3

Female

Male

Figure 3. GAT3 expression across female cortical development. Western blot analysis demonstrates an increase in GAT3 protein expression following postnatal day 0. *statistically different from p0. #statistically different from p7.

Protein expression between the sexes

GAT1

GAT3

RNA expression across development

Female

Male

Figure 7. SLC6A11 mRNA expression across female cortical development. *p, < 0.05

Figure 10. SLC6A11 mRNA expression across male cortical development. *p, < 0.05

Results and Conclusions

- GAT3 mRNA and protein expression showed a surprisingly high expression at postnatal day 7 in both males and females
- GAT1 mRNA expression showed sex-specific differences
 - Males demonstrated little developmental variation, while female expression peaked at postnatal day 7 again

Future Directions

- Due to the unexpected trends of expression and sex differences these transporters will be studied with more in depth experiments, including
 - Determine mRNA and protein expression in isolated astrocytes
 - Spatial and cell-type distribution across brain regions using immunohistochemistry
 - Determination of astrocytic GAT functions and subsequent influence on overall brain functions

References

- Meyer, Beverly. "Episode 52 - GABA Deficiencies: Anxiety, Insomnia, Obesity." *Live Fit Lean - Live Life Healthy, Fit, & Free*, Live Fit Lean, 2016, www.livefitlean.com/podcast/ep52-gaba/.

ed at postnatal day seven and then decreased to approximately 30% of its peak, where it remained.

Conclusions: Our preliminary studies reveal interesting developmental and sex-specific trends in cortical

GAT expression which development and maturation. These studies lay the Olsen lab which will examine GAT expression in isolated astrocyte and neuron populations.

AAV-Mediated Truncated FOXP2 Splice Variant Injections in Developing Rat Brain Alters Vocalization Complexity and Social Interactions

By: Dawn Wright, Makenzie Taylor, Tina Taylor, Clint Roby, Kareem Omeish, J. Michael Bowers
School of Neuroscience, Virginia Polytechnic Institute & State University, Blacksburg, VA

FOXP2 is a member of a large transcription factor family and is one of the 5% most-conserved proteins with only two amino acids separating humans from chimpanzees. An identified mutation of FOXP2, (R553H), has been found in patients that is consistent with speech and cognitive abnormalities. The forkhead domain of the FOX protein is important for nuclear localization and DNA binding. A novel truncated splice variant of FOXP2, first reported by Bruce and Margolis (2002; Hum Genet 2002), prevents the nuclear localization of FOXP2 because it lacks the C-terminal region coding for the forkhead domain. This truncated variant causes the FOXP2 protein to aggregate in the cytoplasm similar to the R553H mutation. We have found an analogous truncated variant in the rat using endpoint qRT-PCR on neonatal brains. My project will investigate the role that this truncated variant contributes to vocal production and its consequential sex-mediated effects in rats.

AAV-mediated truncated FOXP2 injections were administered to 28 neonatal pups and vocalization recordings were compared for communicative differences between sexes and injected versus control animals. Alterations in a downstream signaling target of FOXP2, CNTNAP2, were confirmed with Western Blot analysis in four brain regions: cortex, hippocampus, striatum, and cerebellum. Our study provides sufficient evidence that rats treated with truncated FOXP2 results increase usage of simple calls compared to the more abundant complex vocal calls used by control rats. This study aims at providing a model of the consequences of upregulated truncated FOXP2 expression in the developing autistic brain.

PCR amplification, cloning, and sequencing of the FOXP2 gene and truncated splice variant created plasmids used for cortical injections. Western blot imaging techniques enabled quantification of signaling partners in virus injected and control groups. Blots were later analyzed for sex-differences within experimental groups.

Ultrasonic vocalizations (USV) data collected by Sonotrack software during social play were analyzed for signaling patterns reflective of simple or complex vocalizations after receiving injections.

The evidence that was gathered during this investigation revealed trends supportive of our initial hypothesis. Western Blot data shows a significant decrease in endogenous FOXP2 levels in males injected with truncated FOXP2. There is no significant reduction in FOXP2 in females. In both the cortex and striatum CNTNAP2 is upregulated in the virus-injected group, which further implicates a reduction in endogenous FOXP2 in the presence of truncated FOXP2. Vocalization data reveals a significant shift from complex calls to simple vocal calls in the presence of the truncated FOXP2 splice variant. The reduction in overall vocalization is observed in both sexes of the virus-injected treatment group. In developing autistic human brains there is increased expression of truncated FOXP2. (Bowers,

et al, 2013) AAV-mediated truncated FOXP2 upregulation in rats displaying social and cognitive deficits potentially serves as a model of lingual impairment associated with autism spectrum disorder.

Future studies will include quantification of FOXP2 signaling partners with Western Blot analysis and investigation of sex differences in FOXP2 expression levels after treatment with virus. Additionally, we will be

investigating the molecular signaling patterns that contribute to lingual development in neonatal brains that contribute to cortical maturation. I would like to thank the *EngelNovitt Undergraduate Research Fellowship* for providing me with the opportunity to immerse myself in such a gratifying research project. I would also like to express my gratitude to Dr. Mike Bowers and the rest of the Bowers' Lab for their contributions and support.

AAV-Mediated Truncated FOXP2 Splice Variant Injections in Developing Rat Brain Alters Vocalization Complexity and Social Interactions

Dawn Wright, Makenzie Taylor, Tina Taylor, Clint Roby, Kareem Omeish, J. Michael Bowers, School of Neuroscience, Virginia Tech

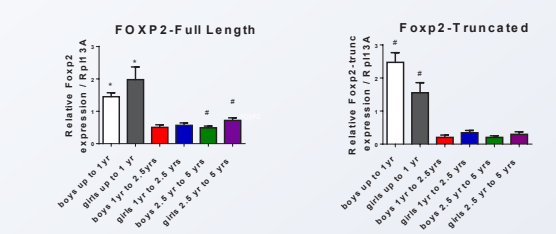
Introduction

FOXP2 is a member of a large transcription factor family and is one of the 5% most-conserved proteins with only two amino acids separating humans from chimpanzees. An identified mutation of FOXP2, (R553H), has been found in patients that is consistent with speech and cognitive abnormalities. The forkhead domain of the FOX protein is important for nuclear localization and DNA binding. A novel truncated splice variant of FOXP2, first reported by Bruce and Margolis (2002; Hum Genet 2002), prevents the nuclear localization of FOXP2 because it lacks the C-terminal region coding for the forkhead domain. This truncated variant causes the FOXP2 protein to aggregate in the cytoplasm similar to the R553H mutation.

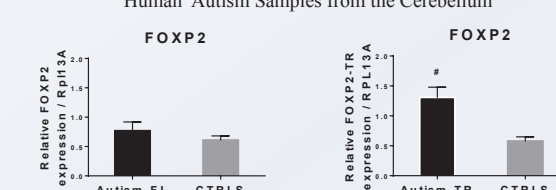
We have found an analogous truncated variant in the rat using endpoint qRT-PCR on neonatal brains. AAV-mediated truncated FOXP2 injections were administered to 28 neonatal pups and vocalization recordings were compared for communicative differences between sexes and injected versus control animals. Alterations in a downstream signaling target of FOXP2, CNTNAP2, were confirmed with Western Blot analysis in four brain regions: cortex, hippocampus, striatum, and cerebellum. Our study provides sufficient evidence that rats treated with truncated FOXP2 results increase usage of simple calls compared to the more abundant complex vocal calls used by control rats. This study aims at providing a model of the consequences of upregulated truncated FOXP2 expression in the developing autistic brain.

Endogenous FOXP2 Expression in Human Cerebellum

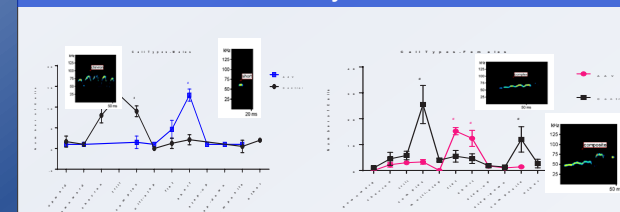
Developmental expression of Full-length and truncated human FOXP2 mRNA in the cerebellum



Human Autism Samples from the Cerebellum



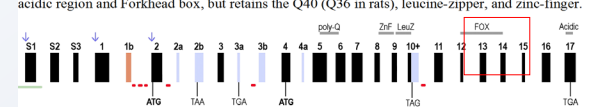
Sex difference for the vocalization call types are different for AAV injected and control



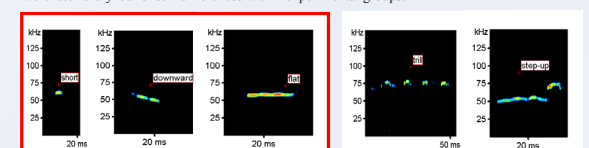
Play partner influences amount of USV
Significant reduction in vocalizations is observed in play groups composed of virus-injected rats. Conversely, this number of vocalizations is starkly increased in groups of only control rats.

Methods

Two C-terminal truncated FoxP2 mRNA reference sequences are listed at NCBI for human. The human truncation occurs when splicing at the 3'-end of Exon-10 does not occur, and the 84-base Exon-10 becomes a 3'-terminal 218bp Exon-10+. This 10+ exon includes an in frame stop codon (TAG) 31 bases down from missed splice site. The human truncation removes the C-terminal acidic region and Forkhead box, but retains the Q40 (Q36 in rats), leucine-zipper, and zinc-finger.



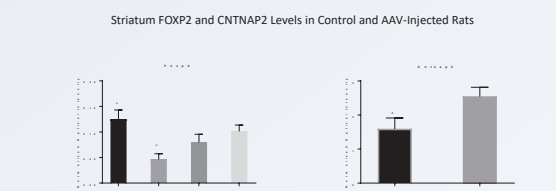
The 30 coding bases in Exon-10+ are identical in rat and human, and noncoding regions are highly similar among the two species. PCR amplification, cloning, and sequencing of the FOXP2 gene and truncated splice variant created plasmids used for cortical injections. Western blot imaging techniques enabled quantification of signaling partners in virus injected and control groups. Blots were later analyzed for sex-differences within experimental groups.



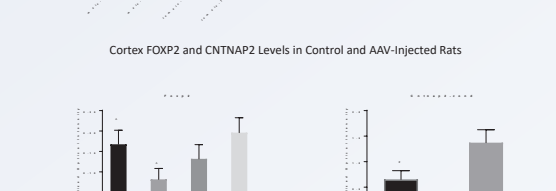
Ultrasonic vocalizations (USV) data collected by Sonotrack software during social play were analyzed for signaling patterns reflective of simple or complex vocalizations after receiving injections.

Western Blot Analysis of FOXP2 and CNTNAP2 Expression

Striatum FOXP2 and CNTNAP2 Levels in Control and AAV-Injected Rats



Cortex FOXP2 and CNTNAP2 Levels in Control and AAV-Injected Rats

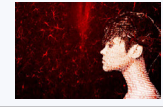


Conclusions

- Western Blot data shows a significant decrease in endogenous FOXP2 levels in males injected with truncated FOXP2. There is no significant reduction in FOXP2 in females. In both the cortex and striatum CNTNAP2 is upregulated in the virus-injected group, which further implicates a reduction in endogenous FOXP2 in the presence of truncated FOXP2.
- Vocalization data reveals a significant shift from complex calls to simple vocal calls in the presence of the truncated FOXP2 splice variant. The reduction in overall vocalization is observed in both sexes of the virus-injected treatment group.
- In developing autistic human brains there is increased expression of truncated FOXP2. (Bowers, et al, 2013) AAV-mediated truncated FOXP2 upregulation in rats displaying social and cognitive deficits potentially serves as a model of lingual impairment associated with autism spectrum disorder.
- Future studies will include quantification of FOXP2 signaling partners with Western Blot analysis and investigation of sex differences in FOXP2 expression levels after treatment with virus.

Acknowledgements

1. Dr. Michael Bowers, Makenzie Taylor, Tina Taylor, Clint Roby, Kareem Omeish, and Dr. Miguel Perez-Pouchoulen
2. EngelNovitt Undergraduate Research Fellowship
3. Virginia Tech School of Neuroscience



3D Bioprinted Gliovascular Units

Sahil A. Laheri, Alexander P. Haring¹, Manjot Singh, Ellen Cesewski and Blake N. Johnson

Department of Industrial and Systems Engineering; School of Neuroscience
Virginia Polytechnic Institute and State University, Blacksburg, VA 24060

Background: Glial cells are the most abundant type of cells in the nervous system and play an essential role in the support of neurons. The gliovascular unit is the complex functional system that maintains proper blood flow to the active brain regions. Glioma, one of the most common brain tumors, arises from glial cells and causes the breakdown of the blood brain barrier. 3D bioprinting is a novel technique that allows for the preservation of cell function and viability within a specifically printed construct. A unique advantage for this technique is the ability to reproduce the higher order function and features associated with human pathophysiology. Although the printing of 3D neurological models is useful, the vascularization of these models remains a challenge. Having the ability to vascularize these models will lead to more detailed understanding of mass transport and other physiological changes associated with the blood-brain barrier. We examined the possibility of leveraging 3D printing to create two different models of vasculature in the brain.

Methods

3D Gliovascular Unit Model

The model was created through a multistep printing process. First, the outer cast and sacrificial, suspended channel was manually written out in code and printed with a 30% Pluronic F127 bioink gel using a 27 GA tapered tip. Next the cast was filled with a heated 10% gelatin methacrylate (GelMA) solution and then cured under ultraviolet (UV) light for 5-8 minutes. The outer cast and sacrificial channel were then washed away with cold water, resulting in an open channel within the cured GelMA filling.

Glioma Migration Chamber

The migration chamber is a 2D model of the gliovascular unit. First, a CAD model of the channel was designed and then translated into code to be printed with SI 595 RTV Silicone Clear using a 27 GA tapered tip. The printed chambers were placed aside to cure over a short time period.



3D Bioprinted Gliovascular Units

Sahil A. Laheri, Alexander P. Haring, Manjot Singh, Ellen Cesewski and Blake N. Johnson

Department of Industrial and Systems Engineering; School of Neuroscience
Virginia Polytechnic Institute and State University, Blacksburg, VA 24060



Background

Glial Cells

- > Plays an essential role in sustaining the brain's physiological activity
- > Glioma arise from these cells and make up a majority of malignant brain tumors
- > Gliovascular system assures necessary blood supply to the active brain regions¹

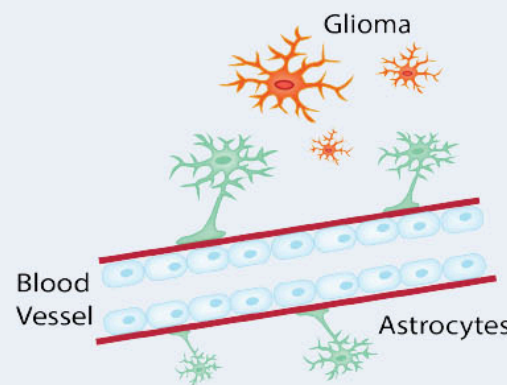
3D Bioprinting

- > Allows for cell function and viability to be preserved within a precise construct²
- > Reproducibility of the neural model is a unique benefit with this approach

Vascularization of Models

- > Huge 3D printing challenge
- > Necessary for long-term cell culture of thick tissues
- > Helps to understand mass transport and reproducing pathophysiological trajectories associated with the blood-brain barrier

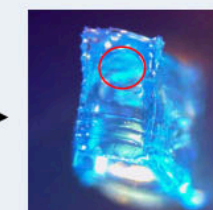
Gliovascular Unit



Printed Pluronic F127

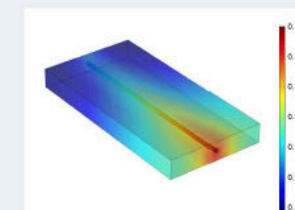
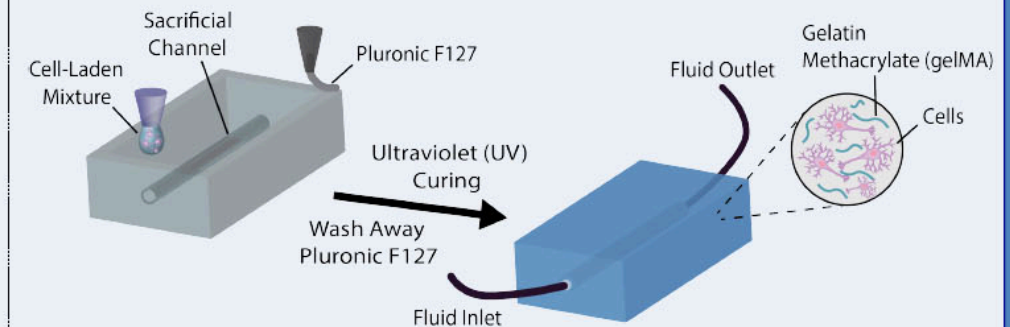


gelMA Filled Box



Vascularized Model

3D Gliovascular Unit Model



Simulated Model

- Day 21
- 10⁶ cells/mL
- Fluid: H₂O
- Flow rate: 100 μL/s
- Full channel still viable for cells

Research Questions

- Can we leverage 3D printing to create a model of the gliovascular unit?
- How can we apply 3D printing to understand the migration of glioma cells due to biochemical cues?

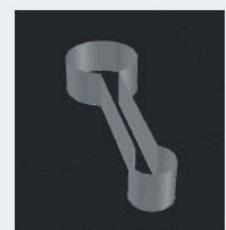
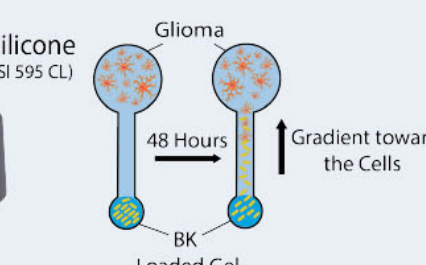
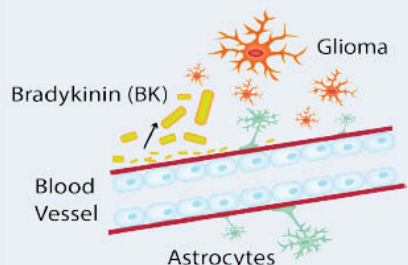
Acknowledgements

We acknowledge the The Virginia Tech School of Neuroscience for their support through the James and Lillian Gay Undergraduate Research Fellowship.

References

1. Kimbrough IF, Robel S, Roberson ED, Sontheimer H. Vascular amyloidosis impairs the gliovascular unit in a mouse model of Alzheimer's disease. *Brain*. 2015;138(12):3716-3733.
2. Kolesky, D. B., Truby, R. L., Gladman, A. S., Busbee, T. A., Homan, K. A. and Lewis, J. A. (2014), 3D Bioprinting of Vascularized, Heterogeneous Cell-Laden Tissue Constructs. *Adv. Mater.*, 26: 3124–3130.

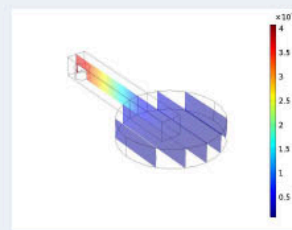
Glioma Migration Chamber



CAD Model



Printed Devices



Simulated Model

- 48 hours
- Peptide concentration gradient forms

Conclusions

1. Printed a gliovascular model with an open channel
2. Printed migration chambers to be used for biochemical studies

Future Studies

Apply the gliovascular model to study fluid effects on the surrounding cells and vasculature

Explore time-lapse studies on how different neuropeptides can affect migration rates

Results/Conclusions: We were able to successfully print gliovascular models with an open channel to be used for fluidic studies. The silicone migration chambers were successfully created and optimized for use

in time-lapse migration studies. Future directions for this study include integration of the 3D printed gliovascular unit with fluid handling components and application of migration chambers in different bio-

chemical settings to understand the effects of cue concentration magnitude and profile on migration rates.

Anorexigenic mechanisms of substance P in alternative vertebrate models

Christopher Buenaventura, Elizabeth R. Gilbert and Mark A. Cline
 Neuroendocrinology Laboratory, Virginia Polytechnic Institute and State University

Background: Substance P (SP) is a member of the neurokinin (NK) family, a group of neuropeptides that are distributed throughout the peripheral and central nervous systems. Substance P is involved in multiple physiological processes, including emesis, pain perception and transmission, and food intake, effects of which are mediated via NK receptors. Central administration of SP elicited anorexigenic effects in rats and our group recently demonstrated a similar effect in domestic broiler chicks (*Gallus gallus*). The central mechanisms underlying the anorexigenic effects of SP are still unclear and elucidating such pathways may provide information that could facilitate a novel strategy to treat eating disorders. The objective of this research was to evaluate the anorexigenic effect of SP in Japanese quail (*Coturnix japonica*), an avian species that has not undergone intense artificial selection for growth-related traits but adapts well to a cage environment, and thus provides evolutionary perspective.

Methods and Results: In Experiment 1, 7 day-old quail were centrally (intracerebroventricularly; into the left lateral ventricle) injected with 0 (vehicle; artificial cerebrospinal fluid), 0.25, 0.5 or 1.0 nmol SP and food and water intake were quantified for 180 minutes. On a cumulative basis, quail that received 0.5 and 1.0 nmol SP reduced food intake during the entire observation period (50% reduction compared to controls at 30 minutes post-injection). Water intake was not affected. In Experiment 2, whole hypothalamus was isolated from SP-injected chicks at 1 hour post-injection, total RNA isolated, and real time PCR performed to measure mRNA abundance of several appetite-associated factors. Quail injected with SP expressed less agouti-related peptide (AgRP) mRNA than vehicle-injected chicks. In Experiment 3, a comprehensive behavior analysis was performed. Quail that were injected with SP displayed fewer feeding pecks and reduced locomotion compared to vehicle-treated birds during the first 30 minutes post-injection. In Experiment 4, c-Fos immunoreactivity (an indicator of

neuronal activity) was quantified in appetite-associated hypothalamic nuclei. There were fewer c-Fos immunoreactive cells in the lateral hypothalamus (LH) of SP-injected chicks than vehicle-injected chicks at 1 hour post-injection. In Experiment 5, the LH was collected for total RNA isolation and gene expression analysis via real time PCR. Quail injected with SP expressed less agouti-re-

lated peptide (AgRP) mRNA than vehicle-injected birds in the LH at 1 hour post-injection.

Conclusions: Central injection of SP was associated with decreased food intake in Japanese quail, similar to rodents and chickens. Molecular mechanisms appear to differ between the

two avian models. In chickens, we found that SP injection was associated with increased c-Fos immunoreactivity and urotensin 2 mRNA in the paraventricular nucleus of the hypothalamus, whereas in quail there was a reduction in c-Fos and AgRP mRNA in the LH. While AgRP is expressed in several hypothalamic nuclei, especially the arcuate nucleus, the whole hypothalamus and LH gene expression results suggest that the decrease in AgRP in SP-injected chicks is of LH origin. Future research will focus on understanding the role of the LH and AgRP in SP-mediated feeding behavior via microinjection and receptor blockage studies.

Differential anorexigenic mechanisms of substance P in alternative vertebrate models

Christopher Buenaventura, Elizabeth R. Gilbert and Mark A. Cline | Neuroendocrinology Laboratory | Virginia Polytechnic Institute and State University | Sponsored by Engelnovitt Fellowship

Background

- Substance P (SP) is an excitatory central neurotransmitter [RPKKQFFGLM-NH₂]
- Role in pain transmission & sensation (Hanson & Geppert, 2001; Otsuka & Konishi, 1976)
- Potent vasodilator (Elska Mistrova, Peter Kruzik, Magdalena Chotkova Dvorakova, 2016)
- Released from dorsal raphe nuclei (Felpe et al., 1996)
- Found in central and peripheral nervous system (Otsuka & Yoshioka, 1993; Galagher et al., 1992; Quartara & Maggi, 1999)
- Binds 3 different SP G-protein-coupled receptors (Gerard et al., 1993)
- Also stimulates the neurokinin 1 receptor (Elska Mistrova, Peter Kruzik, Magdalena Chotkova Dvorakova, 2016)
- SP affects appetite in mammals (insert) and birds (Tachibana et al., 2010)
- In some cases, central appetite control is different between birds and mammals: orexins, melanin concentrating hormone, & motilin stimulate hunger in mammals, but not chickens (Furuse et al., 1999, Ando et al., 2000, Ohkubo et al., 2002), ghrelin causes hunger (Wren et al., 2000) in rodents, but inhibits it in chicks (Furuse et al., 2001, Saito et al., 2002), and peptide YY and pancreatic polypeptide stimulate food intake in chicks (Kuenzel et al., 1987, Ando et al., 2001), but inhibit it in rodents.

Figure 1 (Above) Several nuclei are considered key in homeostatic appetite regulation including the paraventricular nucleus (PVN), dorsal medial nucleus (DMN), lateral hypothalamic area (LHA), ventromedial hypothalamus (VMH) and the arcuate nucleus (ARC). The ARC has numerous projections to the superior nuclei and has a dense concentration of neuropeptide Y (NPY) and proopiomelanocortin (POMC) somata.

Gallus gallus

- Intensely selected for rapid growth and muscle development
- Has lost the ability to self regulate food intake which results in development of obesity
- May provide insight on eating disorders in humans

Coturnix japonica

- Dramatically less selection pressure than in chicken
- Much closer to wild-type bird than chicken
- Can be studied in laboratory settings with hypothesis-driven experimental designs without confounds of stress
- Results can provide an evolutionary perspective on appetite regulation

SP in *Gallus gallus*

Figure 5 (right) To determine if a hypothalamic mechanism was responsible, c-Fos immunoreactivity was quantified in the hypothalamus of SP-injected chicks. The paraventricular nucleus was activated.

Figure 6 (right) Representative c-Fos immunoreactive staining in the PVN of SP-injected (A) or vehicle-treated (B) chicks. The borders of the PVN are outlined by the dashed line.

Figure 7 (left) Whole hypothalamus samples were screened for appetite-associated factor mRNA abundance, but no differences were detected.

Figure 8 (right) Paraventricular nucleus biopsy revealed increased expression of urotensin in SP-injected chicks.

SP in *Coturnix japonica*

Figure 12 (left). c-Fos immunoreactivity was quantified to determine which hypothalamic nucleus was responsible for SP-injected anorexia. The only difference was detected in the rostral LHA, a reduction in the number of c-Fos positive soma. This is different than chickens where the PVN was activated after SP injection. This difference is likely the result of artificial selection in the chicken.

Figure 13 (left). Based on c-Fos quantification, LHA was collected from SP-injected quail and AgRP mRNA measured. AgRP mRNA expression was decreased in the LHA. To compare to chicken, PVN was collected but UTS mRNA was not affected, lateral hypothalamus (LHA). Values are the mean ± SE, asterisks denote significant difference from vehicle, n = 15 vehicle and 18 SP-injected. Insert is a representative hypothalamus post-LHA punch.

A comprehensive behavior analysis was performed on SP-injected quail. Behaviors including distance traveled, food pecks, exploratory pecks, jumps, defecations, steps, escape attempts, standing time, sitting time, resting time, preening time, drinking time. SP-injected quail moved more, but no other behaviors were affected. This implies that the effect on food intake is primary, not secondary to some competitive behavior. Additionally, that the quail did not show signs of malaise, implies that the reduction in food intake is likely a true appetite effect, not secondary to sickness.

SP in *Gallus gallus*

Figure 2 (left). When centrally administered to young chickens, SP was associated with a dose-dependent reduction in food intake. Values are the mean ± SE, bars with different superscripts are different from each other within a time point (P < 0.05), n = 5-7 chicks per dose.

Figure 3 (right). Although food intake was reduced, there were no dipsogenic effects observed. Data are expressed as mean ± SE, n = 5 to 7 chicks per dose.

Figure 4 (left). To start elucidating the central mechanism of action, dienocephalon were collected from SP-injected chicks and real-time PCR performed. No differences were detected.

Figure 4 (right). To start elucidating the central mechanism of action, dienocephalon were collected from SP-injected chicks and real-time PCR performed. No differences were detected.

SP in *Coturnix japonica*

Figure 9 (left & right). SP caused reduced food intake in quail on a non-cumulative (left) and cumulative (right) basis. The threshold of dose response was 4X lower in quail than chickens. Compensatory food intake was not observed (right) - SP exerted a sustaining effect.

Figure 10 (left). Water intake was not affected on either a non-cumulative (far left) or cumulative (near left) basis. This lack of a dipsogenic effect is consistent with chicken. Data are expressed as mean ± SE, n = 12 chicks per dose.

Figure 11 (right). Whole hypothalamus from SP-injected quail were isolated 1 h post-injection and a variety of appetite-associated factor mRNAs were measured. It was expected that anorexigenic factors would have increased expression, but this hypothesis was not supported. Agouti-related peptide (AgRP) mRNA was reduced in SP-injected quail. AgRP was not measured in chicken. Data are expressed as mean ± SE, n = 12 chicks per group.

Conclusions

- Central SP is a more potent satiety signal in quail than chicken.
- The central SP-satiety hypothalamic circuit is different in quail than chicken.
- In chicken, it appears that SP induces satiety, but in quail it appears that SP reduces hunger.
- The reduction in SP efficacy in chicken is likely due to artificial selection. Selection likely reduced the potency of anorexigenic factors, which contributes to the chicken's accelerated growth.
- This may have implication in understanding a variety of eating disorders across species, including humans.
- SP is likely a reasonable target for the pharmacological reversal of over eating.

Works Cited

Smallbone, G., Jeffrey, G., Maitland, N., Shillington, K., Hagg, D. et al. (2012). Whole-brain gene expression of feeding and food intake. *Behavioral Brain Research*, 232, 304-311.

Smallbone, G., Jeffrey, G., Maitland, N., Shillington, K., Hagg, D. et al. (2013). Whole-brain gene expression of feeding and food intake. *Behavioral Brain Research*, 242, 1-11.

Smallbone, G., Jeffrey, G., Maitland, N., Shillington, K., Hagg, D. et al. (2014). Whole-brain gene expression of feeding and food intake. *Behavioral Brain Research*, 255, 1-11.

Smallbone, G., Jeffrey, G., Maitland, N., Shillington, K., Hagg, D. et al. (2015). Whole-brain gene expression of feeding and food intake. *Behavioral Brain Research*, 278, 1-11.

Smallbone, G., Jeffrey, G., Maitland, N., Shillington, K., Hagg, D. et al. (2016). Whole-brain gene expression of feeding and food intake. *Behavioral Brain Research*, 300, 1-11.

Smallbone, G., Jeffrey, G., Maitland, N., Shillington, K., Hagg, D. et al. (2017). Whole-brain gene expression of feeding and food intake. *Behavioral Brain Research*, 320, 1-11.

Smallbone, G., Jeffrey, G., Maitland, N., Shillington, K., Hagg, D. et al. (2018). Whole-brain gene expression of feeding and food intake. *Behavioral Brain Research*, 340, 1-11.

Smallbone, G., Jeffrey, G., Maitland, N., Shillington, K., Hagg, D. et al. (2019). Whole-brain gene expression of feeding and food intake. *Behavioral Brain Research*, 360, 1-11.

Smallbone, G., Jeffrey, G., Maitland, N., Shillington, K., Hagg, D. et al. (2020). Whole-brain gene expression of feeding and food intake. *Behavioral Brain Research*, 380, 1-11.

Smallbone, G., Jeffrey, G., Maitland, N., Shillington, K., Hagg, D. et al. (2021). Whole-brain gene expression of feeding and food intake. *Behavioral Brain Research*, 400, 1-11.

Smallbone, G., Jeffrey, G., Maitland, N., Shillington, K., Hagg, D. et al. (2022). Whole-brain gene expression of feeding and food intake. *Behavioral Brain Research*, 420, 1-11.

36 Month EEG Predicts Reading Achievement at Age Six through Executive Function

Katherine Vlahcevic, Alleyne Broomell, and Martha Ann Bell
Virginia Polytechnic Institute & State University, Blacksburg VA

Background: Electroencephalogram (EEG) is a measure of electrical activity in the brain. (Britton, 2016). EEG is used to measure cortical maturity and is associated with an increase in executive function skills (Almas, 2012). Executive function and contributes to children's word and non-word reading skills (Cartwright, 2012). At 6 years old, reading skills improve from understanding basic sight words to major phonological and comprehension development. Children at 6 years old begin to identify words by sounding them

We hypothesized that EEG at 3 years old would predict 6-year-old executive function which would then predict 6 year old reading achievement in a typically developing sample.

Our structural equation model shows that EEG at 36 months predicts executive function at 6 years, $p = .007$. Subsequently, concurrent EF predicts reading achievement at 6 years, $p < .001$.

Methods: At 36 months the baseline EEG was recorded with a 16 channel cap while the child watched a one-minute clip of turtles swimming from Finding Nemo. At 6 years old the children completed the reading achievement tests and the EF tasks. To test for reading achievement the children completed Woodcock-Johnson Passage Comprehension and Woodcock-Johnson Reading Fluency, which are standardized measures of academic achievement. For the EF battery three tasks were completed. The first task was the Dimension Change Card Sort (DCCS), a card sorting task that measures cognitive flexibility. Children sorted a series of cards by either color or shape then were instructed to sort by one dimension if the card had a border and the other dimension if the card did not have a border. Proportion correct on the borders condition was the variable of interest. The Number Stroop is an age appropriate measure of inhibitory control. The child was given a set of numbers, ex: 444 and asked to report the number of digits on the screen, not the numbers themselves. Response time or how long it took them to answer was the variable of interest. The Backwards Digit Span task asked children to repeat a string of numbers backwards as measure of working memory, with the number of digits increasing until the child could no longer perform the task. The highest correct span was the variable of interest.

	β	B	SE
EEG 3Yrs ---> EF 6Yrs	-.300	-.135	.050
EF 6Yrs ---> Reading 6Yrs	.863	30.990	8.318
EF 6Yrs ---> DCCS	.389	.240	.069
EF 6Yrs ---> Stroop	-.500	-.516	.131
EF 6Yrs ---> BD	.384	1.000	
Reading 6Yrs ---> Reading Fluency	.952	1.000	
Reading 6Yrs ---> Passage Comprehension	.955	.525	.034

Table 1: Table of Beta and B values

The fit statistics for our model are mixed, with a chi-square value of 15.976, $df = 8$, $p = .043$, suggesting the model is not a good fit for the data and we should reject the null. However, the Root Mean Square Error of Approximation (RMSEA) was .057, suggesting a statistically acceptable fit and the Comparative Fit Index (CFI) value for the model was .973, which indicates the model to be a good fit for the data. The significant chi-square value may be due to the large sample size and taken in conjunction with the other goodness-of-fit statistics does not warrant a rejection of the model.

Discussion: Our findings show that the EEG, a measure of cortical maturity, at 36 months is able to predict EF at 6 years old, which in turn predicts reading achievement. The path between EEG and EF is negative showing that less power during baseline the higher EF skills the child will have later in development. When looking at the EF battery, DCCS and backwards digit span both loaded positively to executive function. However, the Stroop loaded negatively because a lower response time indicated the child was able to inhibit their response more quickly, therefore demonstrating greater EF.

Results: EF was measured through three tasks, DCCS, stroop, and backwards digit span, all of which loaded onto a single EF factor, $p < .001$. The tests for reading achievement were Woodcock-Johnson Passage Comprehension Test and Woodcock-Johnson Reading Fluency, which loaded onto a reading achievement factor, $p < .001$.

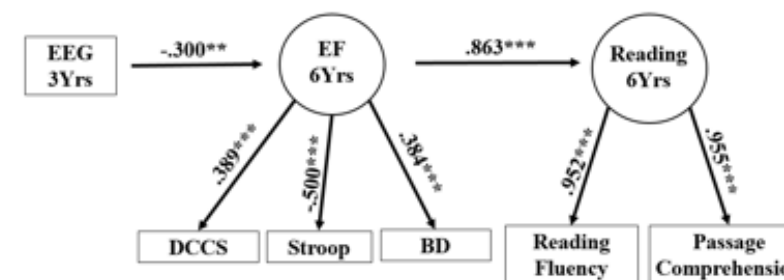


Figure 1: Structural Equation Model

36 Month EEG Predicts Reading Achievement at Age Six through Executive Function

Katherine Vlahcevic, Alleyne Broomell, and Martha Ann Bell
Virginia Tech

kvlah13@vt.edu

Introduction Method Results cont.

Electroencephalogram (EEG) is the measure of electrical activity in the brain. (Britton, 2016). EEG is used to measure cortical maturity and is associated with an increase in executive function skills (Almas, 2012).

Executive function (EF) is a higher cognitive processes that controls goal-directed behaviors. EF skills include working memory, inhibitory control, cognitive flexibility and more. EF is critical for reading development in elementary school years and contribute to children's word and non-word reading skills (Cartwright, 2012).

At 6 years old, reading skills improve from understanding basic sight words to major phonological and comprehension development. Children at 6 years old begin to identify words by sounding them out and even begin to read on their own (Carnine, 2014).

Developing basic reading skills is essential because they provide basic building blocks of education and contribute to the future success of in school. (Dickinson & Porche, 2011)

We hypothesized that EEG at 3 years old would predict 6 year old executive function which would then predict 6 year old reading achievement in a typically developing sample.

Participants

At 36 months old, 199 children came in for testing. All children were born full term with no complications, representing a typically developing sample. At 6 years old, 185 children completed DCCS, 190 completed digit span, 187 completed number stroop, 146 completed Woodcock Johnson Reading Fluency and 191 completed Woodcock Johnson Passage Comprehension

References

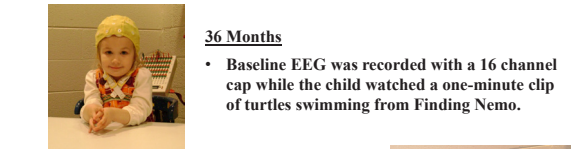
Almas, A. N., K. A. Depress, A. Bahadrasa, C. A. Nelson, C. H. Zeanah, and N. A. Fox. "Effects of early intervention and the moderating effects of brain activity on developmental outcomes in low-income children." *Proceedings of the National Academy of Sciences* 113(2012): 11218-11223. Web.

Britton, J. E., J. C. Hogg, J. H. Gilmore, M. L. Lomb, E. K. Fry, C. Gilmore. *Electroencephalography (EEG): An Introductory Text and Atlas of Normal and Abnormal Findings in Adults, Children, and Infants* (Harcourt, Chicago: American Epilepsy Society; 2016). Available from:

Cartwright, B. W., S. Sherrill, J. R. Kover, et al. (2012). Reading Development: Child's Model. Direct Instruction Reading. *Curriculum, Instruction, and Assessment* 2(1), 24-30. doi:10.1080/19402022.2012.641922.

Dickinson, D. K., & Porche, M. V. (2011). Relations Between Language Experiences in Preschool Classrooms and Children's Kindergarten and Fourth-Grade Language and Reading Abilities. *Child Development* 82(3), 879-886. doi:10.1111/j.1467-8624.2011.01877.x

Goldman, R., & Schneider, L. (1997). Early Language Development and Kindergarten Phonological Awareness as Predictors of Reading Proficiency From 3 to 8 Years of Age. *Cross-Language Studies of Learning to Read and Spelling* 20(1), doi:10.1080/0709-9442.1997.10551316



- 36 Months**
- Baseline EEG was recorded with a 16 channel cap while the child watched a one-minute clip of turtles swimming from Finding Nemo.

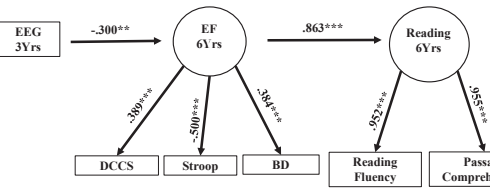
- 6 Years**
- Woodcock-Johnson Passage Comprehension Test and Woodcock-Johnson Reading Fluency Test
 - EF Battery
 - Dimension Change Card Sort (DCCS)
 - Card sorting task that measures cognitive flexibility. Borders condition was the variable of interest.
 - Number Stroop
 - An age appropriate measure of inhibitory control. Response time during the mixed condition was the variable of interest.
 - Backwards Digit Span
 - Asked children to repeat a string of numbers backwards as measure of working memory. Highest span was the variable of interest.

Results

EF was measured through three tasks, cognitive flexibility, inhibitory control and working memory, all of which loaded onto a single EF factor, $p < .001$. The tests for reading achievement were Woodcock-Johnson Passage Comprehension Test and Woodcock-Johnson Reading Fluency, which loaded onto a reading achievement factor, $p < .001$. Our structural equation model shows that EEG at 36 months predicts executive function at 6 years, $p = .007$. Subsequently, concurrent EF predicts reading achievement at 6 years, $p < .001$. The fit statistics for our model are mixed, with a chi-square value of 15.976, $df = 8$, $p = .043$, suggesting the model is not a good fit for the data and we should reject the null. However, the Root Mean Square Error of Approximation (RMSEA) was .057, suggesting a statistically acceptable fit and the Comparative Fit Index (CFI) value for the model was .973, which indicates the model to be a good fit for the data. The significant chi-square value may be due to the large sample size and does not warrant that the model be completely discarded.

Table 1.

	β	B	SE
EEG 3Yrs ---> EF 6Yrs	-.300	-.135	.050
EF 6Yrs ---> Reading 6Yrs	.863	30.990	8.318
EF 6Yrs ---> DCCS	.389	.240	.069
EF 6Yrs ---> Stroop	-.500	-.516	.131
EF 6Yrs ---> BD	.384	1.000	
Reading 6Yrs ---> Reading Fluency	.952	1.000	
Reading 6Yrs ---> Passage Comprehension	.955	.525	.034



Model 1. Structural Equation Model * $p < .05$, ** $p < .01$, *** $p < .001$

Discussion

Our findings show that the EEG, a measure of cortical maturity, at 36 months is able to predict EF at 6 years old, which in turn predicts reading achievement. Major executive function skills start to development at 3 years old (Cartwright, 2012). This information could help children from a young age who are at risk for developing issues with reading obtain professional guidance. If children start to develop greater executive function skills at a younger age then this may increase their school readiness.

Grant sponsor - NIH/NICHHD
R01 HD049878; R03 HD043057

(EF) is a higher cognitive processes that controls goal-directed behaviors. EF skills include working memory, inhibitory control, cognitive flexibility and others. EF is critical for reading development in elementary school years out and even begin to read on their own (Carnine, 2014). Developing basic reading skills is essential because they provide basic building blocks of education and contribute to future success in school. (Dickinson & Porche, 2011).

Future directions could include investigating an indirect between EGG at 36 months old and reading achievement at 6 years old. Additionally, future work could be to see if cortical maturity at even younger ages predicts EF and reading with the same pattern demonstrated here.

Extracellular Matrix Degradation Causes Reactive Astrogliosis

Kalirroi Engel, Bhanu P. Tewari, and Harald Sontheimer

Virginia Tech School of Neuroscience, Virginia Tech Carilion Research Institute Undergraduate Research Fellowship Recipient, School of Neuroscience at Virginia Tech

Background: Extracellular matrix has been known to influence the neuronal activity and synaptic plasticity. In different regions of the brain, extracellular matrix forms lattice like structures known as perineuronal nets (PNNs). The PNNs are specialized assemblies of chondroitin sulfate proteoglycans (CSPGs), tenascin-R, hyaluronan and link proteins that surround fast spiking parvalbumin interneurons in the cerebral cortex. PNNs ensheath cell soma, axon and proximal dendrites, and lattice holes are the only access points for the interaction with astrocytes. Due to this space constrain, astrocytes may have a unique physiological relationship with the PNN surrounded neurons. The spatial proximity of astrocytic processes and neurons is critical for the smooth ongoing of astrocytic housekeeping functions such as extracellular K⁺ buffering and glutamate clearance. We hypothesized that to balance this space constrain astrocytic processes in contact with the PNN holes might possess specialized activity domains. These domains might have differential expression of astrocytic proteins involved in neuron glia information exchange and housekeeping functions.

Methods: Adult B16 (Black 6) mice were intracranially injected with Chondroitinase ABC (ChABC) enzyme, which degrades the chondroitin sulfate chains in PNNs and interstitial matrix. Animals were transcardially perfused with paraformaldehyde for whole body fixation and brains were dissected out. Brains were sectioned with a vibratome to obtain 50 micrometer thin sections and stored in phosphate buffer saline for storage until usage. Sections were immunostained with primary antibody for PNN marker WFA (wisteria Floribunda Agglutinin), 2B6 (an antigen stub which is exposed after CSPG degradation), and GFAP (glial fibrillary acidic protein) to stain the astrocytes. Appropriate fluorophore tagged secondary antibodies were used to detect the antigen bound primary antibodies. On staining completion section were mounted on slides and images were taken with the Nikon A1 confocal microscope.

Results: First we confirmed the PNN/CSPG degradation by WFA staining. We observed that ChABC injection causes widespread ECM/PNN degradation exhibited as negligible WFA staining and disintegrated PNNs. Contrary to the injected hemisphere, the contralateral half as well as the PBS injected brain exhibited normal WFA staining and intact PNNs. Secondly, the 2B6 staining in the injected area confirmed ECM degradation by ChABC. Chondroitin sulfate cleavage by ChABC exposes 2B6 antigen which can be stained with Anti-2B6 Igs. The combined staining of 2B6 and WFA further proved PNN degradation due to ChABC, showing an inverse relationship between the 2B6 and WFA stains. Most importantly, we observed a global reactive astrogliosis in the ChABC injected hemisphere as evident by in-

Extracellular Matrix Degradation Causes Reactive Astrogliosis

Kalirroi Engel *1, Bhanu P. Tewari PhD 2, and Harald Sontheimer PhD 1,2

1. Virginia Tech School of Neuroscience, 2. Virginia Tech Carilion Research Institute Undergraduate Research Fellowship Recipient, School of Neuroscience at Virginia Tech

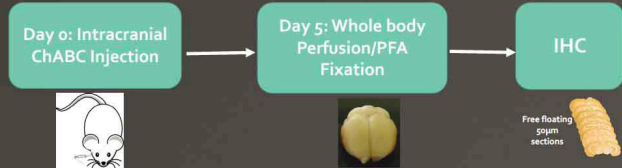


Introduction

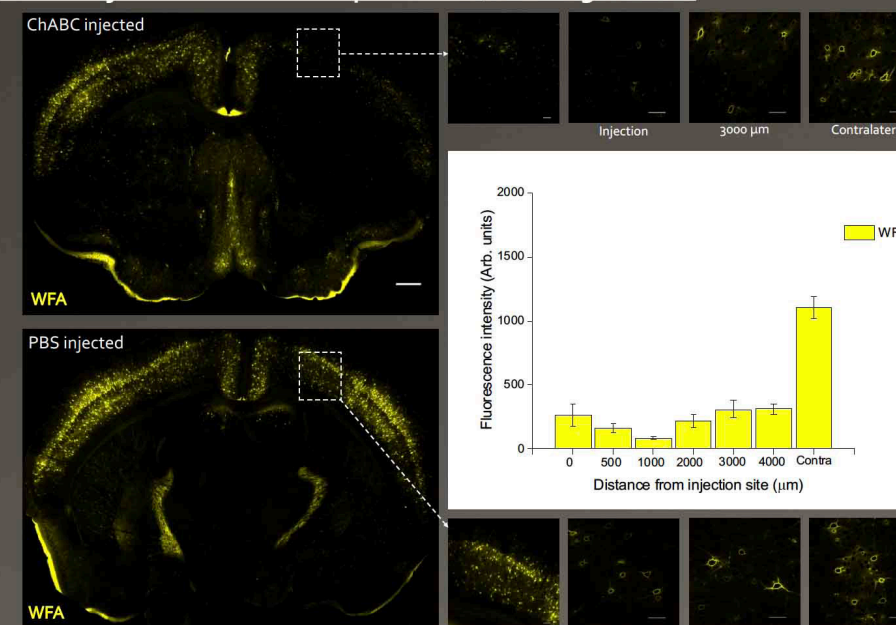
- ❑ The extracellular matrix (ECM) in the central nervous system constitutes: 1) basement membrane, 2) Interstitial matrix, and 3) Perineuronal Nets (PNNs).
- ❑ PNNs are specialized lattice like structures consisting of chondroitin sulfate proteoglycans (CSPGs), hyaluronic acid (HA), Tenascin R, aggrecan and various linker proteins.
- ❑ PNNs are believed to maintain ionic homeostasis and consequently neuronal function owing to the high density of negative charges on CSPGs.
- ❑ Alterations in PNNs have been reported in various CNS disorders.
- ❑ **Aim of the study:** Present study intends to explore the consequences of ECM degradation on physio-chemical attributes of neurons and glial cells.

Methods

Adult B16 mice were intracranially injected with Chondroitinase ABC (ChABC) enzyme, which degrades the chondroitin sulfate chains of PNNs and interstitial matrix leading to disintegration of PNN architecture. PNNs can be visualized by wisteria floribunda agglutinin (WFA) staining.

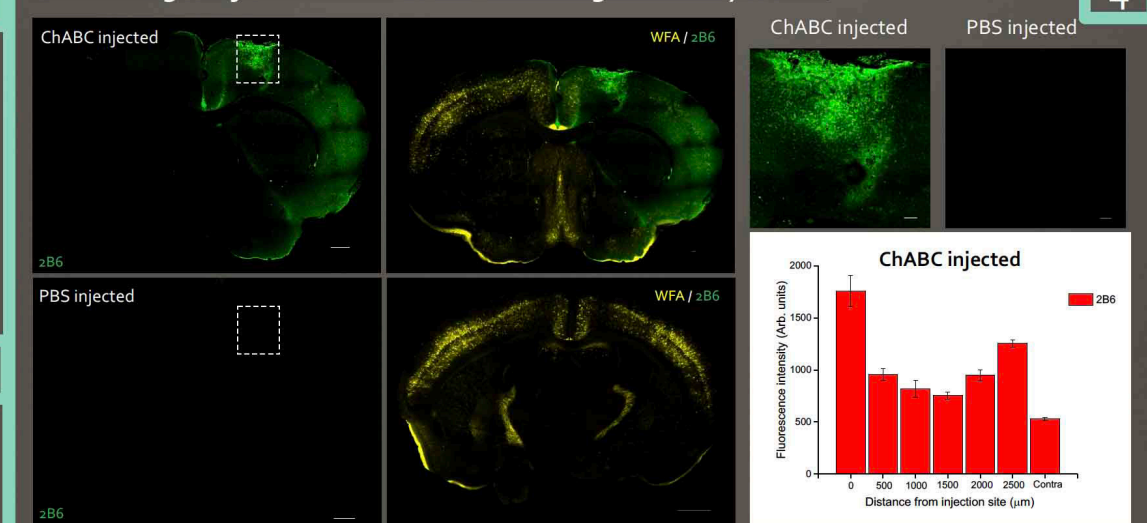


ChABC Injection Causes Widespread ECM/PNN degradation



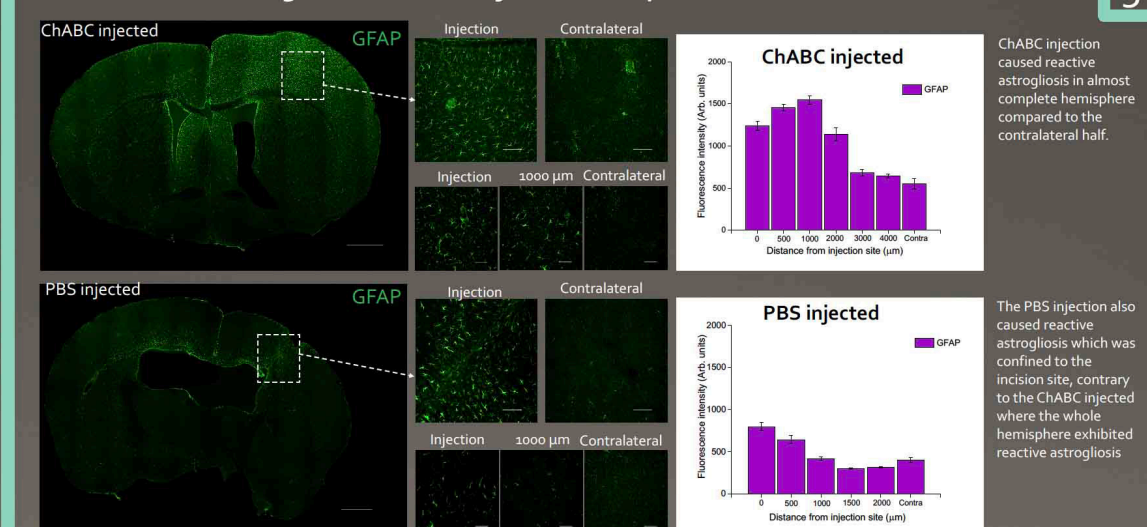
The ChABC injected hemisphere exhibited negligible WFA staining (Top Right) indicative of PNN degradation. Contrary to the injected hemisphere, the contralateral half and PBS injected brain halves exhibited normal WFA staining. The above bar diagram shows the mean±SEM of WFA fluorescence intensity at different distances from the site of ChABC injection.

2B6 Staining in Injected Area Confirmed ECM Degradation by ChABC



Chondroitin sulfate cleavage by ChABC exposes 2B6 antigen which can be stained with Anti-2B6 Igs. The images above further confirm the PNNs degradation by ChABC. Inverse relationship of WFA and 2B6; the more intense 2B6 stain, the less intense WFA and vice versa.

Global Reactive Astrogliosis in ChABC Injected hemisphere



ChABC injection caused reactive astrogliosis in almost complete hemisphere compared to the contralateral half.

The PBS injection also caused reactive astrogliosis which was confined to the injection site, contrary to the ChABC injected where the whole hemisphere exhibited reactive astrogliosis.

Summary: ❖ ChABC injection in mice brain leads to widespread PNN disintegration and reactive astrogliosis.
❖ Next is to investigate spatial and temporal aspects of PNN degradation and reactive astrogliosis by ChABC and the mechanisms by which PNN degradation causes reactive astrogliosis

Acknowledgements: Lata Chaunsali, Dipan Patel, Ian Kimbrough and Paul Youmans

creased GFAP positive cells. Spatially, the ChABC injection causes reactive astrogliosis in almost the complete hemisphere compared to the contralateral half. In the sham animal we observed that reactive astrogliosis, which was confined to the injection site. This suggests that reactive astrogliosis in ChABC injected animals was a

consequence ECM degradation rather than the incision.

Conclusion: In conclusion, we observed that ChABC injection in mice brains can lead to widespread PNN disintegration and reactive astrogliosis, which may have pathological consequences.

Dysfunctions of the Gliovascular Unit in Alzheimer Disease

Emily Barritt, Ian F. Kimbrough, William A. Mills III, Lata Chausali, Chris Liao, Harald Sontheimer
 Virginia Polytechnic Institute, Virginia Tech School of Neuroscience, VT Carillion Research Center, Center for Glial Biology

The gliovascular unit (GVU), consisting of astrocytes and its processes, associated neurons, and microvessels blood vessels functions to maintain homeostasis. In this unit, astrocytes function to regulate local blood flow. In addition to this role, astrocytes also serve to maintain tight junction proteins, which make up the blood brain barrier (BBB)—the brain's main line of defense against blood borne toxins. These roles are carried out by the release of vasoactive factors, which signal to the associate blood vessels. In a recent publication, our lab showed that an invading glioma tumor cell has the ability to invade the intimate space along the vasculature and displace the astrocytic end foot. The end foot, displaced by the tumor cell, was no longer able to signal the vasculature. Subsequently, breaches of the blood brain barrier, the brain's main line of defense, occurred. Associated down-regulations of tight junction proteins occurred as well.

Alzheimer's disease shows pathology that mirrors that of glioma. The larger amyloid beta aggregates, referred to as vascular amyloid, deposit along the vasculature in a similar location as the tumor cells. This similar placement lead to questions about how the GVU is affected in Alzheimer's disease (AD).

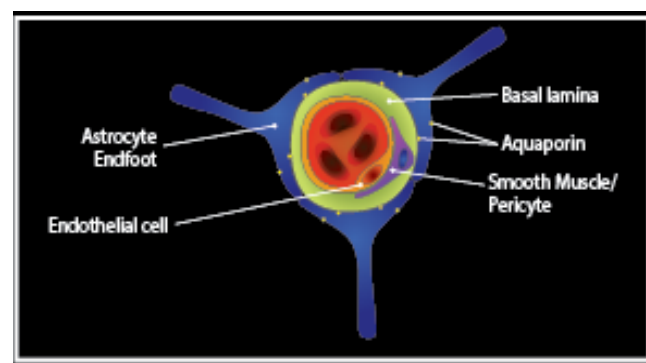


Figure 1 : The GliovascularUnit

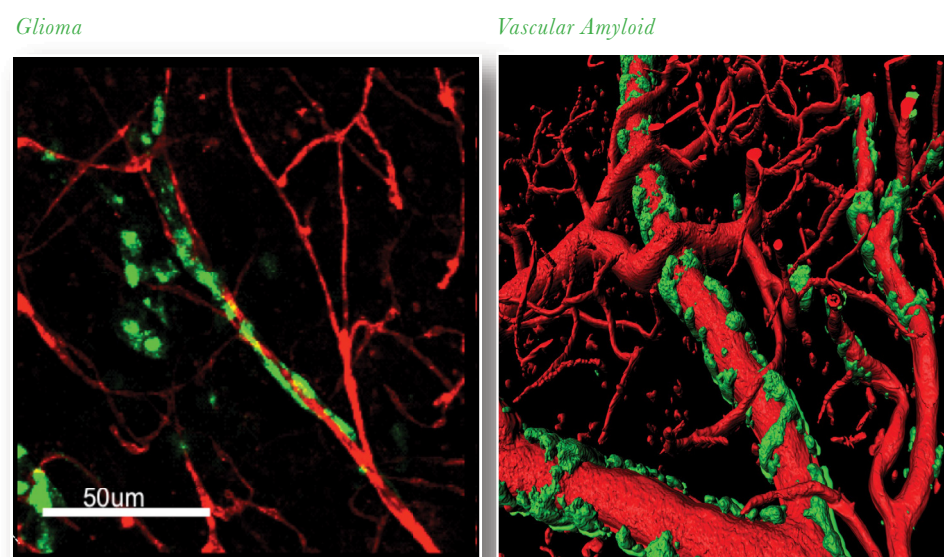
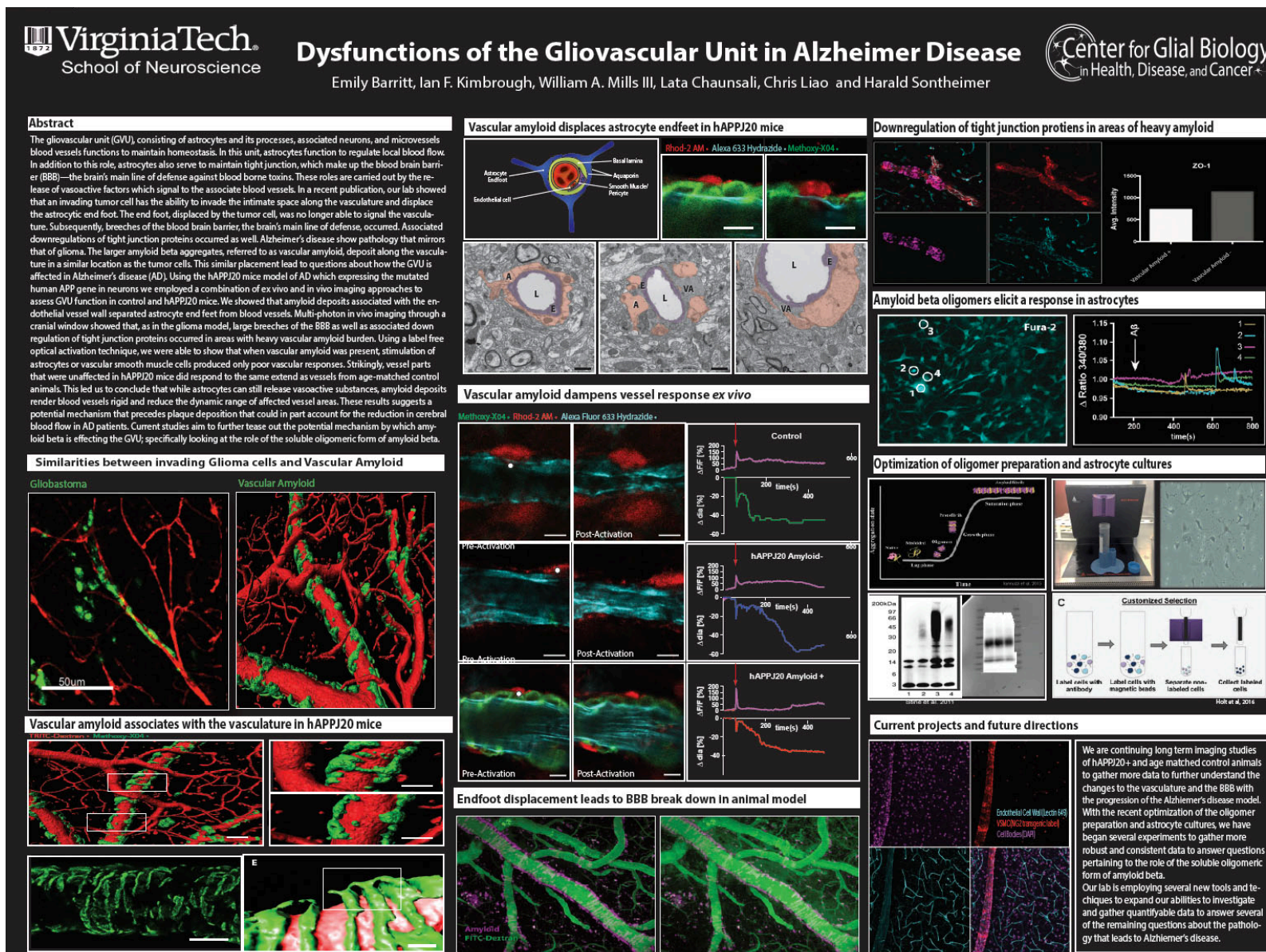


Figure 2: Glioma and Vascular Amyloid deposit in a similar area along the vasculature.

express the mutated human APP gene in neurons we employed a combination of ex vivo and in vivo imaging approaches to assess GVU function in control and hAPPJ20 mice. We showed that amyloid deposits associated with the endothelial vessel wall separated astrocyte end feet from blood amyloid was present, stimulation of astrocytes or vascular smooth muscle cells produced only poor vascular responses. Strikingly, vessel parts that were unaffected in hAPPJ20 mice did respond to the same extent as vessels from age-matched control animals. This led us to conclude that while astrocytes can still release vasoactive substances, amyloid deposits render blood vessels rigid and reduce the dynamic range of affected vessel areas. One interpretation of these results, is the aggregation of vascular amyloid is physically separating the endfeet from the vessel wall. Alternatively, another mechanism may exist that precedes plaque deposition that could in part account for the endfoot displacement and the reduction in cerebral blood flow in AD patients.

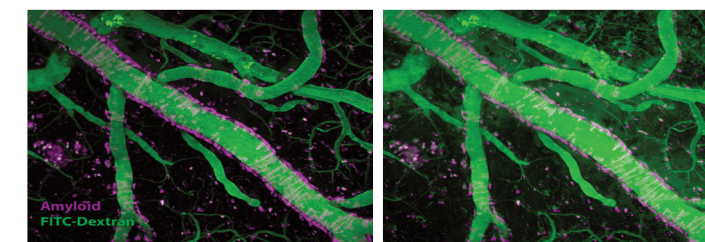


Figure 3: End foot displacement leads to BBB breach in animals with heavy vascular amyloid burden

Using the hAPPJ20 mice model of AD which express the mutated human APP gene in neurons we employed a combination of ex vivo and in vivo imaging approaches to assess GVU function in control and hAPPJ20 mice. We showed that amyloid deposits associated with the endothelial vessel wall separated astrocyte end feet from blood vessels. Multi-photon in vivo imaging through a cranial window showed that, as in the glioma model, large breaches of the BBB as well as associated down regulation of tight junction proteins occurred in areas with heavy vascular amyloid burden. Using a label free optical activation technique, we were able to show that when vascular

Current studies aim to further tease out the potential mechanism by which amyloid beta is effecting the GVU; specifically looking at the role of the soluble oligomeric form of amyloid beta. Our lab is employing several new tools and techniques to expand our abilities to investigate and gather quantifiable data to answer several of the remaining questions about the pathology that leads to Alzheimer's disease.

We are continuing long term imaging studies of hAPPJ20+ and age matched control animals to gather more data to further understand the changes to the vasculature and the BBB with the progression of the Alzheimer's disease model. In addition to the BBB long-term studies, we have begun several experiments to test the effects of soluble amyloid beta on astrocytes.

Lead induces widespread toxic effects in the developing tadpole brain

Erica Johnson, Alexa Figueroa Baiges, Shaan Sharma, Zahabiya Husain,

Husain,

Christopher K. Thompson

School of Neuroscience, Virginia Tech, Blacksburg VA

Background: Lead is known to be toxic to humans and has been shown to affect almost every organ system in the human body, particularly the central nervous system. Lead has the ability to take the place of calcium ions and cross the blood brain barrier inducing widespread toxic effects in the brain. The developing central nervous system is particularly sensitive, and lead toxicity has been shown to be associated with impaired cognition and behavioral disorders in children. Humans can be exposed to lead through drinking water or contaminated soil, and it is also used in car batteries. There is no known safe level of exposure, and the usage of lead in paint and gasoline has been banned. The Lead and Copper Rule imposed by the U.S. Environmental Protection Agency requires action to be taken if lead concentration in drinking water exceeds fifteen parts per billion (ppb). For perspective, during the Flint Water Crisis in Flint, Michigan, the average concentration of lead in home tap water was 27 ppb and as high as 158 ppb in the Virginia Tech study of 2015. *Xenopus laevis* served as our model because their external development allows observation of the early stages of brain development that occur in utero in many mammalian systems. This model is also useful because they are acutely sensitive to changes in thyroid hormone which critical to metamorphosis and whose signaling is thought to be disrupted by lead toxicity. An experiment in zebrafish showed that lead is an endocrine disruptor and caused a decrease in thyroid hormone signaling. In this experiment, we looked at overall widespread toxic effects of lead in the brain of *Xenopus laevis*. We also examined if lead toxicity is associated with a decrease in transthyretin, a protein that transports thyroid hormone in the blood.

Methods: *Xenopus laevis* served as our model because their external development allows observation of the early stages of brain development that occur in utero in many mammalian systems. This model is also useful because they are acutely sensitive to changes in thyroid hormone which critical to metamorphosis and whose signaling is thought to be disrupted by lead toxicity.

We worked with albino tadpoles NF stage 46-47 (7-10 days old). The tadpoles were placed into one of eight groups: a control bath or seven concentrations of lead (II) acetate trihydrate (10 ppb, 50 ppb, 100 ppb, 500 ppb, 1,000 ppb, 10,000 ppb, and 100,000 ppb) for four days. These concentrations were made with two different stock solutions of 26.3 M and 0.263 M in water and then diluted into 1X Steinburg's solution. Groups of tadpoles were reared in 200ml of solution for four days. Tadpoles were killed on Day 4 with an overdose of MS222 and fixed overnight in 4%PFA. Standard immunohistochemistry methods were used to stain whole-mount brains for H2AX (Millipore-Sigma, 1:400), Caspase-3 (AbCam, 1:400), and Sytox-O (Life Sciences, 1:500).



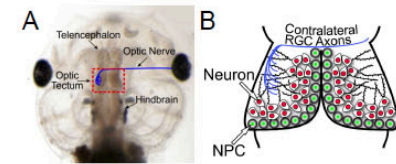
Lead induces widespread toxic effects in the developing tadpole brain

Erica Johnson, Alexa Figueroa Baiges, Shaan Sharma, Zahabiya Husain, Christopher K Thompson
School of Neuroscience, Virginia Tech, Blacksburg VA



Introduction

Lead is known to be toxic to humans and has been shown to affect almost every organ system in the human body, particularly the central nervous system. Lead has the ability to take the place of calcium ions and cross the blood brain barrier inducing widespread toxic effects in the brain. The developing central nervous system is particularly sensitive, and lead toxicity is shown to be associated with impaired cognition and behavioral disorders in children. Humans can be exposed to lead through drinking water or contaminated soil, and it is also used in car batteries. There is no known safe level of exposure, and the usage of lead in paint and gasoline has been banned. The Lead and Copper Rule imposed by the U.S. Environmental Protection Agency requires action to be taken if lead concentration in drinking water exceeds fifteen parts per billion. For perspective, during the Flint Water Crisis in Flint, Michigan, the average concentration of lead in home tap water was 27 ppb and as high as 158 ppb in the Virginia Tech study of 2015. *Xenopus laevis* served as our model because their external development allows observation of the early stages of brain development that occur in utero in many mammalian systems. This model is also useful because they are acutely sensitive to changes in thyroid hormone which critical to metamorphosis and whose signaling is thought to be disrupted by lead toxicity. An experiment in zebrafish showed that lead is an endocrine disruptor and caused a decrease in thyroid hormone signaling. In this experiment, we looked at overall widespread toxic effects of lead in the brain of *Xenopus laevis*. We also examined if lead toxicity is associated with a decrease in transthyretin, a protein that transports thyroid hormone in the blood.



A) Dorsal aspect of the head of a *Xenopus laevis* tadpole. B) A schematic diagram of the midbrain area in the red box in A illustrating the retino-tectal circuit. Neural progenitor cells (NPC, green) are found in the ventricular proliferative zone. Neurons (red) are generated from NPCs. They extend dendrites (black) into the neuropil where they form synapses with other tectal neurons and/or RGC axons (blue).

Methods

Animals: *Xenopus laevis* albino tadpoles NF stage 46-47 (7-10 days old).

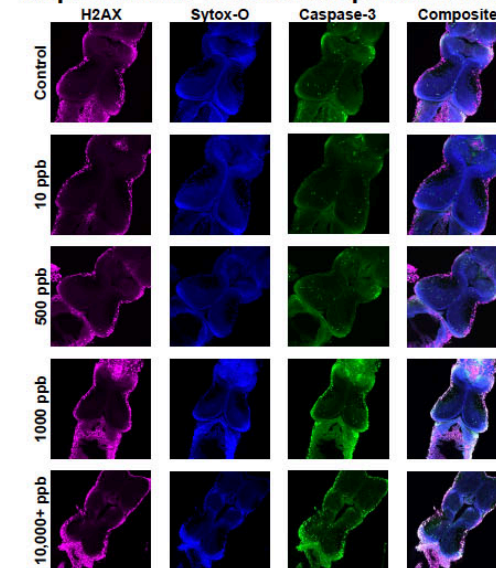
Lead treatment: tadpoles were placed into one of eight groups: a control bath or seven concentrations of Lead(II) acetate trihydrate (10 ppb, 50 ppb, 100 ppb, 500 ppb, 1,000 ppb, 10,000, and 100,000 ppb) for four days. These concentrations were made with two different stock solutions of 26.3 M and 0.263 M in water and then diluted into 1X Steinburg's solution. Groups of tadpoles were reared in 200ml of solution for four days.

Sacrifice and tissue processing: Tadpoles were killed on Day 4 with an overdose of MS222 and fixed overnight in 4%PFA. Standard immunohistochemistry methods were used to stain whole-mount brains for H2AX (Millipore-Sigma, 1:400), Caspase-3 (AbCam, 1:400), and Sytox-O (Life Sciences, 1:500).

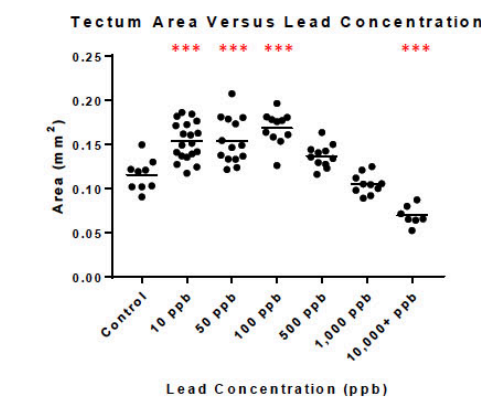
Imaging and analysis: PFA-fixed brains were imaged on a Leica SP8 confocal microscope, and images were analyzed with ImageJ.

10,000, and 100,000 ppb) for four days. These concentrations were made with two different stock solutions of 26.3 M and 0.263 M in water and then diluted into 1X Steinburg's solution. Groups of tadpoles were reared in 200ml of solution for four days. Tadpoles were killed on Day 4 with an overdose of MS222 and fixed overnight in 4% paraformaldehyde. Standard immunohistochemistry methods were used to stain whole-mount brains for H2AX (Millipore-Sigma, 1:400), Caspase-3 (AbCam, 1:400), and Sytox-O (Life Sciences, 1:500), all markers for cell toxicity. PFA-fixed brains were then imaged on a Leica SP8 confocal microscope, and images were analyzed with ImageJ.

Lead exposure induces neural toxicity in tadpole brains in a dose-dependent manner

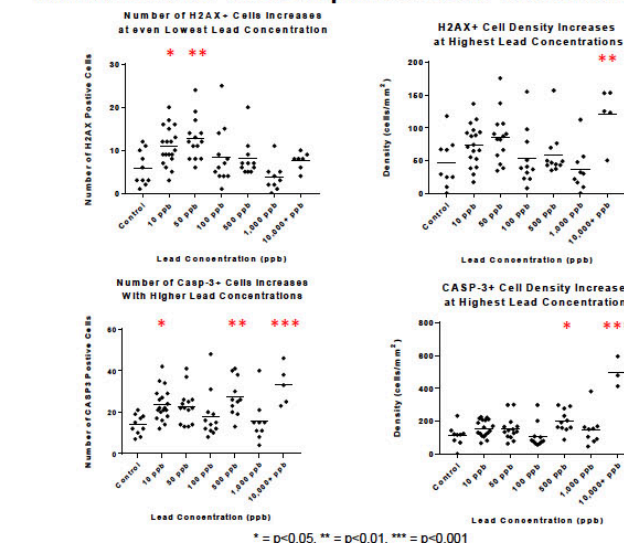


Z-projections of confocal stacks of example optic tecta from Day4. H2AX stain is shown in magenta, sytox stain is shown in blue, and Casp-3 stain is shown in green. These images show an increase in cells positive for markers of cell death with an increase in lead concentration.



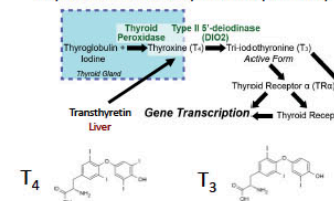
Lead induces a highly significant change in tectum area relative to control across different concentrations. *** = $p < .001$

Lead exposure increases expression of cell death markers H2AX+ and Caspase-3+ cells in the brain



Lead appears to lower expression of transthyretin in the liver

Thyroid hormone synthesis pathway



Conclusions

- Increased lead concentration was associated with higher quantity and density of H2AX and Caspase-3 positive cells.
- Lead also induced changes in tectum area. Lower lead concentrations increased area relative to CNTL, while the highest concentrations of lead decreased tectum area. This dynamic effect may have been caused by swelling in the brain due to the harmful effects of the lead and then a decompensation when cells began to die from the toxicity.
- Lead toxicity in the brain may be associated with a decrease in thyroid hormone signaling or a reduction in circulation of the hormone due to decreased levels of transport protein.
- At even the lowest concentration of lead (10 ppb), there was an increase in cell death and swelling of the brain. This is alarming because this concentration is below the EPA safety standard of 15 ppb in drinking water in the United States.

Acknowledgements

Many thanks to Shaan Sharma, Zahabiya Husain, Alexa Baiges, and Stacy Spitzer, for their assistance with this project. This work is funded by the Engel Novitt James and Lillian Gay and Virginia Tech School of Neuroscience Fellowship and NIEHS grant R00ES022992.

Results: The data shows a significant dose dependent change in the area of the tectum; the lowest concentrations of lead showed an increase in area and then dropped off at the highest concentrations to below control. There was also a significant difference in cells positively marked for both H2AX and caspase-3 even at the lowest concentration of lead, 10 ppb. Density was then considered in order to account for the changes in tectum area. This showed significant increases in positively marked cells at the highest lead concentrations. We also observed that lead decreased expression of transthyretin in the liver in a dose-dependent manner.

Conclusions: Increased lead concentration was associated with higher quantity and density of cell-death markers H2AX and Caspase-3. Lead also induced changes in tectum area. Lower lead concentrations increased area relative to control, while the highest concentrations of lead decreased tectum area. This dynamic effect may have been caused by swelling in the brain due to the harmful effects of the lead and then a decomposition when cells began to die from the toxicity. Lead toxicity in the brain may also be associated with a decrease in thyroid hormone signaling or a reduction in circulation of the hormone due to decreased levels of transport protein. This is thought to be a more long-term process than the acute toxicity shown in this experiment. At even the lowest concentration of lead (10 ppb), there was an increase in cell death and swelling of the brain. This is alarming because this concentration is below the EPA safety standard of 15 ppb in drinking water in the U.S, and may be cause to reexamine the standards for safe drinking water in the United States.

Sulfasalazine as a Treatment for Acquired Epilepsy

Andrew Savoia, Oscar Alcoreza, Lata Chaunsali, Harald Sontheimer, Susan Campbell

Virginia Tech School of Neuroscience, Center for Glial Biology in Health, Disease, and Cancer, Virginia Tech Carilion Research Institute, Virginia Tech Carilion School of Medicine

Background: Epilepsy affects approximately 2.2 million Americans and 1-in-26 people will develop epilepsy within their lifetime. Current therapeutics, targeting neuronal networks, are not effective in 1-in-3 epileptics. A recent study revealed that glutamate release by primary brain tumors induce epilepsy in mice implanted with human glioma cells². System xc (xCT), a glutamate/cystine antiporter, was identified as a major contributor to elevated glutamate levels, which resulted in tumor associated epilepsy in these tumor-implanted mice. This glutamatergic hyperexcitability was also shown to be susceptible to inhibition of xCT via sulfasalazine (SAS), an FDA approved drug. Several mechanisms such as neuronal death, inflammation and gliosis have been suggested to play a role in acquired epileptogenesis, however, no clear consensus has been reached. Previous studies, in Alzheimer and ALS disease models, have shown that activated microglial cells express increased xCT with a corresponding increase in extracellular glutamate³. The effects of sulfasalazine on seizure activity have not been studied in other forms of acquired epilepsy. This project aims to elucidate the role of xCT in acquired epileptogenesis and to test whether sulfasalazine can be used as a broad acting anti-epileptic drug.

Methods: In order to study the effects of SAS, we used the kainic acid (KA) and beta-1 integrin knockout (KO) models of epilepsy. The KA model is a well characterized, chemically induced model of human temporal lobe epilepsy. The beta-1 KO model is a neuroinflammation model characterized by widespread gliosis leading to spontaneous seizures. One round of experiments lasted approximately 5 weeks consisting of EEG implantation, 24/7 video-EEG recording, SAS treatment and tissue analysis. SAS treatment consisted of two injections daily for 1 week. To study the effects of seizure induction and SAS treatment on xCT expression, we conducted qPCR and western blot experiments to look at mRNA and protein expression.

Results: Our preliminary findings showed that KA induced seizures and microglial activation in the hippocampus. The EEG recordings of KA-treated animals showed abnormal activity, which was restored by SAS treatment. In addition, treatment with SAS decreased hippocampal xCT protein levels compared to controls.



Sulfasalazine as a Treatment for Acquired Epilepsy

Andrew Savoia³, Oscar Alcoreza^{1,2}, Lata Chaunsali¹, Harald Sontheimer¹, Susan Campbell¹

¹ Center for Glial Biology in Health, Disease, and Cancer, Virginia Tech Carilion Research Institute

² Virginia Tech Carilion School of Medicine ³ Virginia Tech School of Neuroscience



Background

Epilepsy affects approximately 2.2 million Americans and 1-in-26 people will develop epilepsy within their lifetime. Current therapeutics, targeting neuronal networks, are not effective in 1-in-3 epileptics. A recent study revealed that glutamate release by primary brain tumors induce epilepsy in mice implanted with human glioma cells². System xc (xCT), a glutamate/cystine antiporter, was identified as a major contributor to elevated glutamate levels, which resulted in tumor associated epilepsy in these tumor-implanted mice. This glutamatergic hyperexcitability was also shown to be susceptible to inhibition of xCT via sulfasalazine (SAS), an FDA approved drug. Several mechanisms such as neuronal death, inflammation and gliosis have been suggested to play a role in acquired epileptogenesis, however, no clear consensus has been reached. Previous studies, in Alzheimer and ALS disease models, have shown that activated microglial cells express increased xCT with a corresponding increase in extracellular glutamate³. The effects of sulfasalazine on seizure activity have not been studied in other forms of acquired epilepsy. This project aims to elucidate the role of xCT in acquired epileptogenesis and to test whether sulfasalazine can be used as a broad acting anti-epileptic drug.

Is Increased xCT Expression Involved in the Pathogenesis Of Acquired Epilepsy?

Increased xCT Expression Leading to Neuronal Excitotoxicity

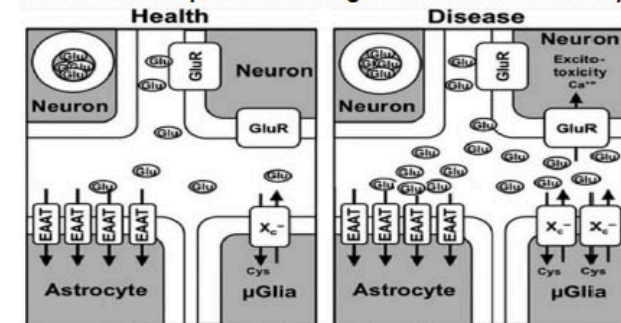
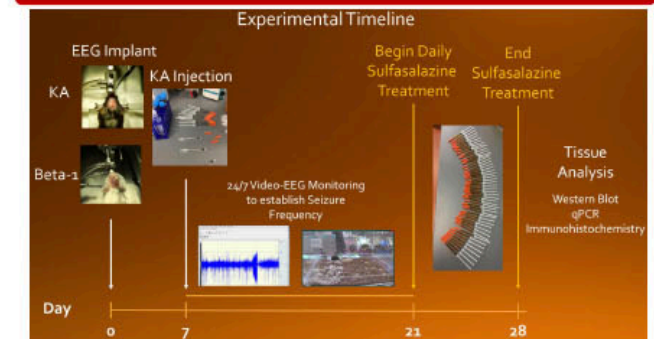


Figure 1: adapted from Massie et al, 2015⁴

Methods



The two mouse models we used to study the effects of sulfasalazine (SAS) in epilepsy are the kainic acid (KA) and beta-1 integrin knockout (KO) models. The kainic acid model is a well characterized, chemically induced model of human temporal lobe epilepsy. The beta-1 KO model is characterized by widespread gliosis leading to spontaneous seizures. To confirm our preliminary findings, future experiments will be performed using the above timelines and methods.

Our KA model allowed us to study the short-term effects of KA seizure induction on xCT expression, however, we found that the chronic seizure frequency was too low to study the effects of SAS long-term. For long-term effects of SAS on seizure activity we conducted EEG recordings

Preliminary Findings

Kainic Acid Induced Gliosis in C57BL/6 Mouse Model

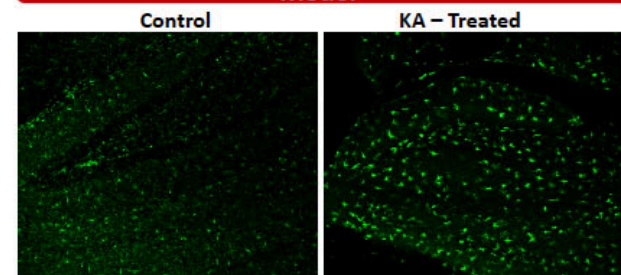


Figure 2: IBA-1, marker for glial activation, expression in hippocampus of KA-treated animal 24 hours post seizure induction compared to control animal. KA-treated hippocampal slice consistent with activated microglia.

Repeated, Low Dose Kainic Acid Results in Spontaneous Seizures

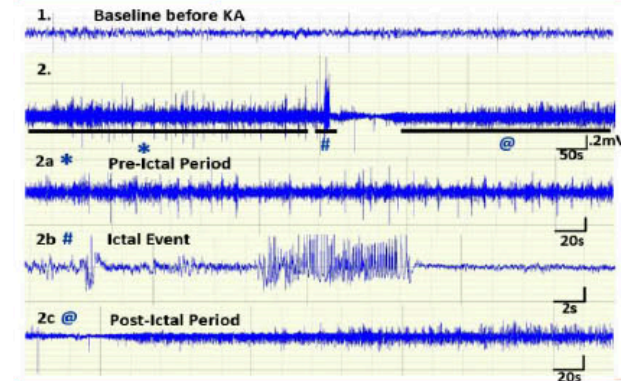


Figure 3. Representative traces of electrographic depiction of spontaneous seizure occurring 2 weeks after repeated, low dose KA administration. 1 – Baseline before KA administration. 2 – Ictal event with pre and post-ictal periods. 2a – Pre-ictal period. 2b – Ictal event. 2c – Post-ictal period.

Sulfasalazine Appears to Restore Pre-Kainic Acid Baseline EEG Patterns

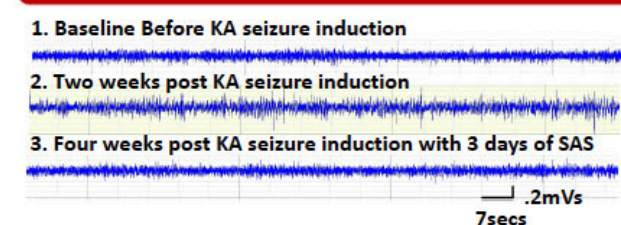


Figure 4. Electrographic depiction of baseline readings from the same animal at three different time points. Pre-KA (1), 2 wks post-KA (2) and 4 wks post-KA with 3 days of sulfasalazine treatment (3).

Sulfasalazine Decreases xCT Expression in Hippocampus of KA treated mice

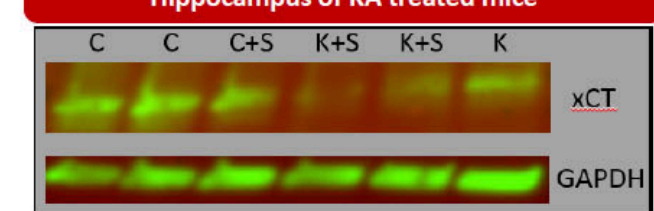


Figure 5: Sulfasalazine treatment (3 days) decreases xCT expression in hippocampal samples from KA-treated mice. C – Control mice. C+S – Control mice treated with sulfasalazine. K+S – Mice treated with KA and sulfasalazine. K – Mice treated with KA and PBS.

Beta-1 Seizure Activity

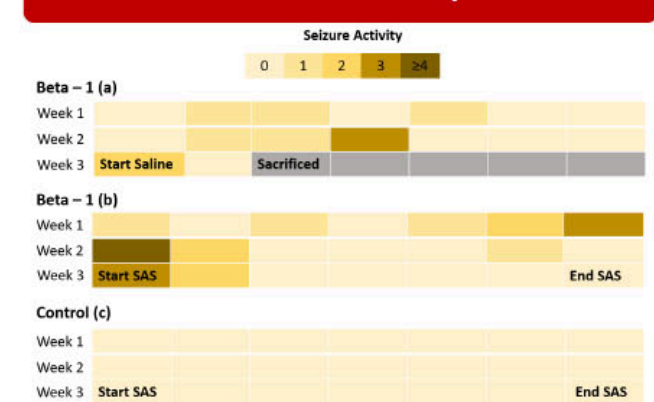


Figure 6. Seizure activity after 3 weeks of 24/7 video EEG recordings. a) Beta-1 KO + saline. b) Beta-1 KO + SAS. c) Control + SAS.

Conclusions

- Sulfasalazine appears to restore KA-induced EEG activity and decrease hippocampal xCT protein levels compared to controls
- Kainic acid induces microglial activation in the hippocampus
- Beta-1 KO mice spontaneously seize at a frequency of ~1 seizure/day and sulfasalazine treatment appears to decrease seizure activity.

References

¹ Kwan, P., Schachter, S. C., & Brodie, M. J. (2011). Drug-resistant epilepsy. *The New England Journal of Medicine*, 365(10), 919-926.
² Buckingham, S. C., Campbell, S. L., Haas, B. R., Montana, V., Robel, S., Ogunrinu, T., & Sontheimer, H. (2011). Glutamate release by primary brain tumors induces epileptic activity. *Nature Medicine*, 17(10), 1269-1274.
³ Mesci, P., Zaidi, S., Lobsiger, C. S., Millecamps, S., Escartin, C., Seilhean, D., ... Boillée, S. (2015). System xc⁻ is a mediator of microglial function and its deletion slows symptoms in amyotrophic lateral sclerosis mice. *Brain: A Journal of Neurology*, 138(Pt 1), 53-68.
⁴ Massie, A., Boillée, S., Hewett, S., Knackstedt, L., & Lewerenz, J. (2015). Main path and byways: non-vesicular glutamate release by system xc⁻ as an important modifier of glutamatergic neurotransmission. *Journal of Neurochemistry*, 135(6), 1062-1079.

from our beta-1 KO mice. Beta-1 integrin KO mice exhibited spontaneous seizures at a frequency of ~1 seizure/day and SAS treatment reduced the seizure activity.

Conclusions: These data suggest that xCT may

play a role in the pathology of acquired epilepsy and that treatment with SAS may work as a broadly acting anti-epileptic drug. Future experiments aim to validate our preliminary data on xCT expression and the effects of SAS treatment on seizure frequency.

Alterations in the Expression of Connexins in the Peritumoral Cortex of Pediatric and Adult Glioma Models

Noah Feld, Lata Chaunsali, Ashley Nyitray, Harald Sontheimer PhD1, and Susan Campbell PhD1

Center for Glial Biology in Health, Disease, and Cancer, Virginia Tech Carilion Research Institute, Virginia Tech Carilion School of Medicine, Virginia Tech School of Neuroscience

Background: Glioblastoma multiforme is a grade IV primary brain cancer with extensive migratory and infiltrative properties. These features highly contributes to the very poor prognosis of glioma patients as it circumvents conventional treatment regimen. A vast majority of glioma patients presents with seizures and a subset develops tumor-associated epilepsy. Growing evidence suggests that gap junction proteins, called connexins, might be markers of glioma progression. In particular, the expression of the connexin 43 subtype was shown to be inversely correlated with tumor grading, and changes in connexin expression occurs in some seizure models. Using an adult glioma model, we previously showed that regions surrounding the tumor mass, peritumoral cortex, exhibited marked hyperexcitability, however it is unknown whether changes in connexin expression in the peritumoral cortex contributes to peritumoral hyperexcitability. Additionally, most studies on connexins are in the context of glioma in adult tissue. The goal of this study is to examine peritumoral neuronal activity in a pediatric glioma model and determine whether changes in connexin expression is associated with changes in neuronal activity.

Methods: We developed a pediatric and adult glioma model where pediatric patient-derived glioma cells were intracranially injected into the cortex of postnatal day 2 and 3 (p2-3) mouse pups and adult glioma cells were implanted into adult mice (p60-p80). After 7 days, the brains were harvested and whole-cell patch clamp recordings of layer 2/3 pyramidal cells were conducted in the peritumoral cortex. Confocal microscopy was used to evaluate the expression of connexin 43 and connexin 30 in peritumoral cortex and compared to distant cortex. The sample size for this procedure was 3-5 brain sections per condition from 3 animals. We used Western Blot to compare connexin 43 protein levels in adult and pediatric glioma cells.

Results: Our results showed for the first time that peritumoral neurons from a pediatric glioma model displayed marked spontaneously occurring epileptiform activity and alteration in neuronal firing properties. The action potential threshold for peritumoral neurons in pups was significantly reduced compared to neurons from sham animals.

Alterations in the Expression of Connexins in the Peritumoral Cortex of Pediatric and Adult Glioma Models

Noah Feld³, Lata Chaunsali¹, Ashley Nyitray^{1,2}, Harald Sontheimer PhD^{1,2}, and Susan Campbell PhD¹

¹ Center for Glial Biology in Health, Disease, and Cancer, Virginia Tech Carilion Research Institute, ² Virginia Tech Carilion School of Medicine, Virginia Tech School of Neuroscience³

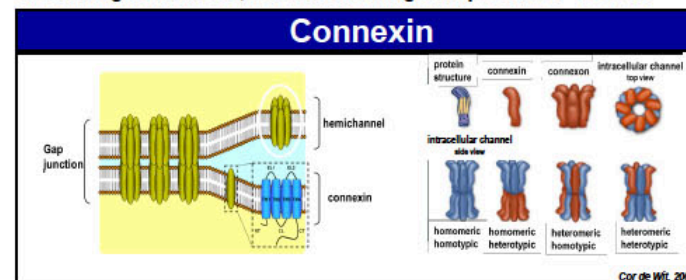


Background

Glioblastoma multiforme, a Grade IV primary brain cancer, is highly invasive, many patients present with seizures and carries a dismal prognosis. This lethality is largely attributed to the ability of glioma cells to aggressively migrate and proliferate in the brain. Growing evidence indicates that gap junction proteins, connexins, could be considered as markers of glioma progression as previous studies showed that expression of a connexin type, connexin43 (Cx43), is inversely correlated to tumor grading. Changes in gap junction communication is also associated with seizure activity. Our previous studies showed that peritumoral (PT) neurons in an adult glioma model displayed hyperexcitability.

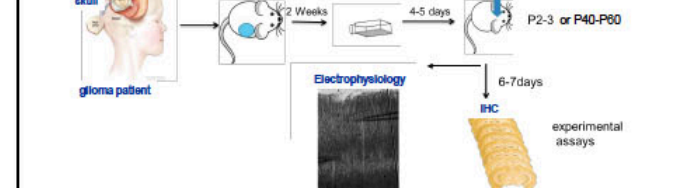
The effect of tumor-induced changes on connexin expression is unknown. Additionally, most studies on connexins in the context of glioma, highly focuses on glioma in adults. Here we examined PT neuronal function in a pediatric and adult glioma model and assess connexin expression in areas surrounding the tumor border.

Here we demonstrate for the first time that PT neurons in a pediatric glioma model display spontaneous epileptiform activity. In addition, we found that connexin expression was decreased in the PT cortex of the adult glioma model, but was unchanged in pediatric PT cortex.



Cor de Wit, 2004

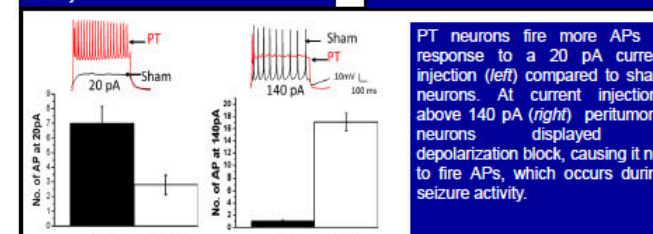
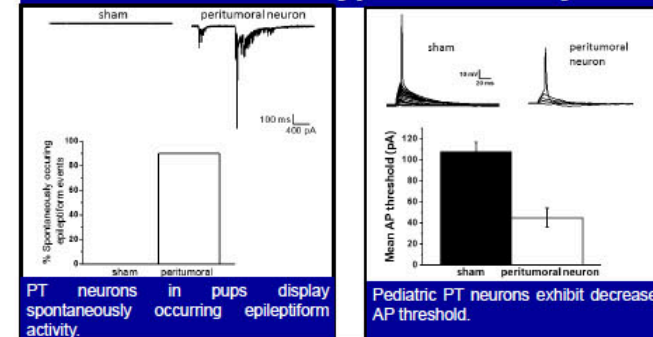
Methods



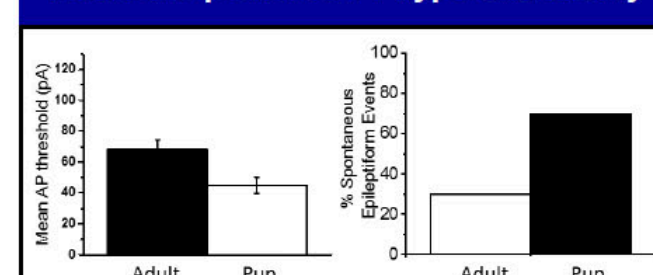
We developed a pediatric glioma and adult glioma model where pediatric patient-derived glioma cells are implanted into the cortex of p2-3 mouse pups and adult glioma cells are implanted into adult mice (p60-p80). The brains are harvested after 7 days and using fresh brain slices, whole-cell patch clamp recordings of layer 2/3 pyramidal cells were conducted in the area of cortex adjacent to tumor (peritumoral cortex) and results were compared to sham-operated controls. We also used immunohistochemistry and confocal microscopy to evaluate expression levels of connexin 43 and 30 in the peritumoral cortex compared to distant cortex. Western blot was used to compare connexin 43 protein levels in adult and pediatric glioma cells.

Results

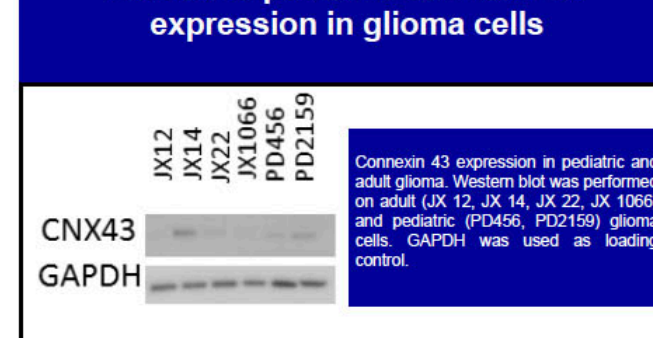
Pediatric PT hyperexcitability



Adult and pediatric PT hyperexcitability

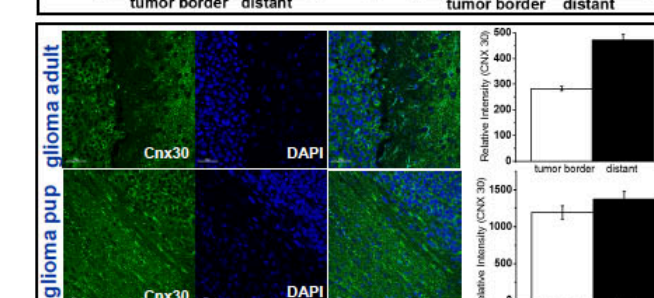
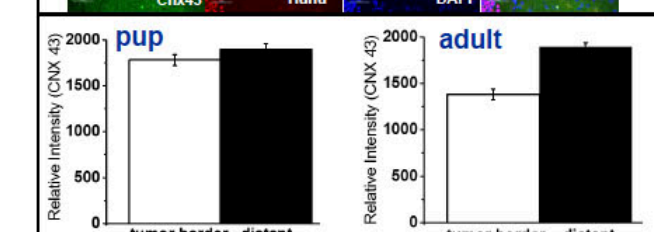
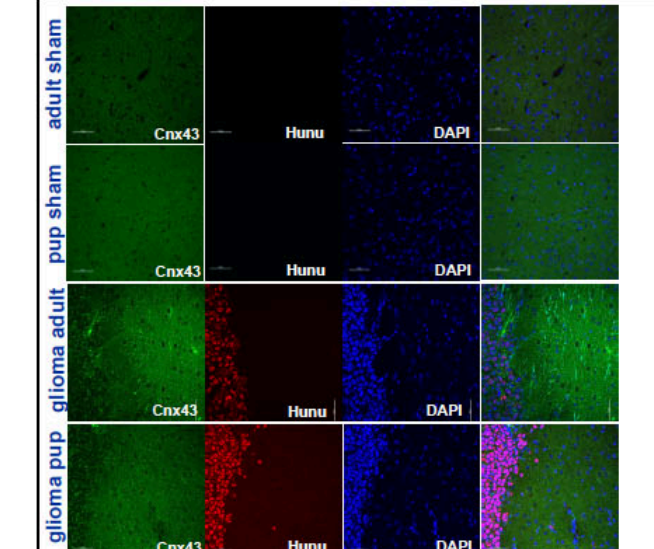


Adult and pediatric connexin 43 expression in glioma cells



Results

Connexin expression PT cortex



Conclusions

Connexin 43 and 30 expression is decreased in adult peritumoral cortex but unchanged in the peritumoral cortex of our pediatric glioma model. Peritumoral hyperexcitability observed in the pediatric glioma model was not associated with changes in connexin 43 and 30 expression in the PT cortex.

In addition, the mean action potential threshold in pediatric peritumoral neurons was lower than that of adult peritumoral neurons. We also found that peritumoral expression of connexin 43 was unchanged in the pups, but was decrease at the tumor border compared to distant regions.

Conclusions: These findings suggest that changes in the peritumoral expression of connexin 43 and connexin 30 were associated with hyperexcitability in the adult glioma model but not the pediatric glioma model. This suggests that connexins may have distinctive interactions with the adult and pediatric brain environment and therefore age should be accounted for in future studies.

Characterizing stress induced sex differences in pre- and post-synaptic plasticity in the Hippocampus and Nucleus Accumbens

Brett Smith, Amanda Patterson, Mariya Tsyglakova, Jennifer Rainville, Georgia E. Hodes
School of Neuroscience, Virginia Tech, Blacksburg, VA

Background: depression and anxiety disorders are more prevalent in females; however, the majority of research in animal models has focused predominantly on males. Major depressive disorder (MDD) is known to affect the hippocampus and nucleus accumbens. Numerous studies have shown that MDD shrinks hippocampal volume (Malykhin & Coupland, 2015). Other studies have shown decreased activation of the nucleus accumbens (NAc), which plays a central role in the reward system of the brain (Pizzagalli et al., 2010). However, little is known about how plasticity in these brain regions may differ in males and females. Previous studies have used immunofluorescent staining of vesicular glutamate transporter 1 (VGLUT1) and post-synaptic density 95 (PSD95) as markers for plasticity in pre-synaptic and post-synaptic regions. Our early research has indicated a significant decrease of pre-synaptic VGLUT1 in the glutamatergic neurons of the nucleus accumbens (NAc) with no detectable changes in post-synaptic density, indicating possible circuit specific reorganization in only female mice that underwent 6 days of variable stress (Brancato et al, 2017). In this model, female mice are susceptible to 6 days of stress and males are resilient. Therefore, we do not know if the female pre-synaptic plasticity effects are due to stress susceptibility vs. resilience or are sex specific. We can test this by extending stress out to 28 days where both males and females show behavioral stress susceptibility. The studies presented here expand on this research by exposing mice to 6 days of sub-chronic variable stress (SCVS) and 28 days of long-term variable stress (LTVS) to measure the effects on glutamatergic neuroplasticity in the nucleus accumbens (NAc) and hippocampus of both males and females.

Methods: We performed alternating stressors of foot shock, tail suspension, and restraint tube on a 6-day sub-chronic variable stress (SCVS) model and a 28-day long-term variable stress (LTVS) model. Each study consisted of 40 mice (n= 10 per group/sex). 24 hours after the last stressors, animals were deeply anesthetized and perfused with saline and 4% paraformaldehyde. Brains were stored, for two days in PFA then 3 days of increasing concentrations of sucrose. We sliced the tissue in to

40-micron sections on a freezing microtome and collected every 6th NAc and hippocampal slice. Immunohistochemistry was optimized to detect the presence of VGLUT1 and PSD95, and most of the time was spent performing immunohistochemistry alterations to optimize the staining. After extensive optimization we ended up switching from a free-floating to a slide mounted staining procedure. Sections were slide mounted, allowed to dry over night and then washed in PBS (1x). Sections were blocked in 3% donkey serum, washed again in PBS (1x) and then incubated overnight in primary (PSD95 from abcam, #ab12093, at 1:500 concentration, and vGLUT1 from milpore, #AB5905, at 1:10000). Slides were washed again and incubated in secondary antibody (by Jackson ImmunoResearch, Cy2 Anti-Goat 705-225-147; Cy5 Donkey Anti-Guinea Pig 706-175-148) for 2 hours at room temperature. After subsequent washing, sections were coverslipped with Vectashield with Dapi (by Vectorlab) and imaged on a confocal microscope (Nikon A1).

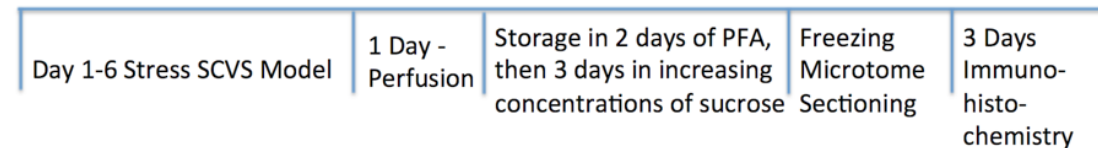
Results: During the initial runs of the free-floating protocol the sections became too fragile to mount, so a new protocol was created. The sections were slide mounted before staining to create a successful immunohistochemistry procedure. However, excess auto-fluorescence detected in unstained controls has caused us to test further concentrations and optimization of secondary antibodies.

Summary: We created a brain bank of 40 SCVS and 40 LTVS mice, which will allow us to examine a number of immunofluorescent markers in both the Hippocampus and Nucleus Accumbens. While much of our time has consisted of optimizing our IHC protocol, we will use this new protocol in the fall to continue this project. Our protocol will allow us to successfully and efficiently stain for VGLUT1 and PSD95 to measure pre- and post-synaptic plasticity, respectively. We will examine the amount of fluorescence, number of puncta, and co-localization of markers in both short-term stress conditions and long-term stress conditions, expanding on our previous research. Our intention is to further explore the sex differences in the complex framework of glutamatergic dysfunctions in susceptibility to stress and depression.

References

- Malykhin, N. V, & Coupland, N. J. (2015). REVIEW. *Neuroscience*, 309, 200–213. <https://doi.org/10.1016/j.neuroscience.2015.04.047>
- Pizzagalli, D. A., Ph, D., Holmes, A. J., Dillon, D. G., Ph, D., Goetz, E. L., ... Fava, M. (2010). *NIH Public Access*, 166(6), 702–710. <https://doi.org/10.1176/appi.ajp.2008.08081201.Reduced>.

Foot shock
Tail Suspension
Restraint Tube



Foot shock
Tail Suspension
Restraint Tube

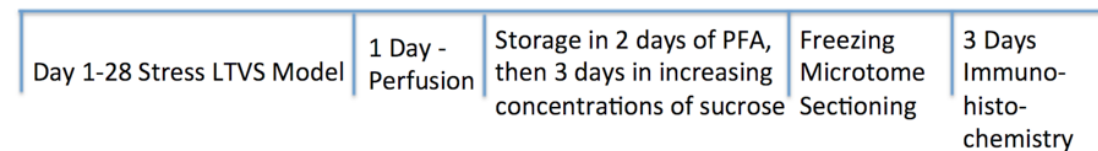


Figure 1. Timeline of SCVS and LTVS Stress Models for Immunohistochemistry

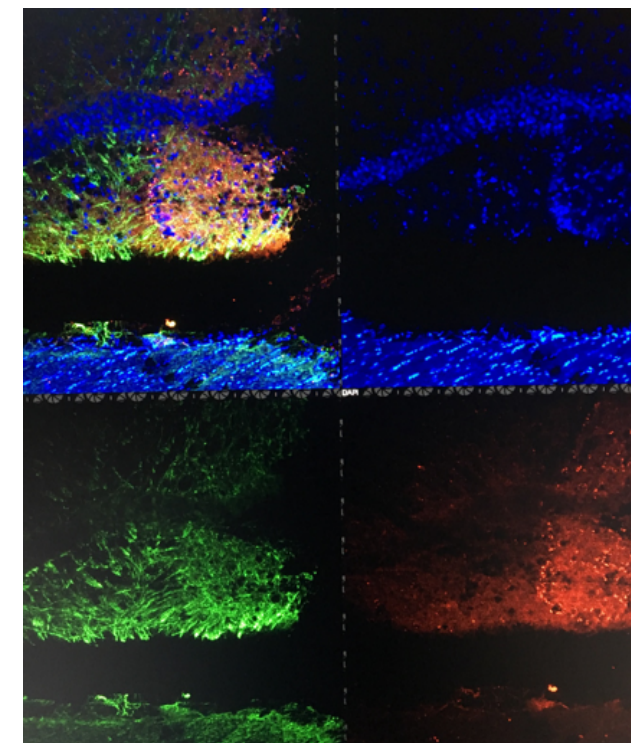


Figure 2. Immunohistochemistry for Dapi for cell bodies (Blue) pre-synaptic marker VGLUT1 (red) and post synaptic marker PSD95(green) in hippocampus



School of Neuroscience
EngelNovitt
Summer Research Program



VirginiaTech®

School of Neuroscience